# Reconstruction of hepatic organoids with functional bile canaliculi using rat small hepatocytes

2004

Ryo Sudo

Ph. D dissertation

Graduate school of science and technology

Keio University

# Abstract

Development of bioartificial livers is an ongoing study for the future therapy of liver diseases. Despite their regenerative capability *in vivo*, functional hepatocytes are difficult to retain *in vitro*. However, recent studies have revealed that hepatic stem/progenitor cells have capabilities to regenerate hepatic organoids *in vitro*. This dissertation focuses on the reconstruction of hepatic organoids using small hepatocytes (SHs) *i.e.*, hepatic progenitor cells. Hepatic cells, including SHs, were isolated from adult rat livers and cultured. For the hepatic organoid formation, individual cells were integrated into tissues in culture. SHs proliferated and formed colonies within 10 days. Some SHs differentiated into mature hepatocytes interacting with hepatic nonparenchymal cells, such as stellate cells and liver epithelial cells. Bile canaliculi (BC) like structures were formed by the differentiated cells. In terms of organoid formation, the BC formations can be considered as the first step in tissue organization because BC are formed between adjacent hepatocytes and pairs of the cells are integrated through the BC formation. The investigations studied how BC developed with the maturation of SHs and whether the tubular structures were functionally active as BC. The results revealed that differentiated SHs possessed membrane polarity and excreted metabolites into the BC-like structures. This suggests that SHs can reconstruct functional BC that are similar to those *in vivo*. Analyses of the BC concentrated on their tissue-level functions. In the liver, hepatocytes secrete bile into BC and the secreted bile is transported into bile ducts through the BC. Investigations were conducted to determine whether the groups of the differentiated SHs moved in a coordinated manner to enable to the BC to transport their contents. Time-lapse microscopy was carried out and reveled that the BC contracted and dilated spontaneously and the movements occurred in a coordinated manner. These results indicate that groups of the cells that form the BC act in a coordinated manner and possess a highly differentiated function that cannot be achieved by individual cells. To expand these organoids, a 3D-culture method was developed by stacking up the 2D tissues of SHs. The studies investigated whether the stacked cells were organized into orchestrated tissues. The results revealed that the SHs of the upper and lower layers adhered to one another, and that BC formed between them. Furthermore, SHs within the structures exhibited the mRNA transcription of hepatic-differentiation markers and retained a relatively high level of albumin secretion. This indicates that differentiated 3D tissues, including functional BC, can be reconstructed by stacking up SH layers. In conclusion, the combination of SHs and 3D stacked-up culture can contribute to successful reconstruction of tissue-engineered livers.

# Abstract (Japanese)

【訳題】ラット小型肝細胞を用いた機能的な毛細胆管を伴う肝臓類似組織の再構築

将来的な肝臓病治療のためにバイオ人工肝臓の開発が進められている．肝細胞は生体内で再生能力を持つにも関わらず，生体外でその機能を維持することは難しい．しかし，最近の研究の成果により前駆細胞あるいは幹細胞と呼ばれる一部の細胞は生体外においても組織を再生する能力を持つことが分かってきた．本研究では，肝前駆細胞である小型肝細胞を用いて生体外で肝臓に類似した組織を再構築することを目的とした．小型肝細胞を含む肝臓構成細胞は，成熟ラットの肝臓から分離して実験に用いた．肝組織を再構築するためにはばらばらの細胞が互いに統合し，多細胞組織を構築していく必要がある．小型肝細胞は生体外で増殖し 10 日程度で細胞集団を形成すると，一部の小型肝細胞は他の肝臓構成細胞である星細胞や肝上皮様細胞との相互作用によって成熟化し，細胞間に生体内の肝細胞で見られるような毛細胆管様の構造を形成する．毛細胆管の形成は細胞間で生じる構造物であることを考えると，隣接する細胞が統合される点で組織再構築の第一段階である．そこで，この毛細胆管様の構造が生体内の毛細胆管と同様の機能を有するかどうか検討した．再構築された毛細胆管の極性や代謝・排出機能を検討した結果，生体内の毛細胆管と同様の機能を持つことが分かった．次の段階として，この毛細胆管の輸送機能について検討した．生体内の毛細胆管は肝細胞から分泌された胆汁の通り道であり，胆汁は毛細胆管の中を通って胆管へ運ばれる．したがって，毛細胆管が組織として機能するためには，隣接する肝細胞が互いに協調することによって毛細胆管を同調して収縮させ，ポンプとしての機能を果たす必要がある．まず，タイムラプス顕微鏡撮影により毛細胆管運動を観察したところ，毛細胆管は自発的な収縮と拡張を繰り返していることが分かった．さらに，この運動は細胞集団全体で協調していることが分かった．すなわち，毛細胆管を形成している小型細胞は個々の細胞として振る舞うのではなく，まとまった集団として協調した振る舞いをすることで高次機能を獲得することが分かった．このような小型肝細胞の組織を三次元に拡張させるために，二次元で培養した小型肝細胞を積層させることで立体的な組織を再構築する培養法を考案し，この方法によって積層された小型肝細胞が組織化するかどうか検討した. その結果, 積層された上下の細胞は互いに接着し，細胞間には毛細胆管が形成されることが明らかになった．さらに，この三次元積層組織内の小型肝細胞は，肝細胞分化マーカーの mRNA を発現しており，肝細胞機能の指標となるアルブミン分泌量も高いレベルを維持していた．これらの結果は，小型肝細胞の三次元積層培養によって肝組織に類似した三次元組織が再構築されうることを示している．以上の結果をまとめると，肝前駆細胞である小型肝細胞と三次元積層培養の組み合わせは組織工学における肝臓の再生に役立つと考えられる．

# Contents

# List of abbreviations and symbols

2D: two-dimensional (1-8)*
3D: three-dimensional (1-6)
5′NT: 5′-nucleotidase (2-5-1)
ABC: avidin-biotin comlex (2-5-3)
AFP: α-fetoprotein (1-5)
Asc2P: L-ascorbic acid 2-phosphate (1-4)
AP-1: activating protein-1 (1-3)
BAL: bioartificial liver (1-6)
BC: bile canaliculi (1-1)
BEC: biliary epithelial cell (1-1)
BrdU: bromodeoxyuridine (Fig. 1-5)
CB: cytochalasin B (2-5-5)
C/EBP: CCAAT enhancer binding protein (1-3)
CK: cytokeratin (1-5)
CMFDA: CellTracker™ 5-chloromethylfluorescein diacetate (2-7-2)
CMTPX: CellTracker™ red-fluorescent CMTPX (2-7-3)
Connexin: Cx (2-5-1)
DAB: 3, 3′-diaminobenzidine (2-6-1)
DAPI: 4′, 6-diamino-2-phenylindole (2-5-2)
DDC: 3, 5-diethocycarbonyl-1, 4-dihydrocollidine (1-5)
DPPIV: dipeptidylpeptidase IV (2-5-1)
DMEM: Dulbecco's modified Eagle's medium (1-4)
DMSO: dimethyl sulfoxide (1-5)
ECM: extracellular matrix (1-1)
EDTA: ethylene diamine tetraacetic acid (1-6)
EGF: epidermal growth factor (1-1)
EGFP rat: transgenic SD rat carrying the enhanced green fluorescent protein transgene (2-1)
EGTA: ethyleneglycol tetraacetic acid (1-4)
ELISA: enzyme-linked immunosorbent assay (2-9)
ES: embryonic stem (1-5)
FACS: fluorescent-activated cell sorter (1-5)
FBS: fetal bovine serum (1-6)
FD: Fluorescein diacetate (2-7-1)
GAPDH: glyceraldehyde-3-phosphate-dehydrogenase (2-11)
GFP-labeled cell: cell isolated from EGFP rats (2-7-3)
H-CFU-C: hepatic colony-forming units in culture (1-5)

* Section where the abbreviation or the symbol first appears

HEPES: 2-[4-(2-hydroxyethyl)-1-piperazinyl] ethanesulfonic acid (1-6)
HGF: hepatocyte growth factor (1-1)
HNF: hepatic nuclear factor (1-6)
HRP: horseradish peroxidase (2-6-1)
HSC: hematopoietic stem cell (1-5)
ICAM-1: intercellular adhesion molecule 1 (1-5)
IL: interleukin (1-3)
LEC: liver epithelial cell (1-6)
LETF: liver-enriched transcription factors (1-6)
MAPC: multipotent adult progenitor cell (1-5)
mdr: multidrug resistance protein (1-5)
MH: mature hepatocyte (1-5)
MHC: major histocompatability complex (1-5)
MRP2: multidrug-resistance associated protein 2 (2-5-1)
NF-κB: nuclear factor kappa B (1-3)
NOD-SCID: nonobese diabetic severe combined immunodeficient (1-5)
NPC: nonparenchymal cell (1-1)
PBS: phosphate buffered saline (2-5-3)
PHx: partial hepatectomy (1-3)
PPD: p-phenylenediamine (2-5-2)
ROI: region of interest (2-4)
RT-PCR: reverse transcription-polymerase chain reaction (2-11)
SD: Sprague-Dawley (2-1)
SDH: serine dehydratase (1-6)
SDS-PAGE: sodium dodecyl sulfate-polyacrylamide gel electrophoresis (2-10)
SEC: sinusoidal endothelial cell (1-1)
SH: small hepatocyte (1-6)
SP: side population (1-5)
STAT3: signal transducer and activator of transcription 3 (1-3)
TAT: tyrosine aminotransferase (2-11)
TEM: transmission electron microscopy (1-6)
TGF: transforming growth factor (1-1)
TNF: tumor necrosis factor (1-3)
TO: tryptophan 2, 3-dioxygenase (1-6)
ZO-1: zonula occludens-1 (2-5-1)

$R_{xy}$: correlation coefficient (2-4)

# Chapter 1

# General introduction

## 1-1 Liver organization

The liver is the largest organ in the body, weighting about 1,500 g in the adult human. The structure of the liver can be divided into functional components, which are called hepatic lobules. We can see this polygonal unit, about 0.7 mm in diameter and 2.0 mm long, in a histological section of the liver (Fig. 1-1). The hepatic lobule is the smallest module of the liver, in which various types of cells are organized into tissues (Fig. 1-2). About 60% of the cells in the liver are hepatocytes, the main parenchymal cells of the liver. They are arranged in plates and cords, which are interconnected to each other as shown in Fig. 1-2. Bile canaliculi (BC) are formed by adjacent hepatocytes in the hepatic cords and they are connected to bile ducts, which are composed of biliary epithelial cells (BECs), the other parenchymal cells in the liver. BC are tubular structures, which are about 1 μm in diameter and function as pathways of bile secreted from hepatocytes.

The hepatic lobule also consists of hepatic nonparenchymal cells (NPCs), such as sinusoidal endothelial cells (SECs), stellate cells, kupffer cells and pit cells. SECs are liver-specific endothelial cells, which have characteristic fenestrae in their cytoplasm (Braet *et al.*, 2001). Sinusoids are characteristic blood vessels in the liver, which are lined by single layers of SECs, running between the hepatic cords. SECs are separated from the underlying hepatocytes by the space of Disse, a perisinusoidal minute space containing sparsely distributed extracellular matrix (ECM), such as collagens, fibronectins and a basement membrane-like matrix (Martinez-Hernandez *et al.*, 1995). Stellate cells locate in the space of Disse. They can store vitamin A in their cytoplasm, secrete cytokines, *e.g.* transforming growth factor (TGF) α, epidermal growth factor (EGF) and hepatocyte growth factor (HGF); produce variety of the ECM, such as type I, III, IV, VI and XIV collagens, proteoglycans and laminins; and function as liver-specific pericytes

which regulate blood flow through their contractility (Li *et al.*, 2001). Kupffer cells are the liver-specific macrophages that are located in the lumen of the sinusoids (Kuiper *et al.*, 1994). Pit cells are liver-specific natural killer cells, which inhabit the sinusoids and often adhere to SECs. They have an ability to kill certain tumor cells and virus-infected cells without prior sensitization (Braet *et al.*, 2001). Thus, hepatocytes, BECs and NPCs are assembled and organized into hepatic tissues.

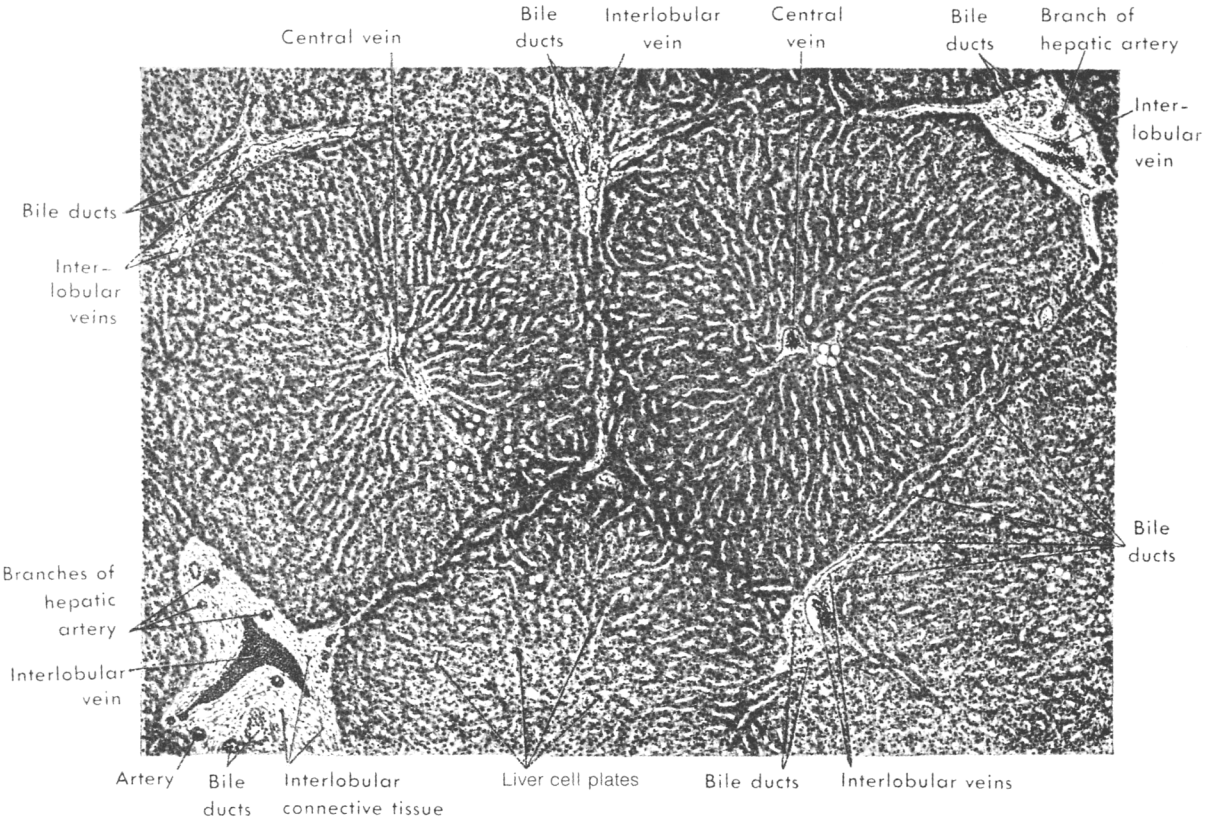


Fig. 1-1 A histological section of the liver of a 22-year-old man showing the polygonal unit, in which cell plates distributed in the radiating pattern (Fawcett, 1994).

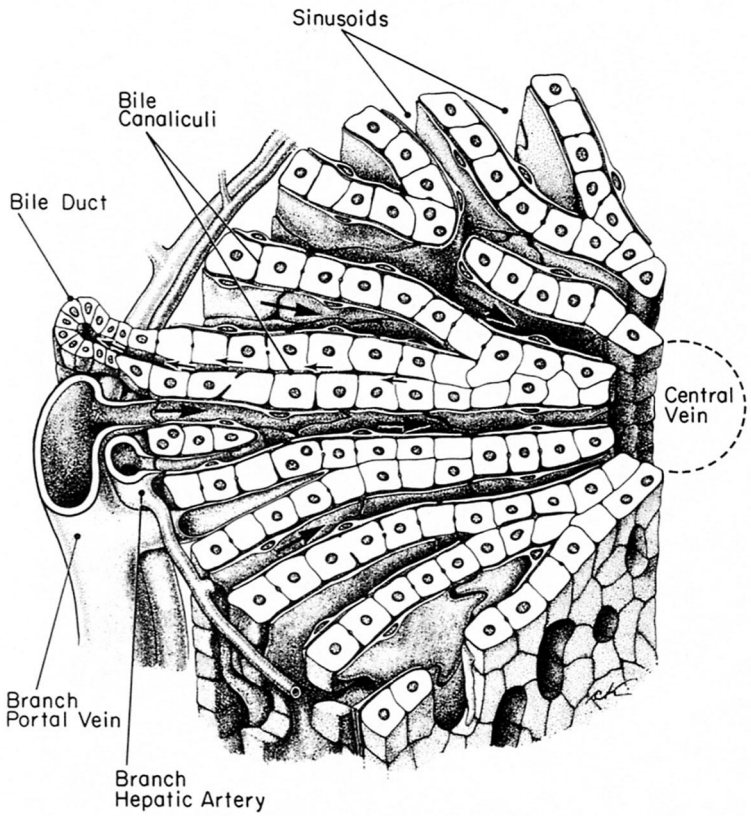


Fig. 1-2 Schematic representation of a portion of the hepatic lobule (Fawcett, 1994).

## 1-2 Liver functions

Liver functions are essential for life because of the functional diversity and complexity. The liver has various physiological functions, such as detoxification, synthesis, storage and excretion (Ross *et al.*, 2003), most of which are carried out by hepatocytes. 1) Detoxification: hepatocytes detoxify drugs and toxins, such as ammonia products and alcohols. They convert drugs and toxins into more water-soluble forms, which can be transported to the kidney and removed. 2) Synthesis: the liver metabolizes carbohydrates, fats and proteins. It synthesizes various circulating plasma proteins: albumins, lipoproteins, glycoproteins, prothrombins, fibrinogens and nonimmune globulines. Hepatocytes also synthesize glucose and release it into the bloodstream in response to demand. 3) Storage: the liver absorbs nutrients from blood that has already circulated through the intestine, and stores glycogen, proteins and vitamins. 4) Excretion: hepatocytes produce bile and excrete it into BC. The secreted bile flows into bile ducts and it is finally excreted into the duodenum. The bile contains metabolites, such as urea and bile acids that help to digest fats. Thus, the liver has complex functions as well as structural complexity.

## 1-3 Liver regeneration

Liver regeneration is a unique phenomenon, which is never happened in the other organs. Hepatocytes rapidly start to proliferate in response to the loss of the tissue although the liver is normally a quiescent organ, in which the hepatocytes live for a year or more and are renewed at a slow rate. When two-thirds of the liver of a rat is removed, the hepatocytes in residual lobes rapidly proliferate, which results in the recovery of the total mass of the liver within 2 weeks. With a human living-donor liver transplantation, the volume of the residual liver in the donor doubles within 7 days after partial hepatectomy (PHx) and the recovery of the transplanted liver in the recipient progesses within 7–14 days after transplantation. The volume recovers the optimal liver mass/body mass ratio to achieve the functional requirements of the body by the 60th day after transplantation (Fausto, 2001).

Liver regeneration was first introduced by Higgins and Anderson (1931) who demonstrated PHx and the following restoration of tissue mass using rats. The regenerative capability of the liver appears in Greek mythology so it must have been known even then. Many researchers have studied how liver cells restore

lost tissue under the control of various factors (Michalopoulos *et al.*, 1997). When the liver of rats is subjected to PHx, DNA synthesis is first started in the hepatocytes after 10–12 hours and peaks at 24 hours (Fig. 1-3). On the other hand, other cell types, such as Kupffer cells, BECs and stellate cells, start to proliferate about 24 hours after PHx, then peak at about 2 days (Fig. 1-3). SECs finally start to proliferate and peak about 4 days after PHx. The proliferating hepatocytes first form aggregates and then rearrange into typical hepatocyte plates that are seen in the mature liver, interacting with other cell types, such as stellate cells and SECs (Martinez-Hernandez *et al.*, 1995). The sequential rebuilding of the liver is associated with the activation of hepatic transcription factors, cytokines and growth factors, which regulate each other.

The mechanism of liver regeneration has become clearer from recent studies using animals subjected to PHx or chemical injury and appropriate transgenic and knockout mouse models although it is not yet completely understood (Fausto, 2000). Although the activation of more than 100 genes and the participation of growth factors and cytokines are associated with the process of liver regeneration, the major steps in liver regeneration after PHx are described below. The sequential events during liver regeneration are shown in a schematic diagram (Fig. 1-4) on the basis of previous studies integrated by Fausto (2001). The proliferation in response to PHx can be triggered by tumor necrosis factor (TNF) although the source for TNF is still unknown. Cytokines, such as TNF and interleukin-6 (IL-6), increase in the blood and the liver after PHx. Transcription factors, such as nuclear factor kappa B (NF-κB), signal transducer and activator of transcription 3 (STAT3), activating protein-1 (AP-1) and CCAAT enhancer binding protein (C/EBP) β, are also activated during the initial stages of liver regeneration. TNF activates NF-κB by binding its receptor TNFR-1, which results in peak activity of NF-κB at 30 min after PHx. TNFR-1 is needed for the activation of IL-6, which activates STAT3. The protooncogenes, such as c-fos, c-jun and c-myc, are rapidly activated in the first 4 hours after PHx, and they are therefore called ‘immediate early genes’. The expression of immediate early genes and the activation of transcription factors are followed by the expression of ‘delayed genes’ and finally followed by that of cell cycle genes, such as cyclin D1 and cyclin E, which are required for the progression of the cell cycle. At this stage, the hepatocytes are primed to become competent for replication and respond to growth factors, such as HGF, EGF and TGF-α. HGF is the definitive mitogen for liver regeneration, which was first identified as a

blood-derived mitogen for hepatocytes (Nakamura *et al.*, 1984). EGF is made by the Brunner's glands of the duodenum and is thought to play a mitogenic role in liver regeneration. TGF-α is an autocrine growth factor through binding the EGF receptors and it also functions through a juxtacrine mechanism. These growth factors stimulate hepatocyte-proliferation and lead to the recovery of liver-mass.

Although the initiation of liver regeneration has been well investigated, its termination is not so clear. While DNA synthesis in hepatocytes eventually stops during liver regeneration, TGF-β1 mRNA increases and reaches plateau amounts. TGF-β1 is normally synthesized by stellate cells and is an inhibitor of the proliferation in hepatocyte cultures. Therefore, TGF-β1 is a logical candidate as the trigger to end liver regeneration (Michalopoulos *et al.*, 1997).

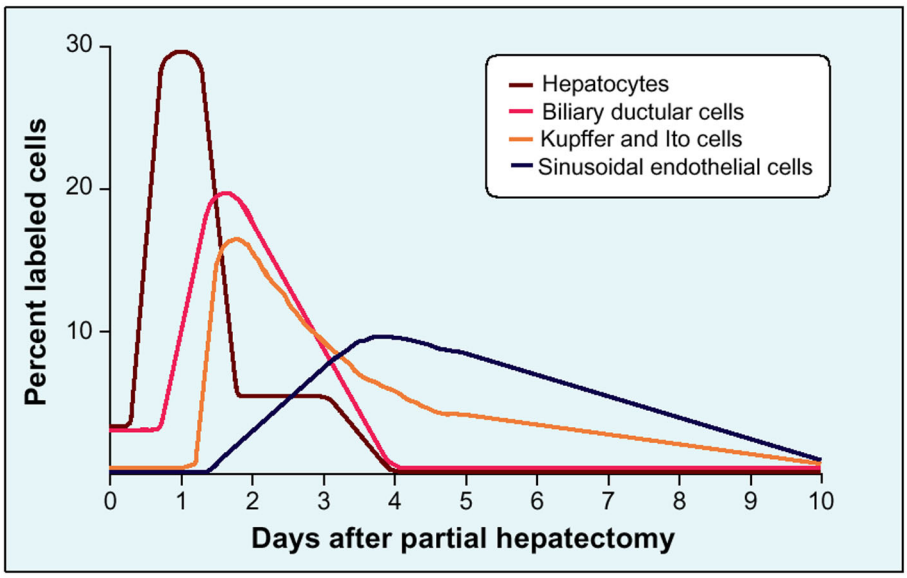


Fig. 1-3 Time kinetics of DNA synthesis in different liver cell types during liver regeneration after PHx (Michalopoulos, 1997). The major types of liver cells, such as hepatocytes, biliary ductular cells (also called BECs), Kupffer cells, Ito cells (also called stellate cells) and SECs, start to proliferate about 24 hours after PHx undergo DNA synthesis at different times. The DNA synthesis of the hepatocytes is first started and peaks at 24 hours, whereas the other cell types proliferate later.

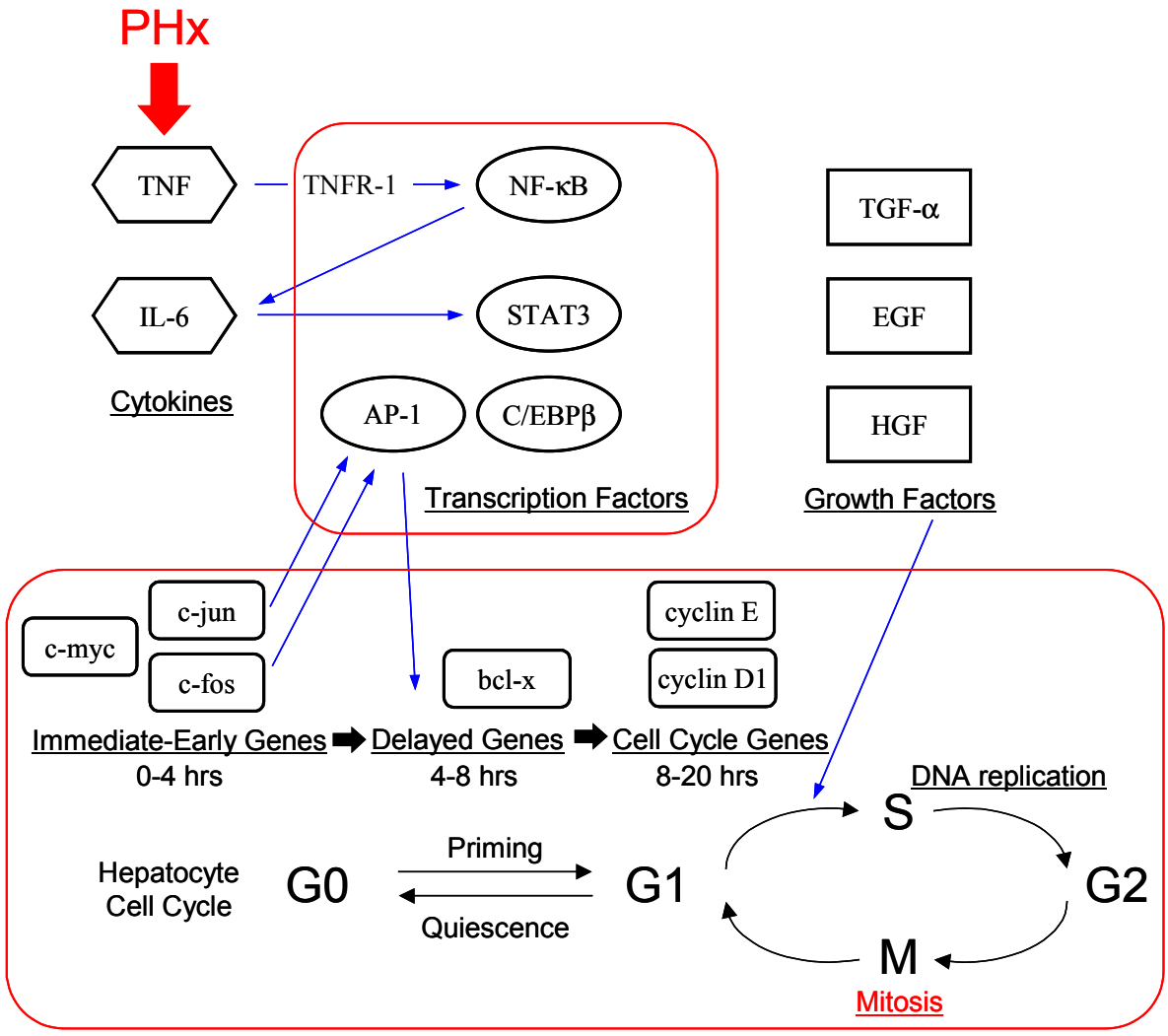


Fig. 1-4 Sequential events during liver regeneration, proposed by Fausto (2001). PHx activates cytokines such as TNF and IL-6 in blood. The proliferation of the hepatocyte can be triggered by TNF. The details of the following events are described in the section 1-3: liver regeneration.

## 1-4 Primary hepatocytes

The isolation of intact hepatocytes was first reported by Howard and Pesch in 1968. They processed liver slices of rats by shaking them with an enzyme solution containing collagenase and hyaluronidase. The *in situ* collagenase perfusion method was developed by Berry and Friend (1969). Finally, the isolation method was improved, and the two-step liver perfusion method was developed by Seglen (1976). The present isolation method of hepatocytes is based on the Seglen's method, in which two solutions are used: ethyleneglycol tetraacetic acid (EGTA) solution for the first perfusion and collagenase solution for the second. Thus, the study using primary hepatocytes was started about 30 years ago.

Bissell *et al.* (1973) first demonstrated a monolayer culture of primary hepatocytes. In Japan, Ichihara *et al.* (1980) reported biochemical functions of adult rat hepatocytes using monolayer culture. Although freshly isolated hepatocytes have impaired functions, the cells recover the activity of a normal liver after culture for a few days. Therefore, primary hepatocytes have been used as an *in vitro* model in the studies of liver metabolism. Although hepatocytes could not proliferate and maintain their functions in the early studies, several additives to the culture media, such as insulin (Richman *et al.*, 1976), dexamethasone (Marceau *et al.*, 1980), EGF (McGowan *et al.*, 1981), proline (Nakamura *et al.*, 1984), dimethyl sulfoxide (DMSO; Isom *et al.*, 1985; Muakkassah-Kelly *et al.*, 1987), L-ascorbic acid 2-phosphate (Asc2P; Senoo *et al.*, 1989) and nicotinamide (Inoue *et al.*, 1989), have improved the culture conditions. When hepatocytes are cultured in Dulbecco's modified Eagle's medium (DMEM) supplemented with these additives, they start to proliferate on the second day after inoculation (Fig. 1-5).

Although many studies have been conducted using monolayer culture of hepatocytes, the cells retain their function only for the limited period. For example, the amount of albumin secreted into the culture medium, a major marker of hepatocyte function, rapidly decreases within a week (Fig. 1-6A). Albumin mRNA transcription also diminishes corresponding to the protein secretion (Fig. 1-6B).

It is difficult to maintain the polarity of hepatocytes as well as mRNA transcriptions and protein production of hepatic differentiation markers. Hepatocytes are highly differentiated epithelial cells, in which membranes are specialized into three functional domains: bile canalicular, lateral and sinusoidal (Fig. 1-7). In the reconstruction of BC on which the experiments described in the following chapters are centered,

the bile canalicular domain is the most important of the three functional domains. The bile canalicular domain of adjacent hepatocytes forms a bile canaliculus, which is a highly differentiated structure and is never seen in other epithelial cells. Bile canalicular membranes have various important proteins and enzymes, which are involved in transportation of bile acids and detoxification products across the membranes. The lateral domain is specialized for cell attachment and cell–cell communication and is separated from the bile canalicular domain by tight junctions. The sinusoidal domain is specialized for the exchange of metabolites with blood. This domain faces the space of Disse and has many microvilli. Thus, hepatocytes have three specialized interfaces: cell–bile, cell–cell and cell–blood. This specialization causes differences in molecular composition among the domains.

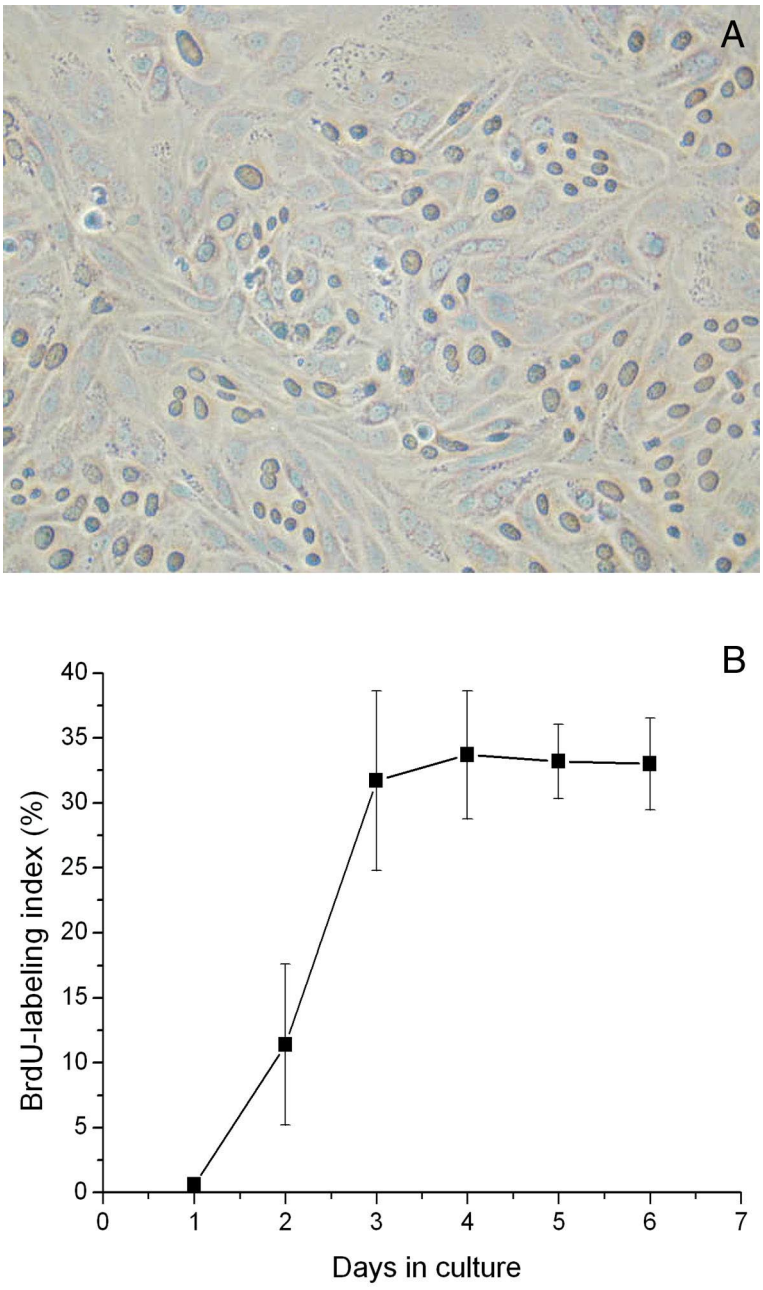


Fig. 1-5 DNA synthesis of primary hepatocytes. A: The cells were treated with 40 μM bromodeoxyuridine (BrdU), which is incorporated in the DNA of proliferating cells. 24 hours later, the cells were fixed in cold absolute ethanol. Thereafter, immunocytochemistry for BrdU incorporation was carried out. The cells with brown nuclei incorporated BrdU into their DNA, which indicates proliferating cells. B: Quantitative representation of the BrdU incorporation (Sudo, unpublished data).

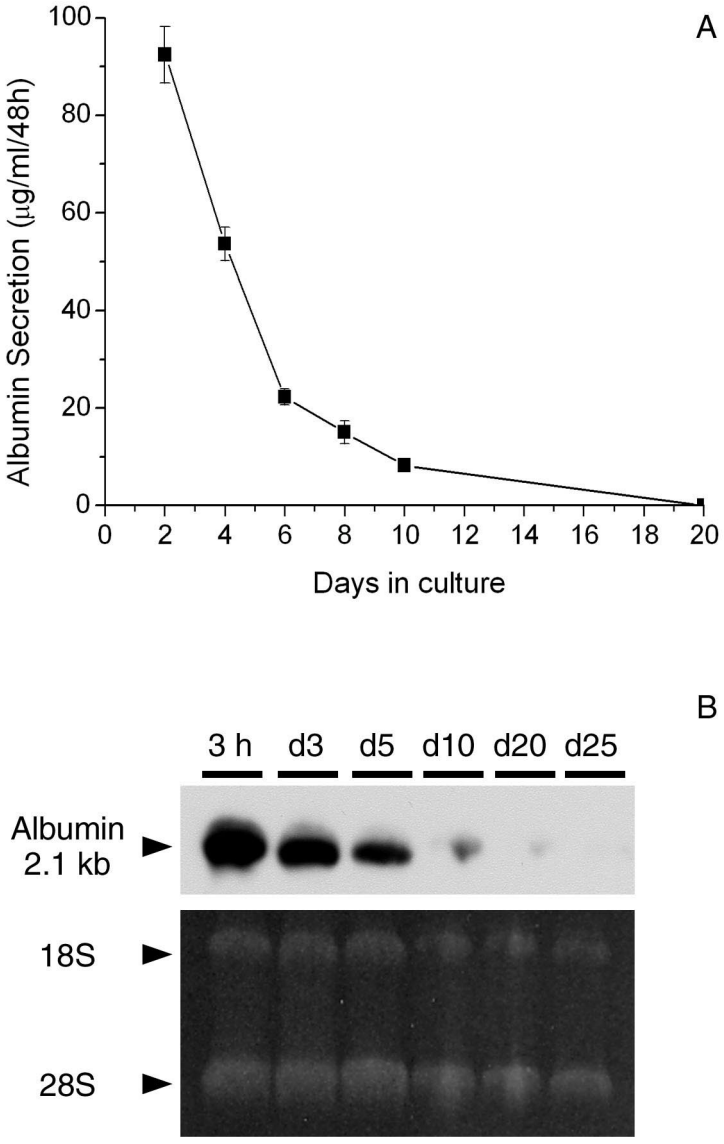


Fig. 1-6 Albumin production and its mRNA transcription of primary hepatocytes. A: Albumin secretion into culture medium by primary hepatocytes (Sudo, unpublished data). Hepatocytes were isolated from a rat liver and cultured on collagen coated dishes with modified DMEM containing 2% DMSO. B: Northern blot analysis for albumin mRNAs of the cells 3 hours, 3, 5, 10, 20, 25 days after inoculation. For each lane, 10 μg of total RNA was applied and hybridized with cDNA probe after blotting.

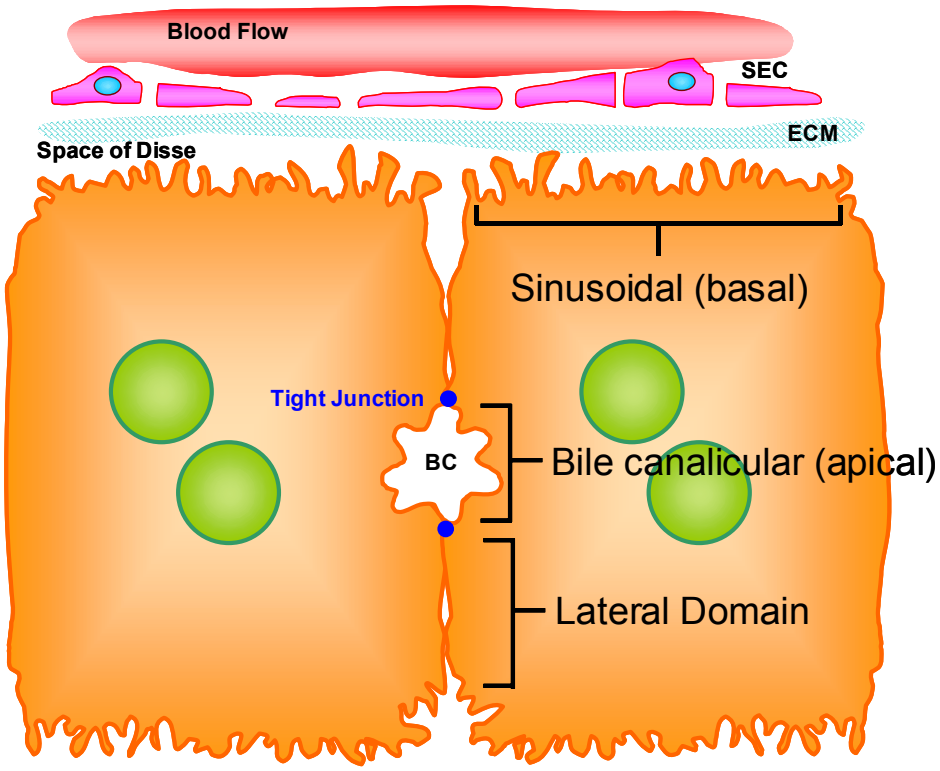


Fig. 1-7 Hepatocyte surface polarity. Membranes of hepatocytes are specialized into 3 functional domains: bile canalicular (other name of apical), sinusoidal (other name of basal) and lateral. The bile canalicular domains of adjacent hepatocytes form a bile canaliculus (BC), a tubular pathway of bile. The BC is about 1 μm in diameter and has luminal microvilli. Tight junctions seal the BC and separate the bile canalicular domain from the lateral domains. The lateral domain is specialized for cell attachments and cell–cell communication. The sinusoidal domain faces the space of Disse, which is minute gap between hepatocytes and SECs and contains sparse ECM. The domain is specialized for the exchange of metabolites with the blood.

## 1-5 Hepatic stem/progenitor cells

Although hepatocytes have great potential for replication in liver regeneration, primary hepatocytes are unable to maintain their specific functions in culture. For the reconstruction of hepatic organoids and hepatocyte transplantations, several kinds of hepatic stem/progenitor cells, such as hepatoblasts, oval cells, bone marrow-derived cells and embryonic stem (ES) cells, have been found in previous studies (Mitaka, 2001, 2002; Fausto, 2004; Alison *et al.*, 2004).

In the embryo, the liver develops as an endodermal evagination from the wall of the foregut to form the hepatic diverticulum. Endodermal-derived hepatoblasts are hepatic stem cells that exist in the liver during development because the cells have bipotential capabilities that give rise to mature hepatocytes (MHs) and BECs. The hepatoblasts express albumin and α-fetoprotein (AFP). In a recent study, Kubota *et al.* (2000) have described bipotential progenitors that could be isolated by a fluorescent-activated cell sorter (FACS) using cell-surface makers, such as intercellular adhesion molecule 1 (ICAM-1) and $RT1A^{1}$, rat classical major histocompatability complex (MHC) class I. They believed that fetal hepatic population could be separated from hematopoietic cell populations by MHC class I expression because adult bone marrow cells other than mature erythrocytes strongly express the MHC class I molecule. In their study, they concluded that hepatoblasts in fetal day 13 in rat livers could be identified as an $RT1A^{1-}$ $OX18^{low}$ $ICAM\text{-}1^{+}$ population. On the other hand, bipotential progenitors were also isolated from a fetal day 13.5 mouse liver. Suzuki *et al.* (2000) believed that a progenitor population could be isolated using markers such as integrins α6 (CD49f) and β1 (CD29), because laminin, a ligand of the α6β1 integrin complex, is expressed in the fetal liver and its expression diminishes with maturation. In their study, $c\text{-}Kit^{-}$ $CD49f^{+}$ $CD29^{+}$ $CD45^{-}$ $TER119^{-}$ cells were isolated using FACS, and the cells that gave rise to a colony containing more than 100 cells were termed hepatic colony-forming units in culture (H-CFU-C). H-CFU-C generated large colonies that exhibited differentiation into albumin-positive hepatocyte and cytokeratin (CK) 19-positive BECs. In a subsequent study, H-CFU-C were further enriched by a selection based on the positivity of c-Met, an HGF receptor (Suzuki *et al.*, 2002). H-CFU-C are considered as a candidate for hepatoblasts in fetal mouse livers.

Although hepatoblasts diminish as development progresses, there are several kinds of cells that can

proliferate and differentiate into both MHs and BECs in adult livers. Oval cells are thought to be the intermediate progeny of hepatic stem cells (Alison *et al.*, 1996). Although oval cells are not present in the liver under physiological conditions, they can be found in certain pathological conditions. When hepatocytes are prevented from proliferating using 2-acetylaminofluorene followed by severe hepatic injury caused by PHx or $CCl_4$ administration, the oval cells are induced inside the smallest branches of the intrahepatic biliary tree in the liver. The oval cells are derived from the canal of Hering, an intermediary tubular structure between BC and bile ducts (Paku *et al.*, 2001), and the cells are positive for markers of BECs (CK 7 and 19) and immature hepatocyte (AFP). Therefore, the cells are more similar to BECs than MHs.

Bone marrow-derived cells also have potential to differentiate into hepatocytes. In terms of a similarity between bone marrow and the liver, the fetal liver is the major site of hematopoiesis during embryonic development. In addition, it was reported that the oval cells and hematopoietic stem cells (HSCs) in the bone marrow had common cell-surface markers, such as c-kit (Fujio *et al.*, 1994), CD34 (Omori *et al.*, 1997) and Thy-1 (Petersen *et al.*, 1998). These findings let us surmise that the oval cells could be derived from bone marrow. Petersen *et al.* (1999) first demonstrated that bone marrow-derived cells initiated development of oval cells and had the capability to differentiate into hepatocytes. Another groups also confirmed the plasticity of the stem cells that were derived from the bone marrow in mice and even in humans (Theise *et al.*, 2000a, b; Alison *et al.*, 2000). Subsequent studies have revealed that bone marrow contained two types of stem cells, HSCs and mesenchymal stem cells that were termed multipotent adult progenitor cells (MAPCs). Laggase *et al.* (2000) reported that an intravenous injection of bone marrow cells in a fumarylacetoacetate hydrolase knockout mouse, an animal model of progressive liver failure, revived the mouse. They also enriched HSCs in the bone marrow by FACS using 13 distinct cell-surface makers and showed that the purified HSCs gave rise to hepatic regeneration. Jiang *et al.* (2002) reported that MAPCs derived from bone marrow could differentiate not only into mesenchymal cells but also into cells with mesoderm, ectoderm and endoderm characteristics *in vitro*.

In a recent study, single HSC was transplanted into lethally irradiated mice and it showed that the transplanted cell did not contribute appreciably to non-hematopoietic tissues including the liver (Wagers *et al.*, 2002). The results indicate that the transdifferentiation of HSCs is an extremely rare event; cell fusion

between hepatocytes and bone marrow derived cells was also reported and therefore stem cell plasticity must be considered controversial (Terada *et al.*, 2002; Wang *et al.*, 2003; Vassilopoulos *et al.*, 2003).

Side population (SP) cells are one kind of HSCs, which has been isolated using a new method based on the ability to efflux the fluorescent DNA binding vital dye, Hoechst 33342 (Goodell *et al.*, 1996). The cells can be isolated by collecting low Hoechst-staining cells by FACS without using cell-surface markers. The dye efflux ability proved to be mediated by a multidrug resistance protein (mdr) because the formation of the Hoechst SP profile was eliminated by the pre-treatment of the cells with verapamil, an inhibitor of mdr. Using a similar purification method, SP cells from muscles were also isolated in mice (Gussoni *et al.*, 1999). Their results suggested that the dye efflux ability might be associated with the characteristics of stem/progenitor cells not only in the bone marrow but also in many tissues. In a recent study, SP cells isolated from a murine liver were directly injected into the recipient liver in which parenchymal-cell-driven regeneration was severely inhibited by treatment with 3, 5-diethocycarbonyl-1, 4-dihydrocollidine (DDC), and then it was shown that the injected cells were involved in liver regeneration (Wulf *et al.*, 2003). It was also shown that bone marrow SP cells contributed to the restoration of liver SP cells after the DDC treatment, which suggests the flow of stem cells from the bone marrow to the liver.

ES cells are pluripotent cells derived from the inner cell mass of the blastocysts that can indefinitely proliferate retaining an undifferentiated state and differentiate to all cell lineages *in vivo*. Differentiation of mouse and human ES cells into hepatocytes was also reported in a recent study (Yamamoto *et al.*, 2003; Rambhatla *et al.*, 2003), but the application of ES cells to research and therapeutics is encumbered by ethical considerations. In a recent study, the transdifferentiation ability of umbilical cord cells was also reported, Newsome *et al.* (2003) isolated mononuclear cells from human cord blood and infused them into sublethally irradiated nonobese diabetic severe combined immunodeficient (NOD-SCID) mice. The results showed that the infused cells had a capability to graft into a NOD-SCID liver and transdifferentiate into hepatocytes.

The several kinds of stem cells investigated in previous studies were summarized in the schematic diagram (Fig. 1-8). Also shown in Fig. 1-8, there is another hepatic progenitor cell that exists in the adult liver, and that was used in the experiments described in the following chapters.

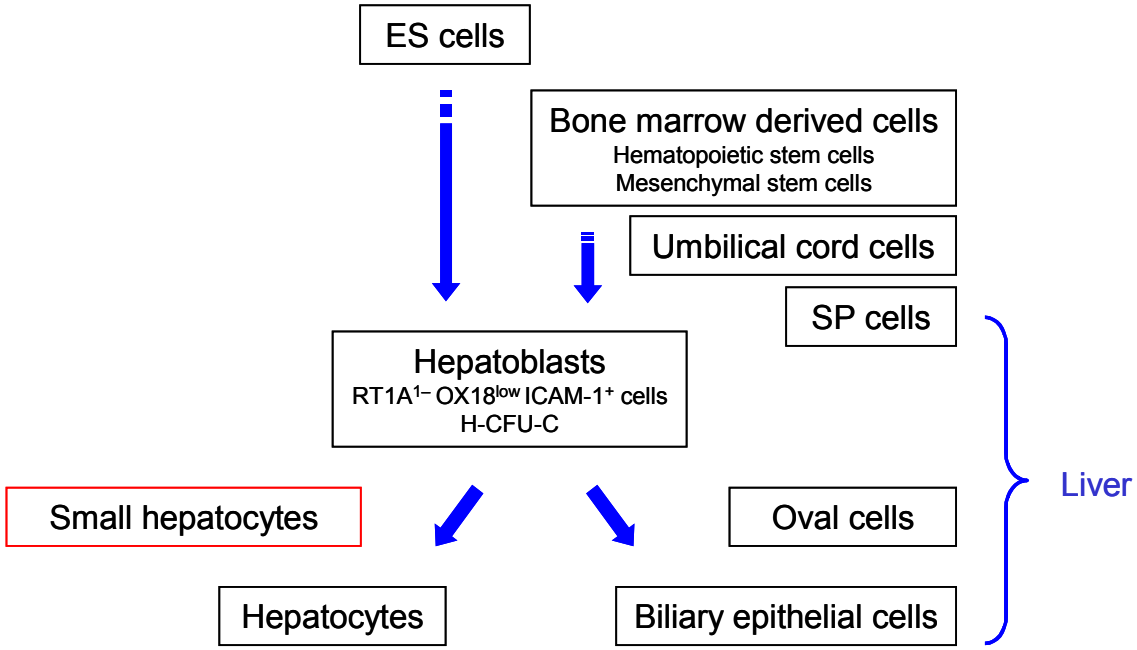


Fig. 1-8 Schematic diagram of hepatic stem/progenitor cells. For detail descriptions of each type of cells except for small hepaotcytes, see the section 1-5: stem/progenitor cells for the tissue engineered liver.

## 1-6 Small hepatocytes

Although the culture conditions of primary hepatocytes have been gradually improved, the number of adult rat hepatocytes could not be sufficiently increased, which led to the conclusion that primary hepatocytes cannot proliferate *in vitro*. Mitaka *et al.* (1992a) found that small mono-nucleate cells proliferated and formed colonies among primary hepatocytes cultured in a serum-free medium supplemented with 10 mM nicotinamide and 10 ng/ml EGF (Fig. 1-9). Immunocytochemistry for hepatocyte-markers showed that the small cells were positive for albumin, transferrin, CK 8 and 18. Transmission electron microscopy (TEM) revealed that the cells had abundant mitochondria, peroxisomes with crystalline nucleoids in their cytoplasm (Mitaka *et al.*, 1992b). These results suggest that the newly developed cells have typical characteristics of MHs. These mono-nucleate cells are different in size from MHs; approximately 1/2–1/3 that of MHs under phase-contrast microscopy. Therefore, these cells are called small hepatocytes (SHs). The sizes of SHs and MHs were further analyzed according to their autofluorescence and granularity using FACS (Tateno *et al.*, 2000). The sorted cells were inoculated on hydrophobic dishes, and their diameters were measured. The results also showed that proliferative hepatocytes are smaller (about 17 μm in diameter) than MHs (about 24 μm in diameter). At this point, SHs are thought to be one kind of hepatic progenitor cells present in adult livers.

Although SHs are found within cultured MHs, moderately purified SHs have been cultured in subsequent studies. A single SH clonally proliferated and finally formed a colony consisting of several hundred cells (Fig. 1-10; Mitaka *et al.*, 1995). SHs also have a capability to reconstruct hepatic organoids with the culture time (Mitaka *et al.*, 1999). The schematic diagram shown in Fig. 1-11 summarizes the reconstruction of hepatic organoids by SHs and NPCs. SHs start to proliferate by day 3 and form colonies within 10 days. Hepatic NPCs such as stellate cells and liver epithelial cells (LECs) also proliferate and surround the SH colonies. Thereafter, the NPCs invade under the colonies and accumulate ECM, type I and IV collagens and laminin. The accumulation of ECM and the formation of a basement membrane-like structure generate the maturation of SHs. The differentiated hepatocytes possess a cuboidal cell shape and form BC between adjacent cells. Finally, SH colonies get overlayed by NPCs, and duct- or cyst-like structures are formed among the reconstructed structures. Thus, SHs can reconstruct hepatic organoids

interacting with NPCs and ECM.

Although SHs have the potential to reconstruct hepatic organoids, it is also necessary to understand the mechanism of their maturation so that organoid formation can be controlled. Sugimoto *et al.* (2002) demonstrated that the maturation of SHs was induced by treatment with Matrigel, a reconstituted basement membrane gel prepared from Engelbreth-Holm-Swarm sarcoma-derived matrix. When SHs were covered with Matrigel, they dramatically changed their shape within several days. The treated cells grew and formed a piled-up shape, morphologically similar to MHs. BC were also formed between the piled-up cells. The alteration of the cell shape was correlated with the maturation of SHs. The cells treated with Matrigel expressed liver-enriched transcription factors (LETFs), such as hepatic nuclear factor (HNF) 4α, HNF 6 and C/EBPα as well as tryptophan 2, 3-dioxygenase (TO) and serine dehydratase (SDH), considered to be markers of terminal hepatic maturation. These results suggest that components of basement membrane, such as laminin and type IV collagen, induce the maturation of SHs. Harada *et al.* (2003) reported that culturing SHs in collagen sponges enhanced the formation of hepatic organoids. In their experiment, SH colonies were collected and re-plated on the absorbable collagen hemostatic sponge used for surgical procedure. Culturing the cells on collagen sponge caused increases in albumin secretion and production of hepatic proteins, such as transferrin, haptoglobin, fibrinogen, carbamoylphosphate synthetase I and cytochrome P450 1A1. BC were formed in the cells, and CK 19-positive duct-like structures were observed within the sponge. These results suggest that three-dimensional (3D) conditions of the cells and cell–ECM interactions are important for the reconstruction of the hepatic organoid. Some knowledge about the reconstruction of the hepatic organoid exists. However, the further mechanism of the maturation of SHs and the interaction with NPCs and ECM for the reconstruction of well-assembled hepatic organoids, the mimic of the liver *in vivo*, is not yet fully understood.

The population of SHs varies according to the age of rats (Mitaka *et al.*, 1993). The population in 4–5-week-old rat livers is estimated to be about 6%, and in 6–8-week-old ones about 2.5%. The number of the cells decreases as they get older. In adult rats, the population is estimated to be 1.5–2.0% of hepatocytes. SHs can be found in adult human livers as well as in rats (Hino *et al.*, 1999). SHs were isolated from normal human liver tissues and inoculated on collagen-coated surfaces. The cells were cultured in DMEM supplemented with 20 mM 2-[4-(2-hydroxyethyl)-1-piperazinyl] ethanesulfonic acid (HEPES), 15 mg/l

L-proline, 0.25 mg/l insulin, $5 \times 10^{-8}$ M dexamethasone, 44 mM $NaHCO_3$, 10 mM nicotinamide, 5 ng/ml EGF, 0.1 mM Asc2P, 5% fetal bovine serum (FBS), 10% freshly prepared normal human serum, 50% conditioned medium derived from Swiss 3T3 cells and antibiotics. The conditioned medium contained pleiotrophin, a potent mitogen for hepatocytes (Sato *et al.*, 1999). The cells steadily replicated and formed colonies. They were cultured for at least 70 days and retained hepatic differentiation markers, such as albumin and α1-antitrypsin.

The cryopreservation of SHs was reported in a recent study (Ikeda *et al.*, 2002). SHs were cultured for 12–15 days and SH colonies were collected using two solutions: first, Hank's balanced salt solution supplemented with 0.02% ethylene diamine tetraacetic acid (EDTA); second, cell dissociation solution (Sigma-Aldrich). The collected colonies were then stored at –80°C for more than 6 months. Rates of attachment on dishes after thawing were about 60%, and the cryopreserved colonies attached on the dishes and then proliferated. The proliferating cells maintained hepatic functions, albumin secretion, transferrin production and TO expression. These results suggest the potential of SHs to use the cryopreserved cells for cell transplantations and a bioartificial liver (BAL).

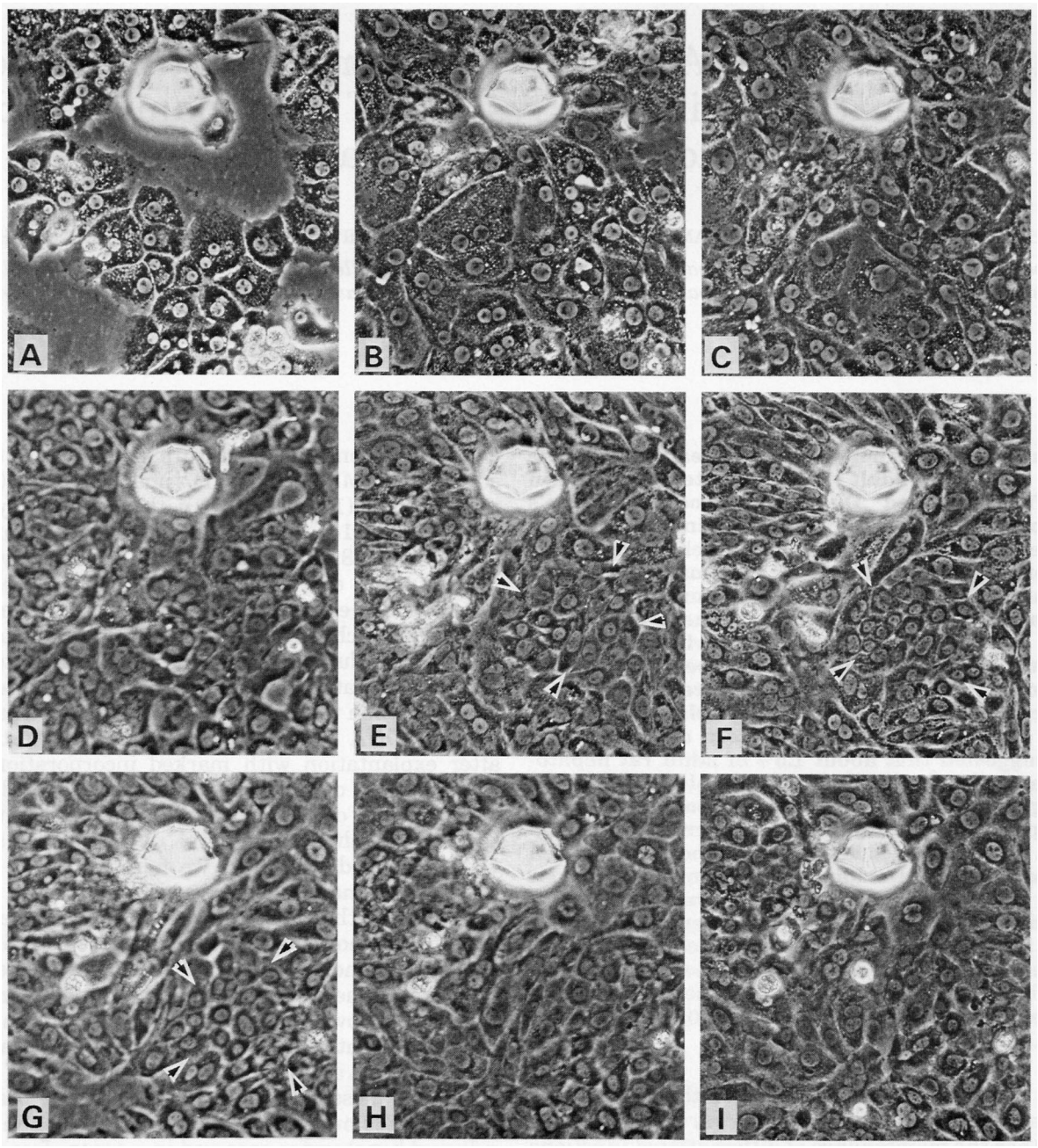


Fig. 1-9 Phase-contrast micrographs of the proliferating cells within primary hepatocytes (Mitaka *et al.*, 1992a). Cells were cultured in modified DMEM supplemented with 10 mM nicotinamide and 10 ng/ml EGF. From day 4 (4 days after inoculation), DMSO was added to the medium at a final concentration of 2%. The same field, marked by a needle, was photographed at day 1–9 (A–I). Small mono-nucleate cells form a colony (arrowheads, E–G).

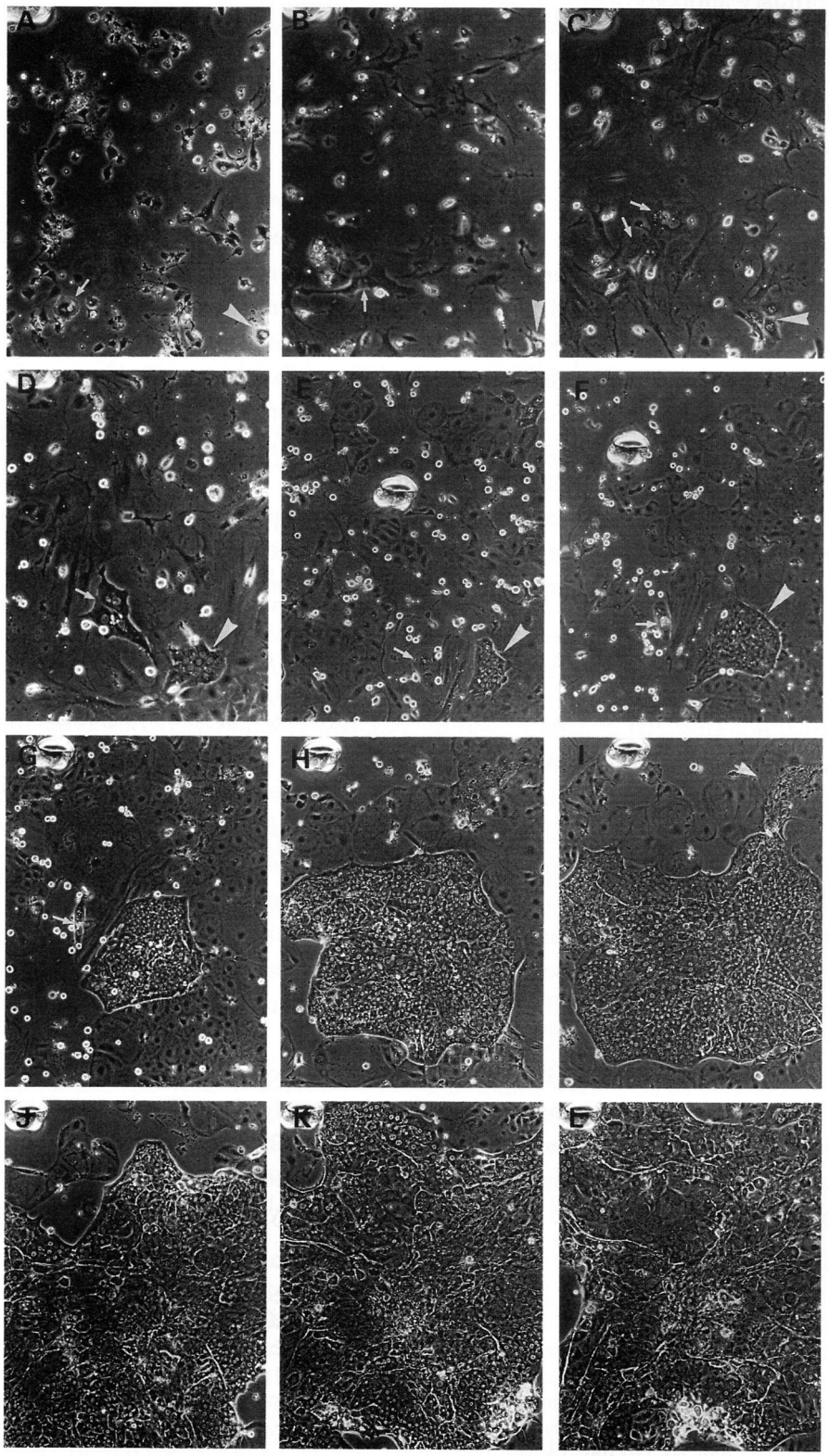


Fig. 1-10 The formation of SH colony (Mitaka *et al.*, 1995). A–L: The cells were cultured in DMEM supplemented with 10 mM nicotinamide, 10% FBS, 1 mM Asc2P, 10 ng/ml EGF and 1% DMSO (after 4 days in culture), and photographed at days 1, 3, 4, 6, 10, 14, 18, 27, 31, 40, 52, 62 (A–D, ×70; E–L, ×48). Single SH proliferates and finally forms a colony consisted of several hundred cells.

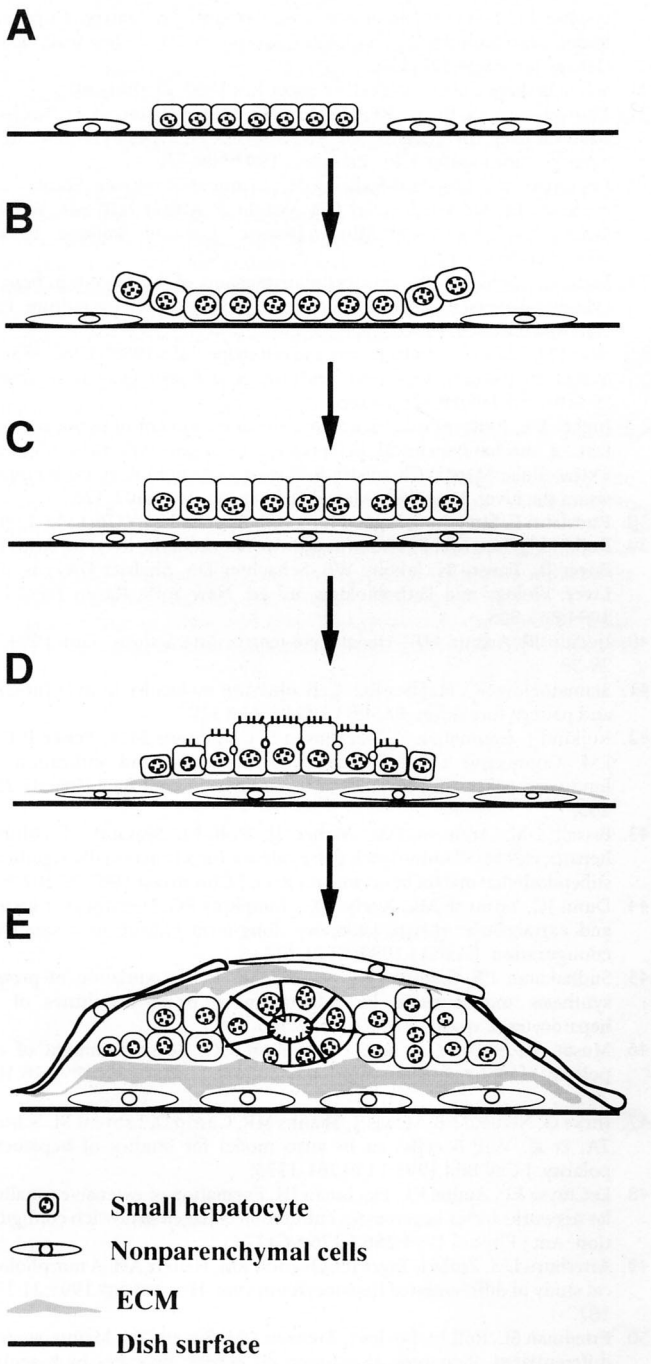


Fig. 1-11 Schematic diagram of hepatic organoid-reconstruction by SHs and NPCs (Mitaka *et al.*, 1999). For detail description of the reconstruction process see the section 1-6: small hepatocytes.

## 1-7 The bioartificial liver

Although the liver can regenerate after hepatic injury, when damaged by chronic conditions, normal regeneration is not possible. Liver transplantation is the only effective therapy in the case of end-stage liver diseases. Many patients suffer from liver diseases all over the world, so, the shortage of donor livers is a serious issue. Patients with chronic liver diseases, such as fibrosis and cirrhosis, are waiting for a liver, and some with acute liver failure will die without a transplantation. There is threore a strong need for the development of BAL.

The most important function of the BAL bioreactor is detoxification of ammonia, because ammonia-increase in the blood (hyperammonemia) is toxic to the central nervous system and causes hepatic encephalopathy. In the early stages of BAL development, non-biomaterials, such as dialysis membranes, activated charcoals and ion-exchange resins, were used for detoxification (Hui *et al.*, 2001). However, they could not function due to their limited absorption of non-biomaterials. These materials absorbed useful ingredients from the blood as well as the toxicants. Development in primary culture of hepatocytes made it possible to use them instead of non-biomaterials. Many researchers have developed a BAL bioreactor by combining freshly isolated hepatocytes and certain reactors (Strain *et al.*, 2002). Patient's plasma is circulated extracorporeally through the bioreactor that houses hepatocytes. The hepatocytes interact with the plasma through semi-permeable membranes. They detoxify chemicals in the plasma, and their metabolites are returned (Fig. 1-12).

Many BAL bioreactors have been developed and tested using experimental animals with acute liver failure (Gerlach *et al.*, 1995; Sussman *et al.*, 1992; Rozga *et al.*, 1993; Funatsu *et al.*, 2001). The first clinical study utilizing a BAL bioreactor loaded with the suspension of isolated hepatocytes was performed by Matsumura *et al.* (1987). They used a BAL bioreactor loaded with cryopreserved rabbit hepatocytes on a patient with hepatic failure due to an inoperable bile duct carcinoma, and the treatment resulted in a decrease in the patient's serum bilirubin level. Other groups subsequently carried out clinical trials using the BAL bioreactors loaded with human hepatoma cell lines or primary porcine hepatocytes in patients waiting for transplants (Demetriou *et al.*, 2004; Ellis *et al.*, 1996; Sauer *et al.*, 2003; Sussman *et al.*, 1994; Watanabe *et al.*, 1997). Although some encouraging results were shown in these studies, the efficacy of the

BAL treatment needs further work.

In addition to the design of the bioreactors, the cell sources are also important. Although porcine hepatocytes have been mainly used as a cell source of BAL bioreactors, there is still an ongoing debate about the risk of cross-species transmission of porcine endogenous retrovirus (Patience *et al.*, 1997; Paradis *et al.*, 1999; Pitkin *et al.*, 1999). Kobayashi *et al.* (2000) reported that intrasplenic transplantation of reversibly immortalized human hepatocytes enabled rats to recover from acute liver failure induced by 90% hepatectomy. They controlled the expansion of the cells using a unique technique, Cre-loxP site-specific recombination system targeting human hepatocytes. The reversibly immortalized hepatocyte is one cell source for BAL bioreactors.

Thus, the BAL bioreactor has been developed as a device to support liver function to maintain the patient's liver before a transplantation (Strain *et al.*, 2002). Because the present goal of BAL is to develop it as a bridging unit, it cannot resolve the donor organ shortage. The ultimate goal is to regenerate hepatic tissues *in vitro* that can be used as alternatives to the BAL bioreactor (Mitaka, 2002). We should develop a tissue-engineered liver as well as the BAL bioreactor by combining an appropriate cell source and tissue engineering.

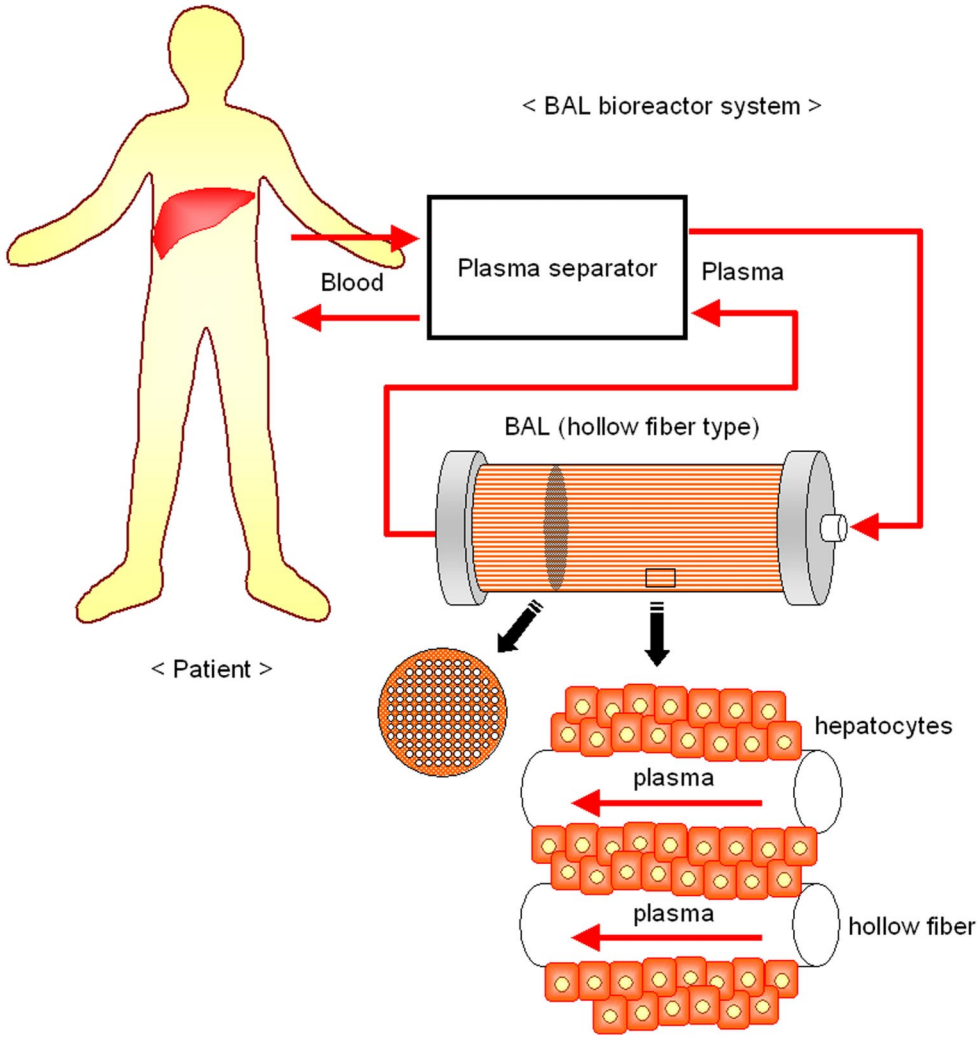


Fig. 1-12 Schematic diagram of the hollow fiber type BAL bioreactor system.

## 1-8 Objectives

This thesis deals with self-organization. Self-organization is a process where the organization of a system increases spontaneously. If we can understand how the organization works in various phenomena, the principle of self-organization can be widely applied in designing artificial systems. From this point of view life is an endless system to search for the principle of self-organization. The liver, in particular, seems to be a good model for the understanding of self-organization, because it regenerates spontaneously to recover lost tissue. It is a typical self-organizing system that can reconstruct tissues with increase in the organization during its regeneration.

A tissue-engineered liver needs to be developed as an alternative method to liver transplantation. Although liver regeneration cannot be produced *in vitro* but only as a potential *in vivo*, several stem/progenitor cells have been discovered in recent studies. The combination of certain cell types and appropriate culture conditions, such as growth factor, ECM and surface topology, will make it possible to reconstruct hepatic organoids *in vitro*. We should consider how the self-organization potential of cells for tissue regeneration can be enhanced.

This thesis focuses on the reconstruction of hepatic organoids by rat SHs and NPCs. SHs were used as a cell source because they retain their capabilities for proliferation and differentiation in culture. The cells start to proliferate 2–3 days after inoculation and then form colonies within 10 days. Some SHs differentiate into MHs that have large cytoplasm and two nuclei. BC-like structures are then formed between the differentiated SHs. In terms of hepatic tissue regeneration, these BC-like structures are extremely important. BC cannot be formed by a single hepatocyte because adjacent hepatocytes share their partial membranes to form BC. In addition, an important function of BC is to excrete the metabolites of hepatocytes. Therefore, BC are highly differentiated structures and their formation is essential in the reconstruction of hepatic organoids. They were studied whether BC-like structures functioned like BC *in vivo* and how SHs possessed differentiated functions with morphological and physiological changes, such as BC formation and repolarization. This was followed by establishing the tissue-level function of the BC. *In vivo*, hepatocytes secrete bile into BC and the secreted bile is transported to bile ducts. To transport the contents of the BC, groups of hepatocytes need to move in a coordinated manner. It is investigated whether

there is any coordination among the SHs that formed BC in the transport of their contents. The analyses of the BC movements were done.

Hepatocytes retain their specific functions by extending three-dimensionally in the liver. The appropriate 3D configuration of the cells seems to be important to the enhancement of their function. Therefore, a 3D culture method was developed. SHs were cultured on microporous membranes and stacked, to develop 3D stacked-up structures. The stacked cells may then attach to each other and form tissues. In order to evaluate the organization of the cells in the 3D stacked-up structures, it was ascertained whether the cells adhered to each other, formed BC in the attached portions, and increased their liver-specific functions.

Thus, tissue organization and cellular functions were investigated in the reconstruction of hepatic organoids. The structure of the reconstructed BC is first investigated in chapter 3. Then, the tissue-level functions of the BC networks are established in chapter 4. In chapter 5, the organization of the cells and BC formation are investigated in the 3D culture of SHs. Finally, these studies are summarized and the conclusions are described in chapter 6.

## References

Alison MR, Golding MH, Sarraf CE. Pluripotential liver stem cells: facultative stem cells located in the biliary tree. Cell Prolif. 1996;29:373–402.

Alison MR, Poulsom R, Jeffery R, Dhillon AP, Quaglia A, Jacob J, Novelli M, Prentice G, Williamson J, Wright NA. Hepatocytes from non-hepatic adult stem cells. Nature. 2000;406:257.

Alison MR, Vig P, Russo F, Bigger BW, Amofah E, Themis M, Forbes S. Hepatic stem cells: from inside and outside the liver? Cell Prolif. 2004;37:1–21.

Berry MN, Friend DS. High-yield preparation of isolated rat liver parenchymal cells: A biochemical and fine structural study. J Cell Biol. 1969;43:506–520.

Bissell DM, Hammaker LE, Meyer UA. Parenchymal cells from adult rat liver in nonproliferating monolayer culture I. Functional studies. J Cell Biol. 1973;59:722–734.

Braet F, Luo D, Spector I, Vermijlen D, Wisse E. Endothelial and Pit cells. In: The liver: biology and pathobiology, 4th edition, edited by Arias IM, Boyer JL, Chisari FV, Fausto N, Schachter D, Shafritz DA. Philadelphia, PA: Lippincott Williams & Wilkins, 2001:437–454.

Demetriou AA, Brown RS Jr, Busuttil RW, Fair J, McGuire BM, Rosenthal P, Am Esch JS 2nd, Lerut J, Nyberg SL, Salizzoni M, Fagan EA, de Hemptinne B, Broelsch CE, Muraca M, Salmeron JM, Rabkin JM, Metselaar HJ, Pratt D, De La Mata M, McChesney LP, Everson GT, Lavin PT, Stevens AC, Pitkin Z, Solomon BA. Prospective, randomized, multicenter, controlled trial of a bioartificial liver in treating acute liver failure. Ann Surg. 2004;239:660–670.

Fausto N. Liver regeneration. In: The liver: biology and pathobiology, 4th edition, edited by Arias IM, Boyer JL, Chisari FV, Fausto N, Schachter D, Shafritz DA. Philadelphia, PA: Lippincott Williams & Wilkins, 2001:591–610.

Fausto N. Liver regeneration. J Hepatol. 2000;32 Suppl:19–31.

Fausto N. Liver regeneration and repair: hepatocytes, progenitor cells, and stem cells. Hepatology. 2004;39:1477–1487.

Fawcett DW. A textbook of histology, 12th edtion. New York, NY: Chapman & Hall, 1994:652–688.

Fujio K, Evarts RP, Hu Z, Marsden ER, Thorgeirsson SS. Expression of stem cell factor and its receptor,

c-kit, during liver regeneration from putative stem cells in adult rat. Lab Invest. 1994;70:511–516.

Funatsu K, Ijima H, Nakazawa K, Yamashita Y, Shimada M, Sugimachi K. Hybrid artificial liver using hepatocyte organoid culture. Artif Organs. 2001;25:194–200.

Gerlach JC, Schnoy N, Encke J, Smith MD, Muller C, Neuhaus P. Improved hepatocyte in vitro maintenance in a culture model with woven multicompartment capillary systems: electron microscopy studies. Hepatology. 1995;22:546–552.

Goodell MA, Brose K, Paradis G, Conner AS, Mulligan RC. Isolation and functional properties of murine hematopoietic stem cells that are replicating in vivo. J Exp Med. 1996;183:1797–1806.

Gussoni E, Soneoka Y, Strickland CD, Buzney EA, Khan MK, Flint AF, Kunkel LM, Mulligan RC. Dystrophin expression in the mdx mouse restored by stem cell transplantation. Nature. 1999;401:390–394.

Harada K, Mitaka T, Miyamoto S, Sugimoto S, Ikeda S, Takeda H, Mochizuki Y, Hirata K. Rapid formation of hepatic organoid in collagen sponge by rat small hepatocytes and hepatic nonparenchymal cells. J Hepatol. 2003;39:716–723.

Howard RB, Pesch LA. Respiratory activity of intact, isolated parenchymal cells from rat liver. J Biol Chem. 1968;243:3105–3109.

Higgins GM, Anderson RM. Experimental pathology of the liver. I. Restoration of the liver of the white rat following partial surgical removal. Arch Pathol. 1931;12:186–202.

Hino H, Tateno C, Sato H, Yamasaki C, Katayama S, Kohashi T, Aratani A, Asahara T, Dohi K, Yoshizato K. A long-term culture of human hepatocytes which show a high growth potential and express their differentiated phenotypes. Biochem Biophys Res Commun. 1999;256:184–191.

Hui T, Rozga J, Demetriou AA. Bioartificial liver support. J Hepatobiliary Pancreat Surg. 2001;8:1–15.

Ikeda S, Mitaka T, Harada K, Sugimoto S, Hirata K, Mochizuki Y. Proliferation of rat small hepatocytes after long-term cryopreservation. J Hepatol. 2002;37:7–14.

Inoue C, Yamamoto H, Nakamura T, Ichihara A, Okamoto H. Nicotinamide prolongs survival of primary cultured hepatocytes without involving loss of hepatocyte-specific functions. J Biol Chem. 1989 25;264:4747–4750.

Isom HC, Secott T, Georgoff I, Woodworth C, Mummaw J. Maintenance of differentiated rat hepatocytes in

primary culture. Proc Natl Acad Sci U S A. 1985;82:3252–3256.

Jiang Y, Jahagirdar BN, Reinhardt RL, Schwartz RE, Keene CD, Ortiz-Gonzalez XR, Reyes M, Lenvik T, Lund T, Blackstad M, Du J, Aldrich S, Lisberg A, Low WC, Largaespada DA, Verfaillie CM. Pluripotency of mesenchymal stem cells derived from adult marrow. Nature. 2002;418:41–49.

Kobayashi N, Fujiwara T, Westerman KA, Inoue Y, Sakaguchi M, Noguchi H, Miyazaki M, Cai J, Tanaka N, Fox IJ, Leboulch P. Prevention of acute liver failure in rats with reversibly immortalized human hepatocytes. Science. 2000;287:1258–1262.

Kuiper J, Brouwer A, Knook DL, Van Berkel TJ. In: The liver: biology and pathobiology, 3rd edition, edited by Arias IM, Boyer JL, Fausto N, Jakoby WB, Schachter D, Shafritz DA. New York, NY: Raven Press, 1994:791–818.

Lagasse E, Connors H, Al-Dhalimy M, Reitsma M, Dohse M, Osborne L, Wang X, Finegold M, Weissman IL, Grompe M. Purified hematopoietic stem cells can differentiate into hepatocytes in vivo. Nat Med. 2000;6:1229–1234.

Li D, Friedman SL. Hepatic stellate cells: Morphology, function, and regulation. In: The liver: biology and pathobiology, 4th edition, edited by Arias IM, Boyer JL, Chisari FV, Fausto N, Schachter D, Shafritz DA. Philadelphia, PA: Lippincott Williams & Wilkins, 2001:455–468.

Marceau N, Goyette R, Valet JP, Deschenes J. The effect of dexamethasone on formation of a fibronectin extracellular matrix by rat hepatocytes in vitro. Exp Cell Res. 1980;125:497–502.

Martinez-Hernandez A, Amenta PS. The extracellular matrix in hepatic regeneration. FASEB J. 1995;9:1401–1410.

Matsumura KN, Guevara GR, Huston H, Hamilton WL, Rikimaru M, Yamasaki G, Matsumura MS. Hybrid bioartificial liver in hepatic failure: preliminary clinical report. Surgery. 1987;101:99–103.

McGowan JA, Strain AJ, Bucher NL. DNA synthesis in primary cultures of adult rat hepatocytes in a defined medium: effects of epidermal growth factor, insulin, glucagon, and cyclic-AMP. J Cell Physiol. 1981;108:353–363.

Michalopoulos GK, DeFrances MC. Liver regeneration. Science. 1997;276:60–66.

Mitaka T. Reconstruction of hepatic organoid by hepatic stem cells. J Hepatobiliary Pancreat Surg. 2002;9:697–703.

Mitaka T, Kojima T, Mizuguchi T, Mochizuki Y. Growth and maturation of small hepatocytes isolated from adult rat liver. Biochem Biophys Res Commun. 1995;214:310–317.

Mitaka T, Mikami M, Sattler GL, Pitot HC, Mochizuki Y. Small cell colonies appear in the primary culture of adult rat hepatocytes in the presence of nicotinamide and epidermal growth factor. Hepatology. 1992a;16:440–447.

Mitaka T, Norioka K, Sattler GL, Pitot HC, Mochizuki Y. Effect of age on the formation of small-cell colonies in cultures of primary rat hepatocytes. Cancer Res. 1993;53:3145–3148.

Mitaka T, Sato F, Mizuguchi T, Yokono T, Mochizuki Y. Reconstruction of hepatic organoid by rat small hepatocytes and hepatic nonparenchymal cells. Hepatology. 1999;29:111–125.

Mitaka T, Sattler GL, Pitot HC, Mochizuki Y. Characteristics of small cell colonies developing in primary cultures of adult rat hepatocytes. Virchows Arch B Cell Pathol Incl Mol Pathol. 1992b;62:329–335.

Mitaka T. Hepatic stem cells: from bone marrow cells to hepatocytes. Biochem Biophys Res Commun. 2001;281:1–5.

Mitaka T. Reconstruction of hepatic organoid by hepatic stem cells. J Hepatobiliary Pancreat Surg. 2002;9:697–703.

Muakkassah-Kelly SF, Bieri F, Waechter F, Bentley P, Staubli W. Long-term maintenance of hepatocytes in primary culture in the presence of DMSO: further characterization and effect of nafenopin, a peroxisome proliferator. Exp Cell Res. 1987;171:37–51.

Nakamura T, Nawa K, Ichihara A. Partial purification and characterization of hepatocyte growth factor from serum of hepatectomized rats. Biochem Biophys Res Commun. 1984;122:1450–1459.

Nakamura T, Teramoto H, Tomita Y, Ichihara A. L-proline is an essential amino acid for hepatocyte growth in culture. Biochem Biophys Res Commun. 1984;122:884–891.

Newsome PN, Johannessen I, Boyle S, Dalakas E, McAulay KA, Samuel K, Rae F, Forrester L, Turner ML, Hayes PC, Harrison DJ, Bickmore WA, Plevris JN. Human cord blood-derived cells can differentiate into hepatocytes in the mouse liver with no evidence of cellular fusion. Gastroenterology. 2003;124:1891–1900.

Omori N, Omori M, Evarts RP, Teramoto T, Miller MJ, Hoang TN, Thorgeirsson SS. Partial cloning of rat CD34 cDNA and expression during stem cell-dependent liver regeneration in the adult rat. Hepatology.

1997;26:720–727.

Paku S, Schnur J, Nagy P, Thorgeirsson SS. Origin and structural evolution of the early proliferating oval cells in rat liver. Am J Pathol. 2001;158:1313–1323.

Paradis K, Langford G, Long Z, Heneine W, Sandstrom P, Switzer WM, Chapman LE, Lockey C, Onions D, Otto E. Search for cross-species transmission of porcine endogenous retrovirus in patients treated with living pig tissue. Science. 1999;285:1236–1241.

Patience C, Takeuchi Y, Weiss RA. Infection of human cells by an endogenous retrovirus of pigs. Nat Med. 1997;3:282–286.

Petersen BE, Bowen WC, Patrene KD, Mars WM, Sullivan AK, Murase N, Boggs SS, Greenberger JS, Goff JP. Bone marrow as a potential source of hepatic oval cells. Science. 1999;284:1168–1170.

Petersen BE, Goff JP, Greenberger JS, Michalopoulos GK. Hepatic oval cells express the hematopoietic stem cell marker Thy-1 in the rat. Hepatology. 1998;27:433–445.

Pitkin Z, Mullon C. Evidence of absence of porcine endogenous retrovirus (PERV) infection in patients treated with a bioartificial liver support system. Artif Organs. 1999;23:829–833.

Rambhatla L, Chiu CP, Kundu P, Peng Y, Carpenter MK. Generation of hepatocyte-like cells from human embryonic stem cells. Cell Transplant. 2003;12:1–11.

Richman RA, Claus TH, Pilkis SJ, Friedman DL. Hormonal stimulation of DNA synthesis in primary cultures of adult rat hepatocytes. Proc Natl Acad Sci U S A. 1976;73:3589–3593.

Ross MH, Kaye GI, Pawlina W. Histology a text and atlas, 4th edition. Philadelphia, PA: Lippincott Williams & Wilkins, 2003:532–563.

Rozga J, Williams F, Ro MS, Neuzil DF, Giorgio TD, Backfisch G, Moscioni AD, Hakim R, Demetriou AA. Development of a bioartificial liver: properties and function of a hollow-fiber module inoculated with liver cells. Hepatology. 199317:258–265.

Sauer IM, Kardassis D, Zeillinger K, Pascher A, Gruenwald A, Pless G, Irgang M, Kraemer M, Puhl G, Frank J, Muller AR, Steinmuller T, Denner J, Neuhaus P, Gerlach JC. Clinical extracorporeal hybrid liver support--phase I study with primary porcine liver cells. Xenotransplantation. 2003;10:460–469.

Sato H, Funahashi M, Kristensen DB, Tateno C, Yoshizato K. Pleiotrophin as a Swiss 3T3 cell-derived potent mitogen for adult rat hepatocytes. Exp Cell Res. 1999;246:152–164.

Seglen PO. Preparation of isolated rat liver cells. Methods Cell Biol. 1976;13:29–83.

Senoo H, Tsukada Y, Sato T, Hata R. Co-culture of fibroblasts and hepatic parenchymal cells induces metabolic changes and formation of a three-dimensional structure. Cell Biol Int Rep. 1989;13:197–206.

Strain AJ, Neuberger JM. A bioartificial liver--state of the art. Science. 2002;295:1005–1009.

Sugimoto S, Mitaka T, Ikeda S, Harada K, Ikai I, Yamaoka Y, Mochizuki Y. Morphological changes induced by extracellular matrix are correlated with maturation of rat small hepatocytes. J Cell Biochem. 2002;87:16–28.

Sussman NL, Chong MG, Koussayer T, He DE, Shang TA, Whisennand HH, Kelly JH. Reversal of fulminant hepatic failure using an extracorporeal liver assist device. Hepatology. 1992;16:60–65.

Sussman NL, Gislason GT, Conlin CA, Kelly JH. The Hepatix extracorporeal liver assist device: initial clinical experience. Artif Organs. 1994;18:390–396.

Ellis AJ, Hughes RD, Wendon JA, Dunne J, Langley PG, Kelly JH, Gislason GT, Sussman NL, Williams R. Pilot-controlled trial of the extracorporeal liver assist device in acute liver failure. Hepatology. 1996;24:1446–1451.

Suzuki A, Zheng Y, Kaneko S, Onodera M, Fukao K, Nakauchi H, Taniguchi H. Clonal identification and characterization of self-renewing pluripotent stem cells in the developing liver. J Cell Biol. 2002;156:173–184.

Suzuki A, Zheng Y, Kondo R, Kusakabe M, Takada Y, Fukao K, Nakauchi H, Taniguchi H. Flow-cytometric separation and enrichment of hepatic progenitor cells in the developing mouse liver. Hepatology. 2000;32:1230–1239.

Tateno C, Takai-Kajihara K, Yamasaki C, Sato H, Yoshizato K. Heterogeneity of growth potential of adult rat hepatocytes in vitro. Hepatology. 2000;31:65–74.

Terada N, Hamazaki T, Oka M, Hoki M, Mastalerz DM, Nakano Y, Meyer EM, Morel L, Petersen BE, Scott EW. Bone marrow cells adopt the phenotype of other cells by spontaneous cell fusion. Nature. 2002;416:542–545.

Theise ND, Badve S, Saxena R, Henegariu O, Sell S, Crawford JM, Krause DS. Derivation of hepatocytes from bone marrow cells in mice after radiation-induced myeloablation. Hepatology. 2000a;31:235–240.

Theise ND, Nimmakayalu M, Gardner R, Illei PB, Morgan G, Teperman L, Henegariu O, Krause DS. Liver

from bone marrow in humans. Hepatology. 2000b;32:11–16.

Vassilopoulos G, Wang PR, Russell DW. Transplanted bone marrow regenerates liver by cell fusion. Nature. 2003;422:901–904.

Wagers AJ, Sherwood RI, Christensen JL, Weissman IL. Little evidence for developmental plasticity of adult hematopoietic stem cells. Science. 2002;297:2256–2259.

Wang X, Willenbring H, Akkari Y, Torimaru Y, Foster M, Al-Dhalimy M, Lagasse E, Finegold M, Olson S, Grompe M. Cell fusion is the principal source of bone-marrow-derived hepatocytes. Nature. 2003;422:897–901.

Watanabe FD, Mullon CJ, Hewitt WR, Arkadopoulos N, Kahaku E, Eguchi S, Khalili T, Arnaout W, Shackleton CR, Rozga J, Solomon B, Demetriou AA. Clinical experience with a bioartificial liver in the treatment of severe liver failure. A phase I clinical trial. Ann Surg. 1997;225:484–93

Wulf GG, Luo KL, Jackson KA, Brenner MK, Goodell MA. Cells of the hepatic side population contribute to liver regeneration and can be replenished with bone marrow stem cells. Haematologica. 2003;88:368–378.

Yamamoto H, Quinn G, Asari A, Yamanokuchi H, Teratani T, Terada M, Ochiya T. Differentiation of embryonic stem cells into hepatocytes: biological functions and therapeutic application. Hepatology. 2003;37:983–993.

# Chapter 2

# Materials and methods

## 2-1 Isolation and culture of small hepatocytes and nonparenchymal cells from the rat (Chapters 3, 4, 5)*

Cells were isolated from male Sprague-Dawley (SD) rats (250–450 g; Nippon Bio-Supp. Center, Tokyo, Japan) and male transgenic SD rats carrying the enhanced green fluorescent protein transgene (EGFP rats; Japan SLC, Shizuoka, Japan), which were established by Okabe *et al.* (1997), using Seglen's (1976) two-step liver-perfusion method with some modifications (Mitaka *et al.*, 1999). A collagenase-digested liver-cell suspension was centrifuged at 50×g for 1 min (Fig. 2-1). The supernatant was centrifuged at 50×g for 5 min, and the pellet was suspended in L-15 medium (Invitrogen, Carlsbad, CA) supplemented with 20 mM HEPES (Dojindo, Kumamoto, Japan), 1.1 g/l galactose (Katayama Chemical, Osaka, Japan), 30 mg/l L-proline, 0.5 mg/l insulin (Sigma-Aldrich, St. Louis, MO), $10^{-7}$ M dexamethasone (Wako Pure Chemical, Tokyo, Japan) and antibiotics. The pellet was re-centrifuged at 50×g for 5 min. Thereafter, it was suspended in the medium and centrifuged at 150×g for 5 min. After this procedure was repeated, the pellet was suspended in the medium and centrifuged at 50×g for 5 min. Finally, the pellet was suspended in DMEM (Sigma-Aldrich) with 20 mM HEPES, 25 mM $NaHCO_3$, 30 mg/l L-proline, 0.5 mg/l insulin, $10^{-7}$ M dexamethasone, 10% FBS, 10 mM nicotinamide (Sigma-Aldrich), 1 mM Asc2P (Wako Pure Chemical), 10 ng/ml EGF (BD biosciences, Bedford, MA) and antibiotics. The number of viable cells was counted using the trypan blue-exclusion test.

The cells were inoculated on culture dishes ($3 \times 10^5$ viable cells/35-mm dish; $6 \times 10^5$ viable cells/60-mm dish; $1.8 \times 10^6$ viable cells/100-mm dish; Corning Glass Works, Corning, NY) coated with rat-tail collagen (50 μg of dried tendon/0.1% acetic acid). For 3D stacked-up culture, the cells were inoculated on 25-mm polycarbonate membranes (Nuclepore® Polycarbonate, Whatman, Clifton, NJ) with a

* Relevant chapters

rated pore size of 12.0 μm, a rated pore density of $1 \times 10^5$ pores/$cm^2$ and a nominal thickness of 8 μm. The membrane was placed in a 35-mm dish (Corning Glass Works, Corning, NY) and coated with rat-tail collagen (50 μg of dried tendon/0.1% acetic acid). The cells were inoculated on 35-mm dishes with the membranes at a cell density of $4.5 \times 10^5$ cells/dish and placed in a humidified, 5% $CO_2$/95% air incubator at 37°C. The medium was changed to remove dead cells 3 hours after inoculation, and was subsequently replaced every other day. After day 4 (96 hours after plating), DMSO (Sigma-Aldrich) was added to the culture medium at the concentration of 1%.

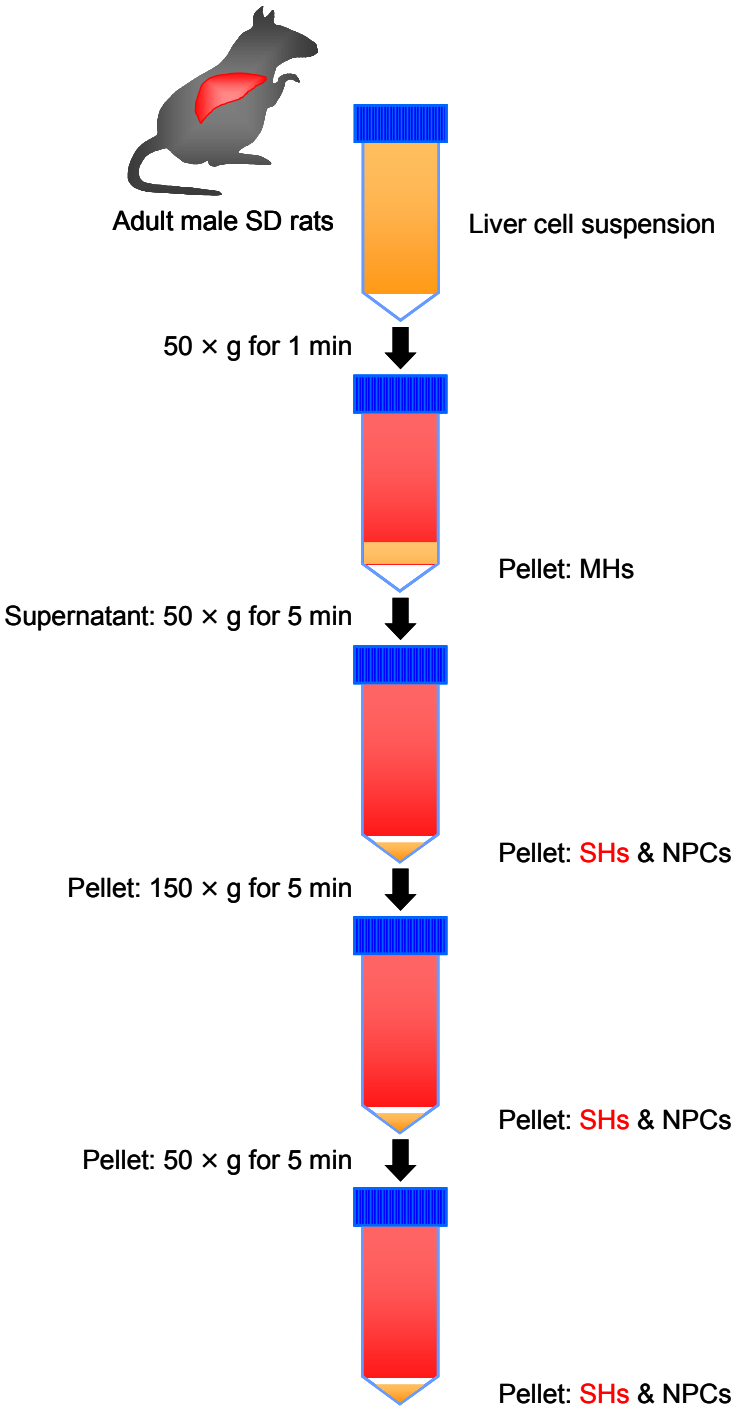


Fig. 2-1 Centrifugation protocol for the separation of SHs and NPCs. For detail description of the cell isolation process see the section 2-1: Isolation and culture of SHs and NPCs from the rat.

## 2-2 Reconstruction of the 3D stacked-up structures (Chapter 5)

In the experiments described in chapter 5, the cells were separately inoculated on pairs of microporous membranes in 35-mm dishes. The SHs were cultured on the membranes for about 20 days to allow them to proliferate and form colonies. Thereafter, four methods of membrane stacking were investigated: first, one membrane was inverted on top of the other, which resulted in the SHs becoming attached to one another (Fig. 2-2A); second, one membrane was stacked on top of the other, which resulted in the membrane being sandwiched between the SHs (Fig. 2-2B); third, one membrane was inverted on top of the cells, which were cultured in another dish (Fig. 2-2C); and fourth, one membrane was stacked on top of the other without reversing (Fig. 2-2D). The method shown in Fig. 2-2A was chosen for use in the following experiments.

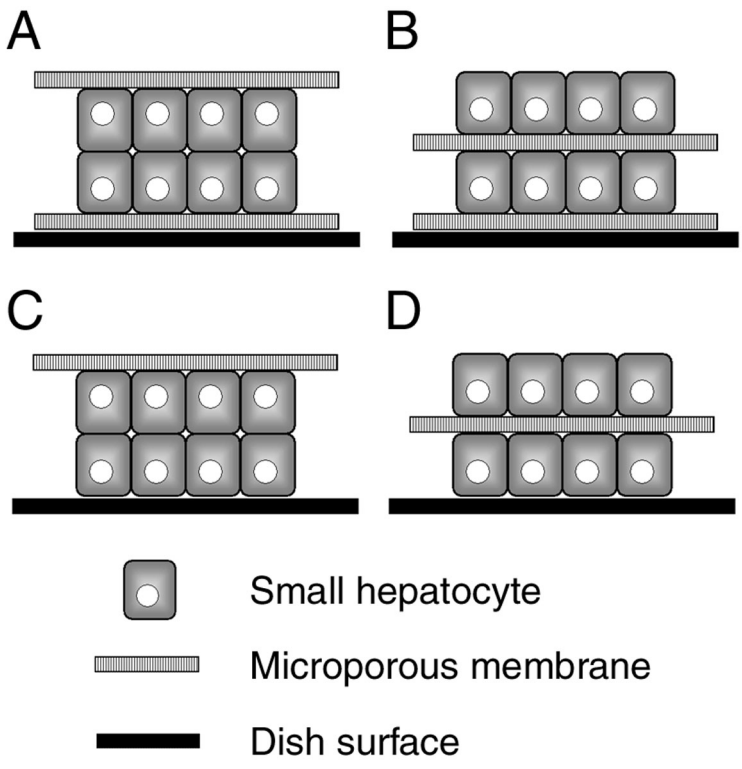


Fig. 2-2 Four different approaches to stack up membranes. Pairs of membranes were prepared for the reconstruction of 3D stacked-up structures. The cells were separately cultured on the membranes for about 20 days in order to form SH colonies. A: One membrane was inverted on top of the other, which resulted in the SHs becoming attached to one another. B: One membrane was stacked on top of the other without reversing the position. C: One membrane was inverted on top of the cells, which were cultured on another dish. D: One membrane was stacked on top of cells that were cultured on another dish, without reversing the position.

## 2-3 Phase-contrast microscopy

### 2-3-1 Photographs and time-lapse movies of cultured cells (Chapter 3)

In the experiments described in chapter 3, cells were photographed on a phase-contrast microscope (Olympus Optical Co., Tokyo, Japan) equipped with a CCD camera (Roper Scientific, Trenton, NJ). To prevent the alkalization of medium during observation, the culture medium was replaced with the fresh L-15 medium. Phase-contrast images of BC-like structures formed in a colony with piled-up cells were recorded at the 20-sec intervals for 2 hours by a phase-contrast microscope (Olympus) equipped with a time-lapse system (Roper Scientific). More than 20 colonies were examined. Four adjacent segments were set in the first image and the average light intensity in each segment was measured. The data were analyzed using the software of IPLab™ (Scanalytics, Billerica, MA).

### 2-3-2 Time-lapse microscopy for the bile canalicular contractions (Chapter 4)

In the experiments described in chapter 4, cells were placed in a humidified 5% CO2/95% air chamber (Sankei, Tokyo, Japan) at 37°C, and photographed using a phase-contrast microscope (TE300; Nikon, Tokyo, Japan) equipped with a CCD camera (Roper Scientific, Trenton, NJ). Images of the BC networks formed in a colony with piled-up cells were recorded at 5-sec intervals for 3 hours. The sequential images (2,160 frames/colony and 17 colonies) were analyzed using the MetaMorph® imaging system (Universal Imaging Corporation™, Downingtown, PA).

## 2-4 Analysis of bile canalicular movements (Chapter 4)

In the experiment described in chapter 4, 17 colonies including well-developed BC networks were photographed using a phase-contrast microscope equipped with a time-lapse device. Measurement of BC movements was based on variations of translucent areas coinciding with BC networks in the sequence of phase-contrast micrographs. To quantify the BC areas, a specific threshold value that distinguished BC from cytoplasm was chosen with reference to translucent belts seen under phase-contrast microscopy. The threshold value was set using the first image of the time-lapse series because pixel intensity of the translucent belts varied in each time-lapse series. The threshold value was adjusted to fit thresholding areas

to the translucent belts. For the quantitative analysis of the BC movement in the time-lapse series, thresholding was applied to the first time-lapse image and the same threshold value of the light intensity was applied to the other sequential images so that consistent thresholding applied. Next, 4 regions of interest (ROIs) were set for each image in the time-lapse series. To investigate the movements of various parts of the BC network, ROIs were randomly placed throughout the colony in the first image, avoiding neighboring cells. The same ROIs were set in the other sequential images of the same time-lapse series. We then measured the thresholding area within each ROI to investigate the width of each BC. The thresholding areas were normalized by dividing the measurement of each time by that of the initial time. Variations of the normalized thresholding areas were compared to analyze the BC movements. Therefore, the results accurately represent BC movements without any biased data. The variations in the thresholding areas reflect the width of the BC. In the experiment that is described in chapter 4, BC in 68 ROIs (4 ROIs/colony and 17 colonies) were analyzed.

To quantify the coordination of BC movements, a correlation coefficient was calculated for each colony. The correlation coefficients between the values of each ROI during the observation period (10 min for fast movements, 30 min for slow movements) were calculated. The correlation coefficient $R_{xy}$ between pairs of the thresholding area in each ROI is given as

$$R_{xy} = \frac{\sum (x_i - \bar{x})(y_i - \bar{y})}{\sqrt{\sum (x_i - \bar{x})^2 \sum (y_i - \bar{y})^2}} \qquad (1)$$

where $\bar{x}$ and $\bar{y}$ are mean thresholding areas in each ROI. $R_{xy}$ ranges from –1 to +1, and –1 and +1 show strong associations in a negative and positive manner, respectively.

## 2-5 Immunocytochemistries

### 2-5-1 Antibodies (Chapters 3, 4, 5)

Antiboies were used for immunocytochemistires for the specific proteins. The primary antibodies were mouse anti-extoATPase (a gift from Dr. T. Mitaka), mouse anti-multidrug-resistance associated protein 2 (MRP2; Alexis Biochemichals, San Diego, CA), rabbit anti-5′-nucleotidase (5′NT; a gift from Dr. I. Wada),

mouse anti-dipeptidylpeptidase IV (DPPIV; Endogen, Rockford, IL), rat anti-zonula occludens-1 (anti-ZO-1; Chemicon International, Temecula, CA) for the protein associated with tight junctions (also called zonula occludens), anti-connexin 32 (Cx 32; Zymed Laboratories, South San Francisco, CA) for gap junctions, rabbit anti-desmin (Lab Vision, Fremont, CA) for stellate cells. Alexa Fluor 594-conjugated phalloidin (Molecular Probes, Eugene, OR) was used for actin filaments, as well as Texas red-conjugated anti-rat albumin (Inter-Cell Technologies, Jupiter, FL). The secondary antibodies were Alexa Fluor 488-conjugated anti-mouse and anti-rabbit IgG, and Alexa Fluor 594-conjugated anti-rat IgG (Molecular Probes).

### 2-5-2 Immunofluorescent staining for bile canalicular proteins (Chapter 3)

In the experiments described in chapter 3, the cells were fixed in cold absolute ethanol and kept at –20°C until use. Double-immunofluorescent staining for BC proteins, such as ectoATPase, 5′NT, DPPIV and MRP2, and actin was carried out. The cells were mounted with 90% glycerol containing 1 g/l p-phenylenediamine (PPD; Sigma-Aldrich) and 1 mg/l 4′, 6-diamidino-2-phenylindole (DAPI; Sigma-Aldrich) for the visualization of nuclei. Digital images of the fluorescent distribution in the cells were obtained using an Axioskop 20 microscope (Carl Zeiss, Hallbergmoos, Germany) equipped for epifluorescence (40 × objective lens) and recorded with the CELLscan System from Scanalytics equipped with a Photometrics CH250 thermoelectrically cooled CCD camera, a piezoelectric z-axis focus device, and a computer-controlled excitation light shutter. The digital images were analyzed using the software of IPLab™ (Scanalytics).

### 2-5-3 Staining reaction for bilirubin and immunocyotochemistry for zonula occludens-1 (Chapter 3)

Bilirubin (100 mg, Kanto Chemicals, Tokyo, Japan) was dissolved in 1 ml of DMSO and then 2 ml of 0.1 M $Na_2CO_3$, 5 ml of FBS, and 2 ml of 0.1 N HCl were added. The solution was diluted tenfold with DMSO and, thereafter, a mixture of the bilirubin solution (500 μl) and the medium (50 ml) was filtrated (0.2 μm). Cells were incubated with the medium containing 10 μg/ml bilirubin for 7 days. The Hall method

(1960) was used for histochemical staining of bilirubin. The cells were washed with phosphate buffered saline (PBS) and immediately photographed with a phase-contrast microscope. Then they were fixed with 4% paraformaldehyde/PBS for 5 min at room temperature and permeabilized with 0.5% Triton X-100 for 5 min. Immunocytochemistry for ZO-1 was performed and the avidin-biotin comlex (ABC) method (Vectastain ABC Elite Kit, Vector Laboratories, Burlingame, USA) was employed.

### 2-5-4 Immunofluorescent staining for gap junctional protein connexin 32 (Chapter 4)

The cells cultured on coverslips coated with rat-tail collagen were fixed in cold acetone for 5 min and double-immunofluorescent staining for Cx 32 and actin was carried out. The cells were mounted with 90% glycerol containing 1 g/l PPD and 1 mg/l DAPI.

### 2-5-5 Cytochalasin B treatment and immunocytochemistry for actin (Chapter 4)

To investigate the effects of cytochalasin B (CB; Sigma-Aldrich) on the behavior of BC networks, SH colonies were treated with CB. Sequential photographs were taken soon after the addition of CB to the medium. The CB solution was prepared from stock solution (25 mg/ml in DMSO). The cells were treated with a final concentration of 0.1, 1.0, 5.0 and 10.0 μg/ml CB in modified DMEM for 3 hours. After images were obtained, the cells were fixed in cold absolute ethanol and kept at –20°C until use. The actin filaments were visualized by incubation with Alexa Fluor 594 phalloidin for 1 hour.

### 2-5-6 Double-immunofluorescent staining for ectoATPase and other cell markers (Chapter 5)

The cells cultured on the membranes and those in the 3D stacked-up structures were fixed with cold absolute ethanol for 10 min. Double fluorescent-immunocytochemistry was carried out for albumin and desmin, ZO-1 and desmin, and ectoATPase and actin. The dishes were mounted with 90% glycerol containing 1 g/l PPD and 1 mg/l DAPI. Images of the cells were collected using a 3D deconvolution-imaging system. A z-axis series of fluorescent images was obtained using an Axiovert 200M motor-driven microscope equipped with a CCD camera (Carl Zeiss). Z-stacks of the fluorescent images

were automatically collected at 0.675/0.650-μm intervals and analyzed using AxioVision software (Carl Zeiss). The blur contributed by the fluorescently labeled structures located above and below the plane of optimal focus was mathematically reassigned to its proper origins using the deconvolution method of the constrained iterative maximum-likelihood algorithm. A theoretical point-spread function, which describes how the light of a point object is distorted by the optical system, was calculated using data from the microscope and the specimen.

## 2-6 Electron microscopy

### 2-6-1 Immunoelectron microscopy for apical membrane proteins (Chapter 3)

The pre-embedding method was used. The cells were fixed with 1.25% glutaraldehyde/0.1 M cacodylate buffer (pH 7.4) for 30 sec and then incubated in 0.5% Triton X-100/PBS for 10 min. The anti-ectoATPase, 5′NT, DPPIV or MRP2 antibody was used as the primary antibody and horseradish peroxidase (HRP)-conjugated anti-mouse Ig or an anti-rabbit Ig antibody was used as the secondary antibody. 3,3′-Diaminobenzidin (DAB; Tokyo Kasei Industories, Tokyo, Japan) was used as a substrate for the staining.

### 2-6-2 Transmission electron microscopy of vertical sections of the 3D stacked-up tissues (Chapter 5)

The cells were fixed with 2.5% glutaraldehyde in 0.1 M phosphate buffer (pH 7.4) overnight at 4°C, then postfixed in 2% $OsO_4$ for 2 hours, dehydrated through a graded series (70–100%) of ethanol, and embedded in Epon-812. Semithin (1 μm) and ultrathin (100 nm) sections were cut perpendicular to the base of the dish using an LKB ultramicrotome. The semithin sections were stained with 0.1% methylene blue and examined using a light microscope. The ultrathin sections were stained with uranyl acetate followed by lead citrate and examined at 80 kV using a JEM-100S transmission electron microscope (JEOL, Tokyo, Japan).

## 2-7 Visualization of bile canaliculi

### 2-7-1 Fluorescein diacetate treatment (Chapter 4)

In hepatocytes, fluorescein diacetate (FD; Sigma-Aldrich) is metabolized by intracellular esterase, to become fluorescein. The cytoplasmic fluorescein is actively transported into the BC via MRP2. To visualize the lumen of the BC networks, FD was added to the medium at a final concentration of 2.5 μg/ml. After 15-min incubation, the cells were rinsed three times with a medium containing no FD and then photographed using a phase-contrast microscope equipped with a fluorescence device.

### 2-7-2 Microinjection of dye into the piled-up cells and transportation of fluorescence (Chapter 4)

Before dye microinjection, the medium was replaced with L-15 medium. To observe flow through BC, 10 μM CellTracker™ green 5-chloromethyl-fluorescein diacetate (CMFDA; Molecular Probes) was microinjected (Eppendorf Micromanipulator system; Eppendorf, Hamburg, Germany) into one of the piled-up cells in each colony. When CMFDA is microinjected into cells, esterase in their cytoplasm hydrolyzes non-fluorescent CMFDA to fluorescent 5-chloromethylfluorescein. In hepatocytes, ATP-dependent multidrug transporters excrete the glutathione-conjugated fluorescent dye into BC (Roelofsen *et al.*, 1998). Fluorescent images of the cells were recorded at 5-sec intervals for 5 min using a fluorescence microscope equipped with a time-lapse system (Roper Scientific). More than 10 microinjections were performed.

### 2-7-3 Fluorescein diacetate and CellTracker™ red-fluorescent CMTPX treatments (Chapter 5)

To investigate whether the cells in the 3D stacked-up structures formed BC, they were treated with FD at a final concentration of 2.5 μg/ml for 15 min. Thereafter, the cells were rinsed three times with the medium and were photographed using a phase-contrast microscope equipped with a fluorescence device. FD is metabolized in hepatocytes by intracellular esterase and becomes fluorescein. The fluorescein in the cytoplasm was actively transported into the BC via MRP2. Thus, the BC formed by differentiated

hepatocytes could be visualized as green fluorescence by the FD treatment. By contrast, when the BC formed by the cells isolated from EGFP rats (GFP-labeled cells) were visualized, they were treated with CellTracker™ red-fluorescent CMTPX (CMTPX; Molecular Probes) at a final concentration of 10 μM for 15 min. CMTPX passes freely through cell membranes, but once inside the cell it is transformed into cell-impermeable reaction products, which might be transported into the BC via MRP2. Thus, the BC could be visualized as red fluorescence by the CMTPX treatment.

## 2-8 DiI treatment (Chapter 5)

DiI is a fluorescent lipophilic tracer that diffuses laterally within the plasma membrane, resulting in staining of the entire cell. In the experiments described in chapter 5, the cells on one membrane were treated with DiI (Molecular Probes) at a final concentration of 5 μM for 15 min in order to distinguish the upper and lower layers of SHs. Thereafter, the cells were rinsed three times with the medium and were cultured. The cells were stacked on top of the GFP-labeled cells 1 day after the DiI treatment. Thus, the cells could be labeled with red fluorescence that could not be transported into the BC.

## 2-9 Enzyme-linked immunosorbent assay for rat albumin (Chapter 5)

The albumin secretions produced by the cells before and after stacking up of the membranes were measured. At 48 hours after the replacement of the medium, the media from three dishes were separately collected into microcentrifugation tubes and centrifuged at 8,000×g for 10 min. The supernatant was transferred to new tubes. Quantification of the secreted rat albumin was carried out using an enzyme-linked immunosorbent assay (ELISA) with the two-antibody-sandwich method. Sheep anti-rat albumin antibody (1.0 μg/well; Bethyl Laboratories, Montgomery, TX) was coated to each well of a 96-well plate (Nunc, Roskilde, Denmark). After incubating with blocking solution (0.05 M sodium carbonate, pH 9.6), samples (1,000-fold dilution of the culture medium) were applied to the wells and incubated for 1 hour. Rat albumin (Bethyl Laboratories) was used as a standard. Horseradish peroxidase-conjugated sheep anti-rat albumin antibody (2.5 ng/well; Bethyl Laboratories) was then added to each well. TMB peroxidase substrate (Kirkegaard and Perry Laboratories, Gaithersburg, MD) was used

for the enzyme-substrate reaction, which was stopped by applying 2 M $H_2SO_4$. A microplate reader was used to measure the wavelength at 450 nm.

## 2-10 Western blot analysis (Chapter 3)

Colonies that expanded in a monolayer or that formed piled-up structures were manually dissected under a phase-contrast microscope and each colony was picked up using a micropipette. The two types (monolayer and piled-up) of colonies were separately collected into microcentrifugation tubes on ice and kept at –35°C until use. The cells were suspended in lysis buffer (20 mM Tris-HCl, pH 7.4, 150 mM NaCl, 0.5% deoxycholate, 1 mM EDTA, 2 mM phenylmethylsulfonic acid [Sigma], 1% NP-40, 200 kIU/ml aprotinin [Sigma], and 1% Triton X-100) and placed on ice for 5 min. Then they were ultrasonically lysed and the protein concentration was measured using a BCA protein assay kit (Pierce, Rockford, IL). Samples were separated by 7.5% sodium dodecyl sulfate-polyacrylamide gel electrophoresis (SDS-PAGE) and transferred to an Immobilon-P membrane (Millipore, Bedford, MA) with a Semi-dry Transfer Cell (Bio-Rad Laboratories, Hercules, CA). Then the anti-ectoATPase, anti-5′NT or anti-MRP2 antibody was applied to the membranes for 1 hour. Thereafter, HRP-conjugated anti-mouse Ig or an anti-rabbit Ig antibody (DAKO, Copenhagen, Denmark) was applied. SuperSignal West Dura Extended Duration substrate (Pierce) was used for the positive-staining. Apical membranes of hepatocytes were used for the positive control. Five rats were used to isolate liver cell membranes. Purification of apical membranes was performed by using the method of Ali *et al.* (1990) with some modifications and the membrane fraction was kept at –80°C until use.

## 2-11 RNA isolation and RT-PCR analysis (Chapter 5)

Reverse transcription-polymerase chain reaction (RT-PCR) analysis was used to identify mRNA transcripts in the cells after the membranes were stacked. Total RNA was isolated from the cells in the 3D stacked-up structures or the cells cultured on membranes without stacking, using the RNeasy RNA isolation kit (Qiagen, Hilden, Germany). As a positive control, those of freshly isolated primary hepatocytes were also prepared. RT was performed on 0.5 μg of total RNA using the oligo$(dT)_{20}$ primer and the SuperScript

III reverse transcriptase (Invitrogen). The gene-specific primers for albumin, MRP2, HNF-4, tyrosine aminotransferase (TAT), TO and glyceraldehyde-3-phosphate-dehydrogenase (GAPDH) are listed in Table 2-1. The PCR analyses were performed in buffer containing the premix Taq (TaKaRa, Otsu, Japan) and 0.2 μM of each primer pair with the Apollo 201 thermal cycler (CLP, San Diego, CA). PCR was carried out at 94°C for 5 min, followed by 24–28 cycles at 94°C, 53–56°C and 72°C each for 30 sec, with a final elongation step at 72°C for 5 min. The PCR products were then analyzed using the electrophoresis of 2% agarose gels stained with ethidium bromide. The gel images were captured using the Molecular Imager FX (Bio-Rad Laboratories).

Table 2-1 Sequences of PCR primers

| Primer | Sequence (5′-3′) | Annealing temp. (°C) | Size (bp) | Cycle | Reference |
|---|---|---|---|---|---|
| Albumin | AAGGCACCCCGATTACTCCG<br>TGCGAAGTCACCCATCACCG | 56 | 649 | 24 | Gordon *et al.*, 2000 |
| MRP2 | ACCTTCCACGTAGTGATCCT<br>ACTGTAGGCTCTGGGAAATC | 54 | 1,085 | 28 | Vos *et al.*, 1998 |
| HNF-4 | TCTACAGAGCATTACCTGGC<br>TGAGGGGAAGATGAAGACGG | 54 | 654 | 28 | Gordon *et al.*, 2000 |
| TAT | TACTCAGTTCTGCTGGAGCC<br>GCAAAGTCTCTAGAGAGGCC | 56 | 512 | 24 | Gordon *et al.*, 2000 |
| TO | GAAGACGGAGCTCAAACTGG<br>AATAGCGTCTGCTCCTGCTC | 56 | 533 | 28 | |
| GAPDH | ACCACAGTCCATGCCATCAC<br>TCCACCACCCTGTTGCTGTA | 53 | 452 | 26 | |

## References

Ali N, Aligue R, Evans WH. Highly purified bile-canalicular vesicles and lateral plasma membranes isolated from rat liver on Nycodenz gradients. Biochemical and immunolocalization studies. Biochem J. 1990;271:185–192.

Gordon GJ, Coleman WB, Grisham JW. Temporal analysis of hepatocyte differentiation by small hepatocyte-like progenitor cells during liver regeneration in retrorsine-exposed rats. Am J Pathol. 2000;157:771–786.

Hall MJ. A staining reaction for bilirubin in sections of tissue. Am J Clin Pathol. 1960;34:313–316.

Mitaka T, Sato F, Mizuguchi T, Yokono T, Mochizuki Y. Reconstruction of hepatic organoid by rat small hepatocytes and hepatic nonparenchymal cells. Hepatology. 1999;29:111–125.

Okabe M, Ikawa M, Kominami K, Nakanishi T, Nishimune Y. 'Green mice' as a source of ubiquitous green cells. FEBS Lett. 1997;407:313–319.

Roelofsen H, Soroka CJ, Keppler D, Boyer JL. Cyclic AMP stimulates sorting of the canlicular organic anion transporter (Mrp2/cMoat) to the apical domain in hepatocyte couplets. J Cell Sci. 1998;111:1137–1145.

Vos, TA, Hooiveld, GJ, Koning H, Childs, S, Meijer DK, Moshage H, Jansen PL, Muller M. Up-regulation of the multidrug resistance genes, Mrp1 and Mdr1b, and down-regulation of the organic anion transporter, Mrp2, and the bile salt transporter, Spgp, in endotoxemic rat liver. Hepatology. 1998;28:1637–1644.

Seglen PO. Preparation of isolated rat liver cells. Methods Cell Biol. 1976;13:29–83.

# Chapter 3

# Bile canalicular formation in hepatic organoid reconstructed by rat small hepatocytes and nonparenchymal cells

## 3-1 Introduction

The hepatocyte is a highly specialized, polarized cell. Its plasma membrane is differentiated into three functionally and structurally distinct domains: the sinusoidal domain, the lateral domain, and the bile canalicular (apical) domain. The apical domain of paired hepatocytes is separated from the lateral domain by tight junctions and forms BC. The structure is rich in microvilli and components of bile metabolized in the cells are secreted into the structure. Secreted bile can pass through BC and pour into bile ducts. Although the morphogenesis and movement of BC have been investigated in liver tissues (De Wolf-Peeters *et al.*, 1974), in hepatoma cell lines like HepG2 (Sormunen *et al.*, 1993), in hepatoma × fibroblast hybrid cells (Bender *et al.*, 1998), and in primary cultures of liver cells (Kawahara *et al.*, 1989; Oshio *et al.*, 1981; Robenek *et al.*, 1982; Watanabe *et al.*, 1983; Watanabe *et al.*, 1984; Watanabe *et al.*, 1988), they are not well understood.

SHs have been identified as proliferating cells with hepatic characteristics (Mitaka *et al.*, 1992a, b). Recently, it was showed that a single SH could clonally proliferate and form a large colony (Mitaka *et al.*, 1995, 1999). Although SH colonies become flat clusters in the early period of the culture, they expand to form large colonies, some of which are composed of piled-up cells. The piled-up cells show the appearance of MHs and express LETFs, such as HNF 4α, HNF 6, and C/EBPα as well as TO and SDH, which are considered to be markers of hepatic maturation (Sugimoto *et al.*, 2002). In addition, between the piled-up cells BC-like structures are formed and develop into anastomosing networks. In such colonies NPCs invade

under the colony and an accumulation of ECM between hepatocytes and NPCs can be observed. Therefore, it was suspected that SHs could differentiate into MHs that interact with hepatic NPCs and ECM (Mitaka *et al.*, 1999).

In the present experiment they were examined how SHs could form BC-like structures in the process of their maturation and whether the structures could be functionally active as BC. The results of immunocytochemistry, immunoblotting and immunoelectron micrographs revealed that BC proteins such as ectoATPase, 5′NT, DPPIV and MRP2 localized in the membranes of the BC-like structures. Furthermore, continuous contraction and dilatation occurred in the BC-like structures and bilirubin added to the medium were secreted into the reconstructed BC and accumulated without leakage. Thus, the reconstructed BC in the differentiated SH colonies may be functional with polarity of the BC membrane, secretory ability, and motility.

## 3-2 Results

### 3-2-1 Appearance of bile canaliculi-like structures on the colonies (2-1, 2-3-1)*

As previously reported (Mitaka *et al.*, 1999), several kinds of hepatic cells were plated on each dish, including MHs, SHs, LECs, Kupffer cells, SECs and stellate cells. SHs, the size of which was less than half that of attached MHs, began dividing from day 3. The SHs rapidly proliferated and formed a colony. LECs and stellate cells also proliferated. About 10 days after plating, many colonies were surrounded by LECs and stellate cells, and, several days later, piled-up cells appeared in the colonies. The piled-up cells gradually grew and BC-like structures were often found between the cells (Fig. 3-1C). The number of colonies with piled-up cells reached about 25% of all colonies at day 30 (Mitaka *et al.*, 2001). Other colonies that were not surrounded by NPCs developed faster than the colonies surrounded by them and maintained a monolayer (Fig. 3-1A). In such colonies, relatively large hepatocytes, which looked like MHs and were sometimes binucleate, sometimes appeared and the number increased with time in culture (Fig. 3-1B).

* For the relevant methods see the written sections.

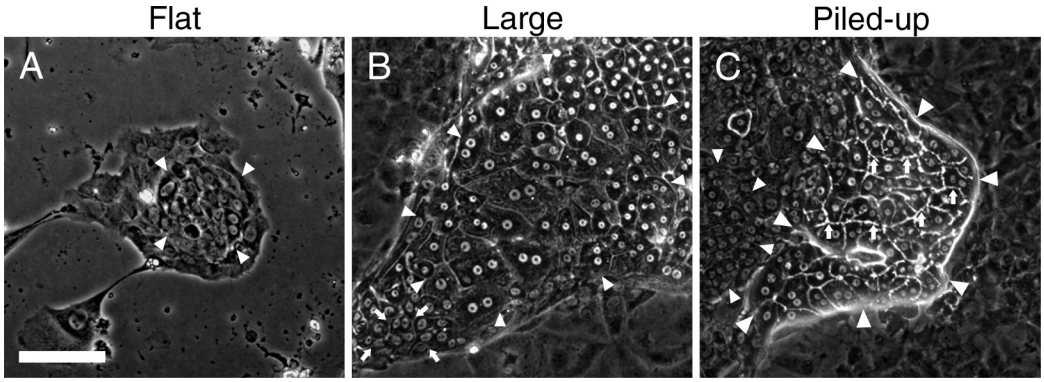


Fig. 3-1 Phase-contrast micrographs of representative SH colonies classified into three types: Flat (A, day 12), Large (B, day 28) and Piled-up (C, day 28). (A) The Flat colony is composed of only SHs (arrowheads) and its shape is flat. (B) The Large colony is composed of SHs (arrows) and large cells (arrowheads), some of which have two nuclei. (C) The Piled-up colony is composed of piled-up cells (large arrowheads). Small arrowheads show SHs. Translucent belts, most of which construct BC-like structures (arrows), are observed between piled-up cells. Scale bar, 100 μm.

## 3-2-2 Localization of bile canalicular proteins in colonies (2-5-2)

The expression and the distribution of ectoATPase, DPPIV, MRP2 and 5′NT proteins were immunocytochemically investigated in the colonies with morphological changes. The colonies were classified into three types according to their morphology. Figure 3-2 shows the expression of the proteins in the three different types of colonies; 1) A flattened colony (Flat, Fig. 3-1A). The colony consists of SHs. Neither ectoATPase (Fig. 3-2A) nor MRP2 (Fig. 3-2D) was expressed in the cells, whereas 5′NT was expressed in both the cytoplasm and cell membrane (Fig. 3-2G). 2) A colony with large hepatocytes (Large, Fig. 3-1B). Positive staining for ectoATPase and MRP2 was found at the corner and/or center of the basolateral domains of the large cells (Figs. 3-2B, E). Although most 5′NT proteins might be localized in the cell membranes, restricted expression was not clearly observed (Fig. 3-2H). 3) A colony with piled-up cells (Piled-up, Fig. 3-1C). Translucent belts were found between the cells under the phase-contrast microscope. Dotted staining of ectoATPase and linear staining of both MRP2 and 5′NT were observed along the belts. In addition, actin was intensively positive around BC-like structures corresponding to the expression of BC proteins (Figs. 3-2C, F, I). The expression of DPPIV was similar to that of MRP2 (data not shown).

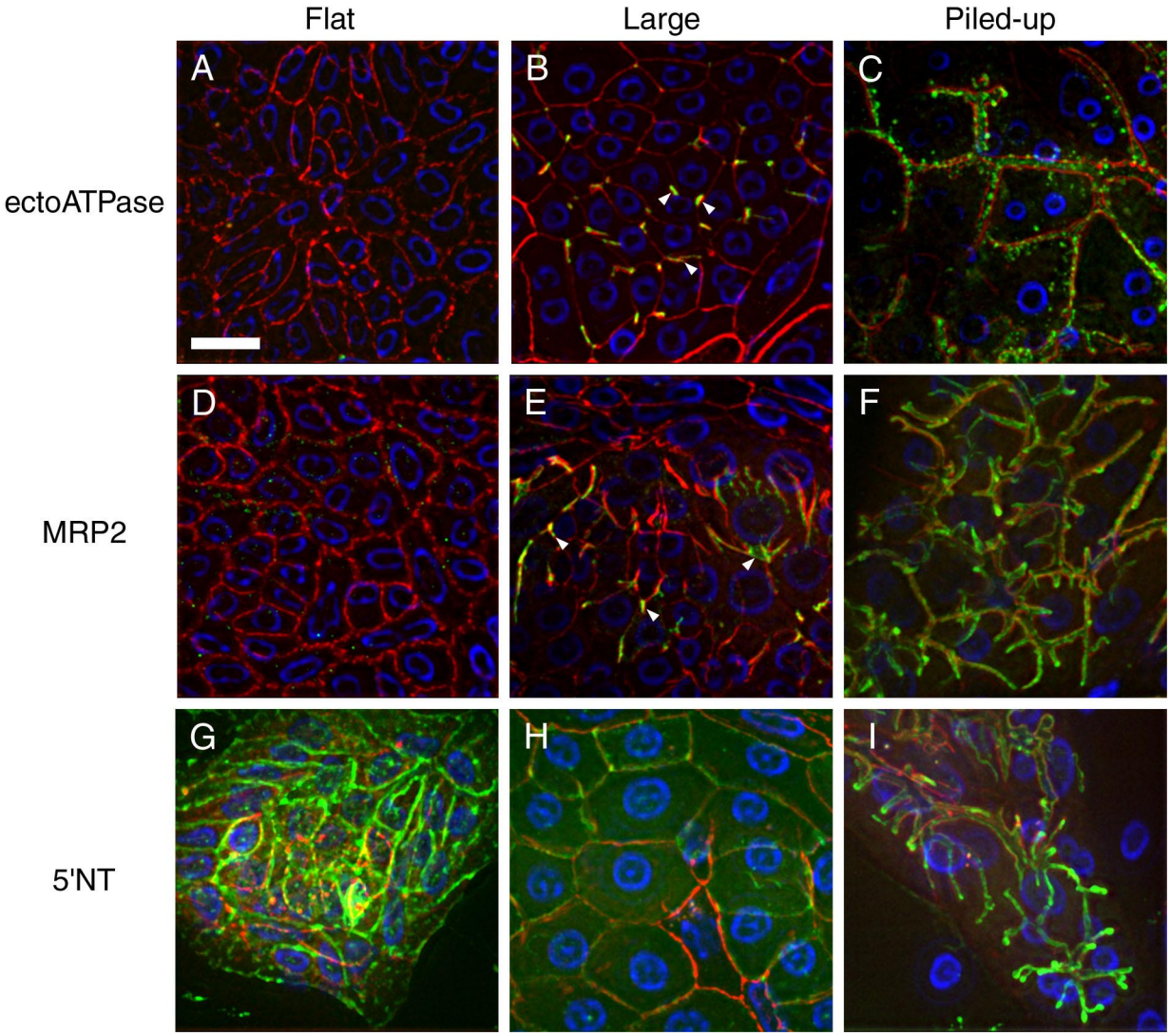


Fig. 3-2 The localization of ectoATPase, MRP2 and 5′NT proteins in colonies. Triple immunostaining for ectoATPase (green), actin (red) and DAPI (blue), for MRP2 (green), actin (red) and DAPI (blue), and for 5′NT (green), actin (red) and DAPI (blue) shown by digital images analyzed using the CELLscan system. Colonies were classified into three types: those consisting of only SHs and having a flat shape (Flat, A [day 15], D [day 15], G [day 10]), those consisting of SHs and large cells (Large, B [day28], E [day28], H [day28]), and those consisting of piled-up cells (Piled-up, C [day28], F [day28], I [day28]). The cells in the Flat colony had no expression of ectoATPase (A) and MRP2 (D) proteins, whereas 5′NT (G) was positive in both cell membranes and cytoplasm. The large cells in the Large colony showed restricted expression of ectoATPase (B, arrowheads) and MRP2 (E, arrowheads) proteins at the corners and the center of the basolateral domains, whereas 5′NT protein (H) was stained in both cell membranes and cytoplasm. The piled-up cells in the Piled-up colony showed were positive for ectoATPase (C), MRP2 (F) and 5′NT (I), and the staining coincided with BC-like structures. The images were three-dimensionally reconstructed by calculating 30 planes at 0.4 μm intervals. Scale bar, 20 μm.

## 3-2-3 Immunoelectron microscopy for bile canalicular proteins (2-6-1)

An immunoelectron micrograph of ectoATPase in piled-up cells is shown in Figure 3-3. BC-like structures with many microvilli were formed in the intercellular space between large hepatocytes and DAB-positive granules localized in the microvilli. DAB-positivity was not observed in either the sinusoidal or basolateral domain of the cell membrane. Furthermore, immunoreactivities to MRP2, DPPIV and 5′NT were also observed in a restricted area, which was coincident with the BC-like structures (data not shown).

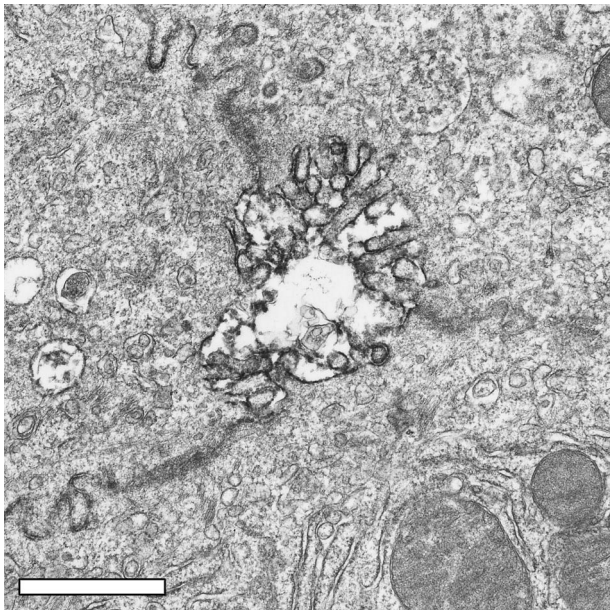

Fig. 3-3 Immunoelectron micrograph for ectoATPase in piled-up cells. A bile canaliculus is formed at the corners of three hepatocytes. Many microvilli developed in the BC lumen and DAB-positive granules are observed along the surfaces of the microvilli. Scale bar, 1 μm.

## 3-2-4 Expression of bile canalicular proteins [2-10]

The expression of BC proteins in the flat colonies and the colonies with piled-up cells was investigated by western blotting (Fig. 3-4). Immunoblots for ectoATPase and MRP2 showed that both proteins were expressed in the colonies with piled-up cells, whereas little of either was detected in the monolayer colonies. The expression of ectoATPase and MRP2 proteins was coincident with the results of the immunocytochemistry. On the other hand, no difference of 5′NT expression was observed between monolayer colonies and colonies with piled-up cells.

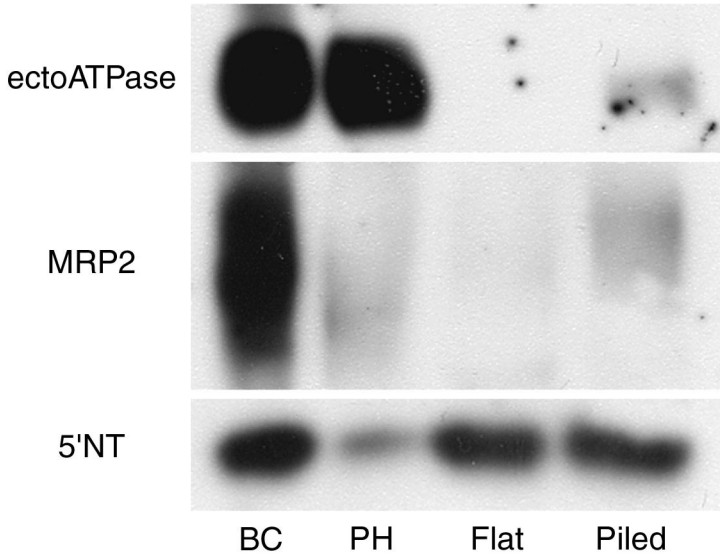


Fig. 3-4 Western blot analysis for ectoATPase, MRP2 and 5′NT of the cells forming colonies. The samples were collected from two types of colonies: those consisting of SHs and having a flat shape (Flat), and those consisting of piled-up cells (Piled). Purified bile canalicular membranes separated from rat livers (BC) and primary rat hepatocytes at 3 hours after plating (PH) were used as positive controls. The samples (PH, Flat, and Piled, 5 μg/lane; BC, 1.5 μg/lane) separated by 7.5% SDS-PAGE were transferred electrophoreically to a PVDF membrane. After transfer, the blots were stained with antibodies against ectoATPase, MRP2 and 5′NT.

### 3-2-5 Secretion of bilirubin into bile canaliculi-like structures [2-5-3]

The piled-up cells could secrete absorbed bilirubin into BC-like structures as we observed that yellowish brown materials accumulated in the structures and cystic regions (asterisk in Figs. 3-5A, B, D, E). DAB-positive dots of immunoreactive ZO-1 proteins (tight junction-associated protein) were arranged along the edges of the structures (Fig. 3-5C). Corresponding images of bright field and ZO-1 staining showed that yellowish brown materials accumulated between the ZO-1-positive lines (insets in Figs. 3-5B, C). In addition, when the cells treated with bilirubin were fixed and histochemically stained, green materials were observed inside the structures (Fig. 3-5F). Corresponding images before and after bilirubin staining showed that the accumulated yellowish brown material changed into a green one, which was bilirubin (Figs. 3-5D–F).

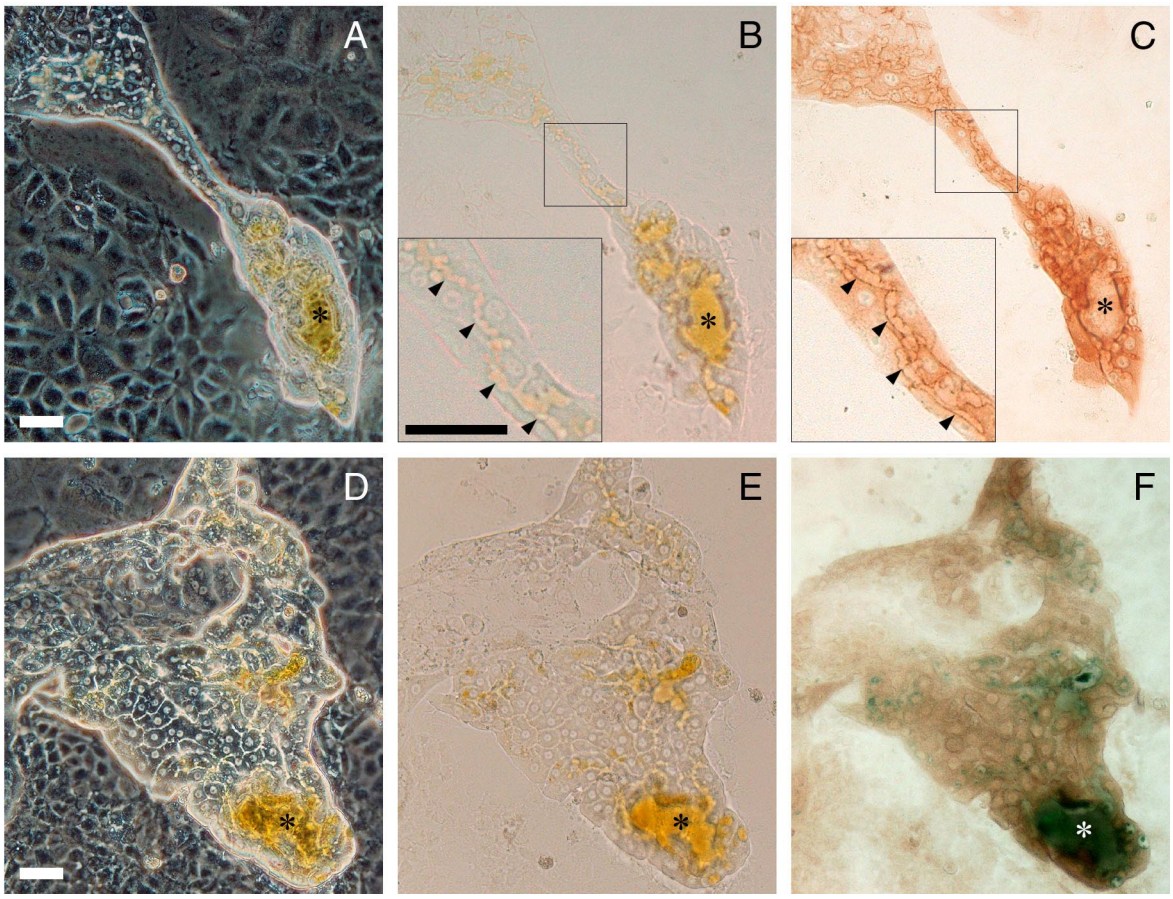


Fig. 3-5 Secretion of bilirubin into BC-like structures in piled-up cells. Cells were treated with medium including 10 μg/ml bilirubin for 7 days. Phase-contrast (A) and bright field (B) images of living cells at day 24, treated with bilirubin, were taken using a microscope equipped with a color digital camera. Yellowish-brown fluid accumulated in a cystic region of a colony (A, B; asterisk). Immunocytochemistry for ZO-1 in the same SH colony (C). Enlarged images of the same part in the colony are shown in each inset (B and C). Corresponding BC-like structures are indicated by arrowheads. At day 27 cells treated with bilirubin were fixed with 10% formalin and stained for bilirubin (F). The piled-up cells treated with bilirubin possess green deposits in intercellular spaces corresponding to yellowish brown BC-like structures in phase-contrast (D) and bright field (E) images. A–C, insets in B and C, and D–F are shown at the same magnification, respectively. Scale bars, 50 μm.

### 3-2-6 Contraction and dilatation of reconstructed bile canaliculi [2-3-1]

BC that were formed between piled-up cells were sequentially photographed using a phase-contrast microscope equipped with a CCD camera. In most colonies one or two big contractions of BC were observed within 2 hours on the monitor with the naked eye. A demonstrative contraction is shown in Fig. 3-6A and the calculated light intensity in the segments is shown in Fig. 3-6B. Alteration of light intensity in the segment reflects the caliber of BC. In the contraction shown in Fig. 3-6, the BC-like structure rapidly expanded and suddenly contracted (Figs. 3-6C–E). It took about 20 min between C and E. In most contractions, although it took much time for the dilatation and the duration of dilatation and contraction varied, the contraction had a tendency to be very rapid. In addition, the movie showed that peristaltic movements were often observed in many regions of BC-like structures and that secreted substances might flow. A pool of secreted substances was often found at the tip of the area consisting of piled-up cells. The pool became larger with time in culture.

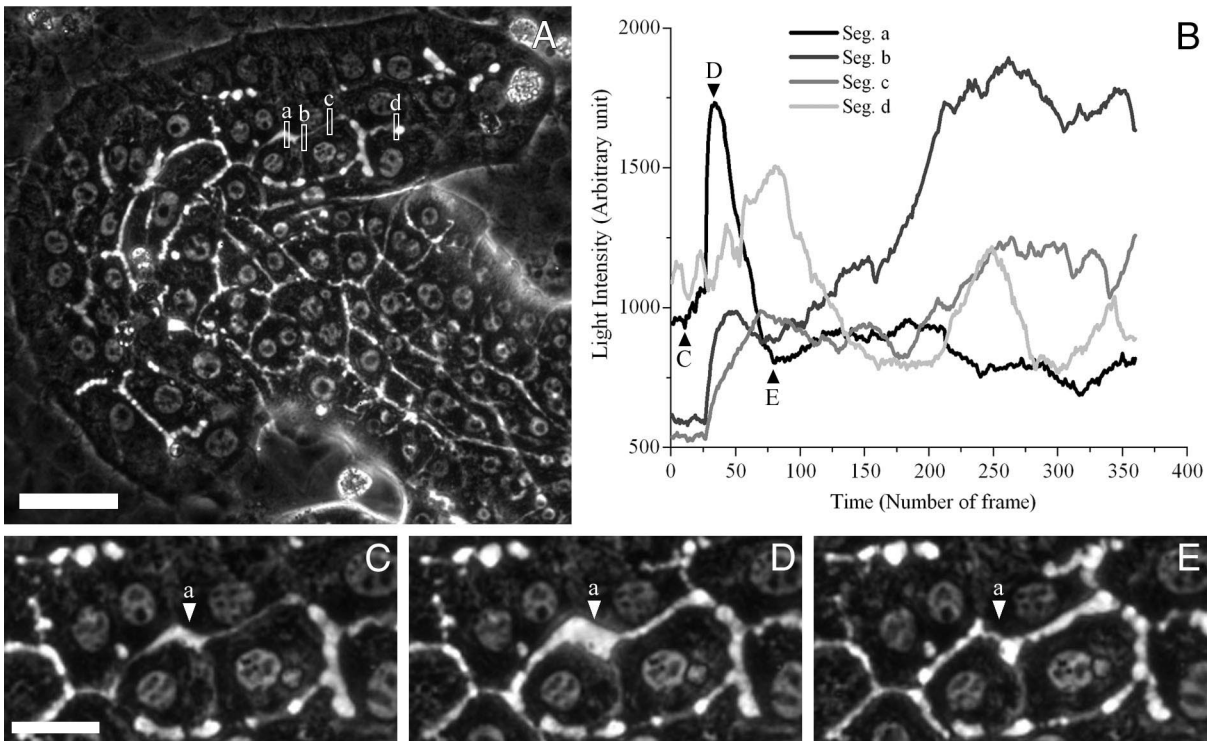


Fig. 3-6 Phase-contrast micrographs and graphical representation of BC contraction. (A) Phase-contrast micrograph of the cells in a colony consisting of piled-up cells forming BC-like structures in the intercellular space. Four segments (*a*–*d*), in which average light intensity was measured, are shown in the image. The calculated light intensity of each segment in (A) is graphically shown in (B). Phase-contrast micrographs (C–E) around segment *a* correspond to the times marked by arrowheads in (B). Scale bars, 50 μm (A) and 20 μm (C).

## 3-3 Discussion

### 3-3-1 Bile canalicular formation in small hepatocyte colonies

The process of BC formation in the liver is not well understood because it is very difficult to develop and to maintain the normal membrane polarity of hepatocytes *in vitro*. Some experimental models developed to analyze the mechanism have been reported. The isolated perfused liver (Hems *et al.*, 1966; Mortimore *et al.*, 1979), hepatocyte couplets (Boyer, 1997; Graf *et al.*, 1984; Sakisaka *et al.*, 1988), and fractionated membrane vesicles (Meier, 1989; Barr, *et al.*, 1995) were used as models. However, in these systems membrane polarity exists before the experiments. Therefore, these models provide little insight into BC development. Recently, progress has been made in obtaining better hepatic polarity by plating primary hepatocytes in sandwiched collagen gels (LeCluyse *et al.*, 1994) and by using differentiated hepatoma cell lines (Sormunen *et al.*, 1993; Chiu *et al.*, 1990) and cell hybrids (Ihrke *et al.*, 1993; Konieczko *et al.*, 1998). Even though these cells can form the BC-like structures, the pre-existence of apical domain proteins and membranes in the cells has to be considered when primary hepatocytes are used. On the other hand, in the colonies consisting of piled-up cells, BC is newly formed and develops into 3D-branched networks.

SHs morphologically and functionally change with time in culture (Mitaka *et al.*, 1999; Sugimoto *et al.*, 2002). The morphology of the large and piled-up cells appearing after long-term culture may be quite different from that of the flat SHs in the early stages of the culture. Piled-up cells are tall, and their height apparently increases from the surface of surrounding flat SHs (Fig. 3-1C). The cells have large cytoplasm and sometimes two nuclei, which are one of the specific characteristics of MHs. Therefore, the shape of the SHs was classified into three types; flat, large and piled-up cells. Interaction between SH–ECM and SH–NPC may be associated with the maturation of SH. It is well known that cell shape is correlated with function. When SHs were treated with Matrigel, they dramatically changed shape from flat to piled-up within several days. Accompanying this alteration of the cell shape, the expression of LETFs, such as HNF 4α, HNF 6, C/EBPα and C/EBPβ reappeared and increased to near the level of proteins in MHs. Furthermore, TO and SDH, which are markers of well-differentiated hepatocytes, were induced in the cells treated with Matrigel (Sugimoto *et al.*, 2002). Therefore, the physiological characteristics of SHs vary

corresponding to their shape during long-term culture.

### 3-3-2 Physiological function of the reconstructed bile canaliculi

To detect the polarity of the BC domain, we carried out immunocytochemistry for ectoATPase, 5′NT, DPPIV and MRP2. Focusing on the process of BC formation, the apical domain was not formed in the cell membranes of flat SHs and the domain formation occurred after more than two adjacent SHs became large/piled-up cells. BC proteins such as ectoATPase and MRP2 first appeared on the cell membrane in the corner and/or center of the membrane between adjacent cells. Although SHs possessed 5′NT protein like large/piled-up cells, the distribution of the protein changed from the cytoplasm to the cell membrane with the alteration of cell shape. The BC proteins first showed a linear arrangement on the cell membrane and then were arranged spherically in the corner and/or center of a segment of the cell membrane. Restricted expression of ectoATPase and MRP2 was observed in BC-like structures, whereas weak expression of 5′NT was also found in the basolateral domain. Similar observations that 5′NT expression was not restricted in BC were reported in other polarized cell models (Ihrke *et al.*, 1993; Luzio *et al.*, 1986). The spherical BC elongated to form tubules along the segment of the cell membrane and, thereafter, the tubules connected to each other to form branches.

EctoATPase and 5′NT are localized in the BC domain, and are ectonucleotidases that are involved sequential degradation of extracellular ATP to adenosine (Che *et al.*, 1997). The concentrations of these proteins on the BC lumen are important, because extracellular nucleotides and their degradation products have multiple effects on hepatic functions by acting through purinergic receptors. The sequential degradation by ectoATPase and 5′NT also plays an important role in purine circulation that may be essential for the liver to provide purine bases for extrahepatic tissues. Western blot analysis revealed that expression of BC proteins in piled-up cells, whereas few expressions were detected in flat cells. Although the amount of ectoATPase protein in the piled-up cells was small compared to that in primary hepatocytes, as much MRP2 protein was expressed in the piled-up cells as in primary hepatocytes. Furthermore, piled-up cells expressed much larger amounts of BC proteins than the flat cells. However, the expression of 5′NT was different from that of ectoATPase and MRP2. Although the amount of 5′NT protein did not

increase in the piled-up cells, the distribution was gradually changed from the cytoplasm in the flat cells to the apical membrane in the piled-up cells.

MRP2 is another BC protein. It plays an important role in a transport system of the hepatocytes. Bilirubin is known to be glucuronized in the cytoplasm and secreted into BC via MRP2. In the present experiment, coincident with the expression of MRP2 in the cells, secretion of bilirubin was observed in the regions of piled-up cells. As the sensitivity of histochemical staining for bilirubin is low, the accumulation and concentration of secreted bilirubin are necessary. Bile plaques were visible within the restricted areas of the cystic and thick-tubular structures. In this experiment, yellowish brown material was retained after washing with PBS. In addition, immunocytochemistry for ZO-1 revealed that the immunoreactivity lined along the tubular structures formed in the piled-up cells and that the accumulation of yellowish brown material was observed in the structure (Fig. 3-5). It was also confirmed that yellowish brown material immediately changed to green after the bilirubin staining (Figs. 3-5D–F). These results indicated that piled-up cells could absorb bilirubin from the medium and secret it into BC-like structures sealed by tight junctions. Unfortunately, it could not be identified whether the secreted bilirubin was the glucuronized form.

In the development of the rat liver, BC are first formed in smooth plasma membranes of two apposed cells at fetal day 12 or 13 (Luzzatto, 1981; Wood, 1965) and then the BC bounded by four or five contiguous cells become apparent after fetal day 16 or 17 (Wood, 1965). BC develop a mature appearance during the perinatal and early postnatal periods (Kanamura *et al.*, 1990). De Wolf-Peeters *et al.* (1974) divided developing BC in rat livers into four types; with an intracellular invagination of the cell membrane into one of the neighboring hepatocytes (type I; at fetal day 16), an irregular lumen (type II; at fetal day 19–20), a wide and regular lumen bearing few or no microvilli (type III; just before and after birth), and a smaller lumen filled with numerous microvilli (type IV; adult type). Type III BC were observed in the early SHs (data not shown) and adult-type BC were observed in the piled-up cells as shown in Fig. 3-3. Thus, the formation of BC with SH maturation appeared to be similar to the development of BC *in vivo*. Thus, the alteration of cell shape and the formation of the BC structure may cause the expression and the distribution of BC proteins, which were restricted to the lumina of the BC-like structures.

### 3-3-3 Movements of reconstructed bile canaliculi

Pericanalicular actin filaments around BC have been suggested to play an important role in the contraction of hepatocyte couplets (Phillips *et al.*, 1983). In this study fluorescent-phalloidin staining also showed that actin filaments were rich in reconstructed BC-like structures. Using isolated hepatocyte couplets and time-lapse microscopy, it has been shown that BC repeatedly open and close and that this motion is accompanied by the expulsion of a bolus of bile (Oshio *et al.*, 1981; Phillips *et al.*, 1982). Concerning this motion of BC, two theories have been proposed: one is that it results from active BC contractions (Oshio *et al.*, 1981; Watanabe *et al.*, 1984; Phillips *et al.*, 1982; Miyairi *et al.*, 1984), the other is that it is due to noncontractile collapses of canaliculi resulting from secretory pressure with rupture of canaliculi (Boyer, 1987; Gautam *et al.*, 1987). Although hepatic couplets are important as a simple model of BC, the BC is artificially closed forming a sealed sphere, whereas the BC-like structures in this study formed a network of tubular structures as observed *in vivo*. Viewing BC movements in our experimental model, an apparent rapid and large contraction as if expelling a bolus of bile was observed. In the movement several pairs of apposed cells contracted synchronously and sequentially. Furthermore, small contractions that seemed to be peristaltic movement of BC were often observed in the reconstructed BC-like structures. Unfortunately, this phenomenon could not be clearly displayed and analyzed because of the limited resolution of our equipment. Contractile activity of BC was reported to vary in the region of the liver lobule (Watanabe *et al.*, 1991). A subcapsular network of BC, which is present on the surface of the liver, showed no contractions, whereas contractions were most frequently observed in periportal canaliculi. Thus, it may be feasible to think that the BC are actively moving. Furthermore, the two types of contractions (a large coordinated one and many small contractions) observed in this experiment may be similar to the regional movements observed in the living liver.

Watanabe *et al.* (1991) observed BC movement in the living state by using sodium fluorescein. They showed that the time interval of the contraction was 20–40 sec, whereas the interval in hepatocyte couplets was 300–360 sec (Phillips *et al.*, 1982). On the other hand, in the reconstructed BC-like structures, the time-lapse movie showed that it took about 1 hour to reach the maximum dilatation and that the region then forcibly contracted to expel the luminal contents. This phenomenon suggests that the BC contraction may be a subthreshold activity and a certain sensor for pressure or stretching, which causes a rapid large

contraction, may exist in the BC. Recently, the existence of stretch-activated channels has been reported in cultured cells (Guharay *et al.*, 1984; Morris, 1990). Although we do not have any direct proof about these sensors, it may be plausible to expect the existence of such channels. On the other hand, between adjacent piled-up cells gap junctional proteins such as Cx 32 and 26 were well expressed (see chapter 4: Fig. 4-8). The coordination of BC contraction in hepatocyte couplets may be mediated by intercellular signals such as ions and molecules through the gap junction (Watanabe *et al.*, 1985).

In the present experiment it was showed that *in vitro* reconstructed BC-like structures might be a useful system to investigate the mechanisms of BC contraction and bile flow. The system may also be useful in the study of hepatic and biliary diseases like cholestasis, especially when human SHs are isolated and used.

## 3-4 Summary

The morphogenesis and movement of bile canaliculi (BC) are not well understood. This is because culture of hepatocytes that maintain polarity of cell membranes and possess highly differentiated functions has never been successful. It was found that small hepatocytes (SHs), which are known to be hepatic progenitor cells, could proliferate and differentiate into mature hepatocytes and that BC-like structures developed between piled-up cells. They were investigated how BC-like structures developed with maturation of SHs and whether the structures were functionally active as BC. Hepatic cells, including SHs, were isolated from an adult rat liver and cultured. Immunocytochemistry and immunoblotting for BC proteins such as ectoATPase, 5′-nucleotidase, dipeptidylpeptidase IV and multidrug-resistance associated protein 2 were examined and time-lapse microscopy was used for the observation of BC contractions. Secretion of bilirubin into the reconstructed BC was also observed. The results of immunocytochemistry, immunoblots and immunoelectron micrographs revealed that BC proteins were localized in the intercellular space that coincided with BC-like structures reconstructed between piled-up cells. Tight junction-associated protein ZO-1 was also expressed along the BC-like structures. Bilirubin added to the medium were secreted into BC-like structure and accumulated without leakage. Time-lapse microscopy showed continuous contractions of reconstructed BC. In conclusion, BC-like structures reconstructed by SHs may be functional with membrane polarity, secretory ability and motility. These results show that this culture system may suitable for investigating the mechanism of the formation of BC and their functions.

## References

Barr VA, Scott LJ, Hubbard AL. Immunoadsorption of hepatic vesicles carrying newly synthesized dipeptidyl peptidase IV and polymeric IgA receptor. J Biol Chem. 1995;270:27834–27844.

Bender V, Buschlen S, Cassio D. Expression and localization of hepatocyte domain-specific plasma membrane proteins in hepatoma × fibroblast hybrids and in hepatoma dedifferentiated variants. J Cell Sci. 1998;111:3437–3450.

Boyer JL. Contractile activity of bile canaliculi: contraction or collapse? Hepatology. 1987;7:190–192.

Boyer JL. Isolated hepatocyte couplets and bile duct units-novel preparations for the in vitro study of bile secretory function. Cell Biol Toxicol. 1997;13:289–300.

Che M, Gatmaitan Z, Arias IM. Ectonucleotidases, purine nucleoside transporter, and function of the bile canalicular plasma membrane of the hepatocyte. FASEB J. 1997;11:101–108.

Chiu JH, Hu CP, Lui WY, Lo SJ, Chang C. The formation of bile canaliculi in human hepatoma cell lines. Hepatology. 1990;11:834–842.

De Wolf-Peeters C, De Vos R, Desmet V, Bianchi L, Rohr HP. Electron microscopy and morphometry of canalicular differentiation in fetal and neonatal rat liver. Exp Mol Pathol. 1974;21:339–350.

Gautam A, Ng OC, Boyer JL. Isolated rat hepatocyte couplets in short term culture-structural characteristics and plasma membrane reorganization. Hepatology. 1987;7:216–223.

Graf J, Gautam A, Boyer JL. Isolated rat hepatocyte couplets: a primary secretory unit for electrophysiologic studies of bile secretory function. Proc Natl Acad Sci U S A. 1984;81:6516–6520.

Guharay F, Sachs F. Stretch-activated single ion channel currents in tissue-cultured embryonic chick skeletal muscle. J Physiol. 1984;352:685–701.

Hems R, Ross BD, Berry MN, Krebs HA. Gluconeogenesis in the perfused rat liver. Biochem J. 1966;101:284–292.

Ihrke G, Neufeld EB, Meads T, Shanks MR, Cassio D, Laurent M, Schroer TA, Pagano RE, Hubbard AL. WIF-B cells: an in vitro model for studies of hepatocyte polarity. J Cell Biol. 1993;123:1761–1775.

Kanamura S, Kanai K, Watanabe J. Fine structure and function of hepatocytes during development. J Elect Microsc Tech. 1990;14:92–105.

Kawahara H, Marceau N, French SW. Effect of agents which rearrange the cytoskeleton in vitro on the structure and function of hepatocytic canaliculi. Lab Invest. 1989;60:692–704.

Kojima T, Mitaka T, Paul DL, Mori M, Mochizuki Y. Reappearance and long-term maintenance of connexin32 in proliferated adult rat hepatocytes: use of serum-free L-15 medium supplemented with EGF and DMSO. J Cell Sci. 1995;108:1347–1357.

Konieczko EM, Ralston AK, Crawford AR, Karpen SJ, Crawford JM. Enhanced $Na^+$-dependent bile salt uptake by WIF-B cells, a rat hepatoma hybrid cell line, following growth in the presence of a physiological bile salt. Hepatology. 1998;27:191–199.

LeCluyse EL, Audus KL, Hochman JH. Formation of extensive canalicular networks by rat hepatocytes in collagen-sandwich configuration. Am J Physiol. 1994;226:C1764–C1774.

Luzio JP, Bailyes EM, Baron M, Siddle K, Mullock BM, Geuze HJ, Stanley KK. The properties, structure, function, intracellular localization and movement of hepatic 5′-nucleotidase. In: Cellular Biology of Ectoenzymes, edited by Kreutzberg GW. Berlin/Heidelberg: Springer-Verlag, 1986:89–116.

Luzzatto AC. Hepatocyte differentiation during early fetal development in the rat. Cell Tissue Res. 1981;215:133–142.

Meier PJ. The bile salt secretory polarity of hepatocytes. J Hepatol. 1989;9:124–129.

Mitaka T, Mikami M, Sattler GL, Pitot HC, Mochizuki Y. Small cell colonies appear in the primary culture of adult rat hepatocytes in the presence of nicotinamide and epidermal growth factor. Hepatology. 1992a;16:440–447.

Mitaka T, Sattler GL, Pitot HC, Mochizuki Y. Characteristics of small cell colonies developing in primary cultures of adult rat hepatocytes. Virchows Arch B Cell Pathol Incl Mol Pathol. 1992b;62:329–335.

Mitaka T, Kojima T, Mizuguchi T, Mochizuki Y. Growth and maturation of small hepatocytes isolated from adult rat liver. Biochem Biophys Res Commun. 1995;214:310–317.

Mitaka T, Sato F, Mizuguchi T, Yokono T, Mochizuki Y. Reconstruction of hepatic organoid by rat small hepatocytes and hepatic nonparenchymal cells. Hepatology. 1999;29:111–125.

Mitaka T, Sato F, Ikeda S, Sugimoto S, Higaki N, Hirata K, Lamers WH, Mochizuki Y. Expression of carbamoylphosphate synthetase I and glutamine synthetase in hepatic organoids reconstructed by rat small hepatocytes and hepatic nonparenchymal cells. Cell Tissue Res. 2001;306:467–471.

Miyairi M, Oshio C, Watanabe S, Smith CR, Yousef IM, Phillips MJ. Taurocholate accelerates bile canalicular contractions in isolated rat hepatocytes. Gastroenterology. 1984;87:788–792.

Morris CE. Mechanosensitive ion channels. J Membr Biol. 1990;113:93–107.

Mortimore GE. Schworer CM. Application of liver perfusion as an in vitro model in studies of intracellular protein degradation. Ciba Found Symp. 1979;75:281–305.

Oshio C, Phillips MJ. Contractility of bile canaliculi: implications for liver function. Science. 1981;212:1041–1042.

Phillips MJ, Oshio C, Miyairi M, Katz H, Smith CR. A study of bile canalicular contractions in isolated hepatocytes. Hepatology. 1982;2:763–768.

Phillips MJ, Oshio C, Miyairi M, Watanabe S, Smith CR. What is actin doing in the liver cell? Hepatology. 1983;3:433–436.

Robenek H, Jung W, Gebhardt R. The topography of filipin-cholesterol complexes in the plasma membrane of cultured hepatocytes and their relation to cell junction formation. J Ultrastruct Res. 1982;78:95–106.

Sakisaka S, Ng OC, Boyer JL. Tubulovesicular transcytotic pathway in isolated rat hepatocyte couplets in culture. Effect of colchicines and taurocholate. Gastroenterology. 1988;95:793–804.

Sormunen R, Eskelinen S, Lehto VP. Bile canaliculus formation in cultured HEPG2 cells. Lab Invest. 1993;68:652–662.

Sugimoto S, Mitaka T, Ikeda S, Harada K, Ikai I, Yamaoka Y, Mochizuki Y. Morphological changes induced by extracellular matrix are correlated with maturation of rat small hepatocytes. J Cell Biochem. 2002;87:16–28.

Watanabe S, Miyairi M, Oshio C, Smith CR, Phillips MJ. Phalloidin alters bile canalicular contractility in primary monolayer cultures of rat liver. Gastroenterology. 1983;85:245–253.

Watanabe S, Phillips MJ. $Ca^{2+}$ causes active contraction of bile canaliculi: direct evidence from microinjection studies. Proc Natl Acad Sci U S A. 1984;81:6164–6168.

Watanabe S, Tomono M, Takeuchi M, Kitamura T, Hirose M, Miyazaki A, Namihisa T. Bile canalicular contraction in the isolated hepatocyte doublet is related to an increase in cytosolic free calcium ion concentration. Liver. 1988;8:178–183.

Watanabe N, Tsukada N, Smith CR, Phillips MJ. Motility of bile canaliculi in the living animal:

implications for bile flow. J Cell Biol. 1991;113:1069–1080.

Watanabe S, Smith CR, Phillips MJ. Coordination of the contractile activity of bile canaliculi. Evidence from calcium microinjection of triplet hepatocytes. Lab Invest. 1985;53:275–279.

Wood RL. An electron microscope study of developing bile canaliculi in the rat. Anat Rec. 1965;151:507–529.

# Chapter 4

# Coordinated movement of bile canalicular networks reconstructed by rat small hepatocytes

## 4-1 Introduction

Liver regeneration is a unique capability of the liver *in vivo* (Fausto, 2000; Michalopoulos *et al.*, 1997). It is well known that hepatocytes can proliferate to recover the lost tissue after two-thirds partial hepatectomy. Although hepatocytes *in vivo* have the potential for liver regeneration, it has been very difficult to reconstruct hepatic tissues *in vitro*. However, reconstruction of hepatic organoids is needed for the transplantation of tissue-engineered organs (Sundbck *et al.*, 2000).

Recently, two approaches for the culture of hepatic organoids have been demonstrated (Michalopoulos *et al.*, 1999; Mitaka *et al.*, 1999). Hepatic progenitor cells, identified as proliferating cells with hepatic characteristics, were found and named SHs (Mitaka *et al.*, 1992a, b, 1995). Although primary hepatocytes rapidly lose their function with time in culture, SHs can reconstruct hepatic organoids interacting with hepatic NPCs, such as LECs and stellate cells (Mitaka *et al.*, 1999). For hepatic organoid formation, ECM, especially components of basement membrane such as laminin and type IV collagen, were shown to be important and treatment with EHS gel (Matrigel™) could induce the maturation of SHs (Sugimoto *et al.*, 2002). On the other hand, Michalopoulos *et al.* (1999) reported that they developed hepatic organoids consisting of hepatocytes and fenestrated endothelium when hepatic cells on polystyrene beads were cultured in roller bottles. Furthermore, when cells isolated from a rat liver were cultured in the roller bottles with rotation, the cells formed a characteristic and reproducible tissue architecture composed of a superficial layer of biliary epithelial cells, an intermediate layer of connective tissue and hepatocytes, and a basal layer of endothelial cells (Michalopoulos *et al.*, 2001). These experiments demonstrated the formation

of hepatic organoids, and revealed the structural features of the organoids. Although the formation of hepatic organoids has been morphologically investigated, tissue-level functions of the cells are not well analyzed.

Bile canalicular contraction is one of the tissue-level functions of the liver, because it is achieved by the coordination of adjacent hepatocytes. BC are tubular structures that form the most proximal channels of the biliary tree and carry bile secreted by hepatocytes. To expel bile through BC, a series of hepatocytes along BC must contract in a coordinated fashion. Therefore, the hepatic tissue needs to have communications and integration among neighboring hepatocytes.

It has been difficult to reconstruct hepatic organoids possessing BC networks with motile activity. However, it is recently demonstrated that SHs could form BC with motility and secretory function (Chapter 3). BC were formed and three-dimensionally extended BC networks were developed in the hepatic organoids. In the reconstructed tissues, BC could continuously contract and dilate. Although the motility of BC was demonstrated, coordination of the movements was not analyzed. To understand the mechanism of bile transportation, the coordination of BC movements should be clarified. Thus, in the present study movements of BC formed in the hepatic organoids were analyzed and it was verified that the BC movements were coordinated. It is revealed that BC contractions occurring in different regions could act synchronously, and that intercellular communication through gap junctions might be important for the coordination of BC movements.

## 4-2 Results

### 4-2-1 Bile canalicular formation and quantification of the bile canalicular area (2-4, 2-7-1)

SHs started to proliferate 2–3 days after inoculation and then formed colonies. Although SH colonies appeared as flat clusters in the early period of the culture, they expanded to form large colonies, some of which were composed of piled-up cells. The piled-up cells had the appearance of mature hepatocytes. In the areas between the piled-up cells BC formed and developed into anastomosing networks (Chapter 3). One-fourth of the SH colonies displayed the piled-up cells that formed BC by day 30 (Mitaka *et al.*, 2001).

BC networks were detected as translucent belts under phase-contrast microscopy (Fig. 4-1A). It was

ascertained whether the translucent belts represented the width of the BC using FD as a probe to visualize BC networks. The BC in the piled-up SHs are functional as an apical domain including the secretory functions for bilirubin and fluorescein (Chapter 3). In addition, secreted fluorescein was not diffused after rinsing with the medium because the BC were sealed by tight junctions as previously reported by immunocytochemistry for tight junction-associated protein ZO-1 (Chapter 3). Therefore, secreted fluorescein can indicate the width of the BC. The fluorescent intensity in intercellular spaces was detected after FD treatment (Fig. 4-1B). The fluorescein localized in the restricted areas of intercellular spaces that represented BC networks. Under phase-contrast microscopy, the merged images showed translucent belts that coincided with fluorescent networks (Fig. 4-1C). These results suggested that the translucent belts observed under phase-contrast microscopy corresponded exactly to the width of the BC. Therefore, BC movements were analyzed based on variations in the translucent areas under phase-contrast microscopy. In order to quantify the translucent areas, thresholding was applied to phase-contrast micrographs to coincide with the translucent belts (Fig. 4-1D). This thresholding was feasible because the thresholding images (red area, Fig. 4-1D) corresponded to the fluorescent images (green area, Fig. 4-1B).

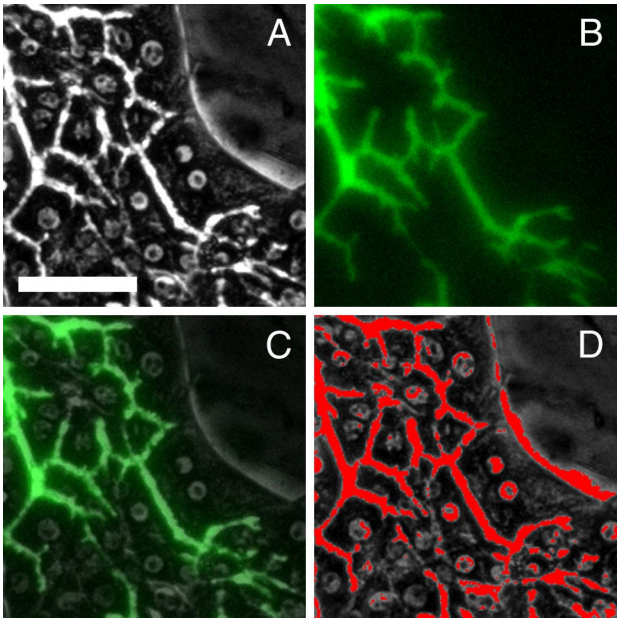


Fig. 4-1 Corresponding images of an SH colony in which piled-up cells formed BC networks. A: phase-contrast micrograph of the cells at day 30 shows translucent networks between the cells representing BC. B: fluorescent image of the cells after FD treatment shows metabolized fluorescein secreted into BC. C: the merged image of the phase-contrast and fluorescent image indicates that the translucent networks under phase-contrast microscopy coincide with the fluorescent networks of fluorescein. D: the merged image of the phase-contrast and thresholding images. Thresholding to the phase-contrast image was applied to clarify the region of the BC, and is shown in red. Scale bar, 50 μm.

## 4-2-2 Bile canalicular movements in the piled-up colonies (2-4, 2-3-2)

Time-lapse microscopy revealed that BC movements occurred in the piled-up cells. Fig. 4-2 shows an SH colony composed of the piled-up cells that form the BC. In the region indicated with rectangle *a* in Fig. 4-2A, the left BC contracted in the early period of the experiment (left arrowheads, Figs. 4-2B, D). The right BC contracted next (right arrowheads, Figs. 4-2D, F). On the other hand, BC in rectangle *b* remained wide or dilated while the BC in rectangle *a* contracted (arrowheads, Figs. 4-2C, E, G, I). In addition, the cystic structure that formed in the tip of the colony (asterisk, Fig. 4-2A) dilated following the BC contraction in rectangle *a* and the dilation in rectangle *b* (data not shown). These sequential movements of BC suggested a flow of the fluid toward the cystic structure.

Some BC contractions were synchronized (Fig. 4-3). BC in the top rectangle (rectangle, Fig. 4-3A) contracted synchronously when the BC in the lower rectangle (rectangle, Fig. 4-3A) contracted (arrowheads, Figs. 4-3C–F). To clarify this phenomenon, the BC movements were analyzed using the thresholding methods. The thresholding was applied to each image of the time-lapse series and ROIs were set on each image (a, b, Fig. 4-3B). Variations of the normalized thresholding areas within each ROI are graphically shown in Fig. 4-3G. The BC contraction that was observed in the time-lapse images was consistent with the variations of the normalized thresholding area in the graph (between 82 min and 107 min, Fig. 4-3G). The maximum amplitude of each graph (amp, Fig. 4-3G), which indicates the degree of the BC movement in each ROI, was calculated by subtracting the minimum value (min, Fig. 4-3G) from the maximum value (max, Fig. 4-3G) in the experimental period.

In the present experiment 68 ROIs of BC in 17 colonies were analyzed. Some BC dramatically contracted or dilated, others showed small morphological changes. Each BC had its own motility, which was represented by a maximum amplitude. To show the motility of the BC, the maximum amplitude of each BC movement was calculated and represented in the form of a histogram (Fig. 4-4). The maximum amplitude had a wide range, varying from 0.2 to 1.8, and no frequency at the range of 0.0–0.2. These results indicate that the BC of each colony had various kinds of motility, and all BC had motility of at least 0.2 in the experimental period. In addition, the most probable motility was in the range of 0.4–0.6 (Fig. 4-4), which suggests the area was increased or decreased by 40–60% when compared with the initial BC area.

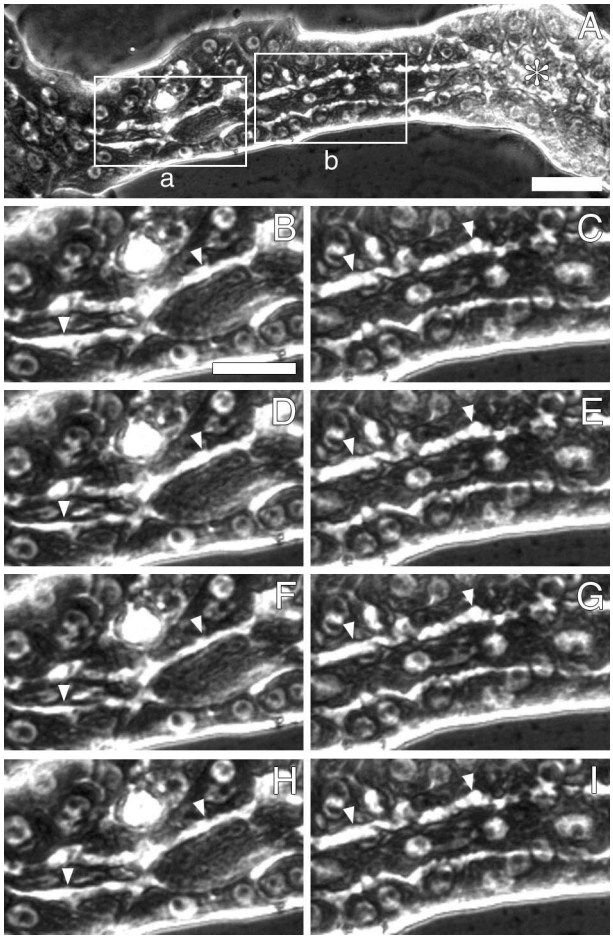


Fig. 4-2 Phase-contrast micrographs of the cells that form BC. A: Parallel BC developed in the piled-up cells at day 27. B–I: Enlarged time-lapse images of the same part indicated by the rectangle *a* (B, D, F, H) and *b* (C, E, G, I) in A. The total number of the time-lapse images was 2160. The frame numbers are 75 (B, C), 79 (D, E), 82 (F, G) and 100 (H, I), respectively. BC contractions were detected in the sequential images (arrowheads). Scale bars, 50 μm (A) and 30 μm (B).

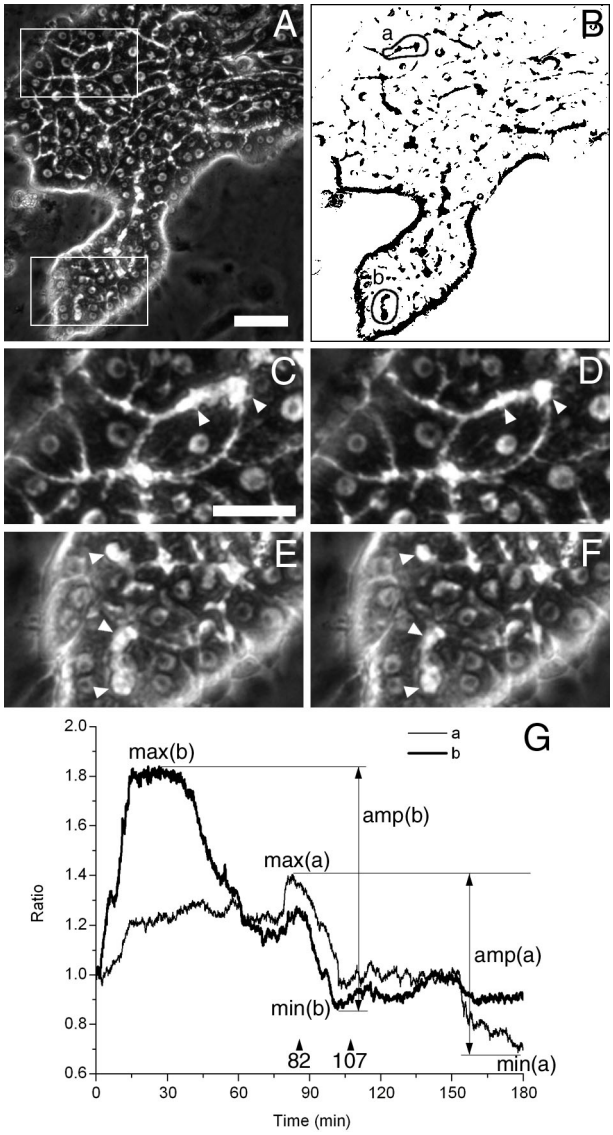


Fig. 4-3 Phase-contrast micrographs and graphical representation of BC movements. A: Phase-contrast micrograph of the piled-up cells at day 23. B: Thresholding was applied to A. ROIs were set on the image (a, b). C–F: Enlarged images of the same parts indicated by rectangles in A (top rectangle: C–D, lower rectangle: E–F). Images correspond to the times of 82 min (C, E) and 107 min (D, F), indicated by arrowheads in G. G: Graphical representation of BC movements in two ROIs (a, b, B). The thresholding area within the ROIs of each time was calculated and the values were normalized by dividing each value by the initial value. Maximum amplitude of each graph is shown by vertical arrows designated amp (a) and amp (b). Scale Bars, 50 μm (A) and 30 μm (C).

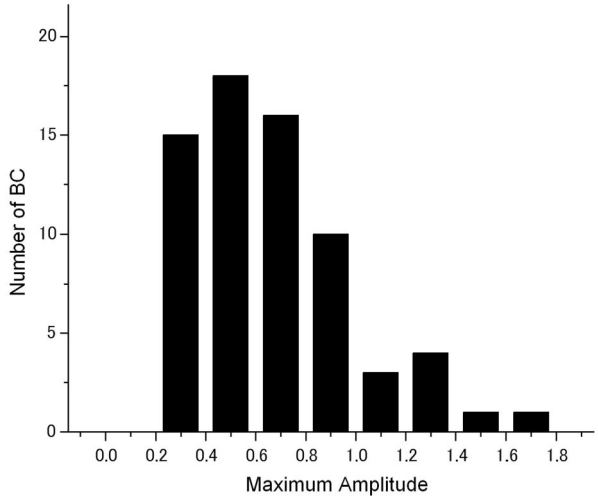


Fig. 4-4 Maximum amplitude histogram of the total BC in ROI. In this experiment, 68 regions of BC (4 ROIs/colony and 17 colonies) were analyzed and the maximum amplitude of the graph in the experimental period (3 hours) was measured. Note that there is a peak at the maximum amplitude of 0.4–0.6. There is no frequency at the maximum amplitude of 0.0–0.2.

## 4-2-3 Coordination of the bile canalicular movements (2-3-2, 2-4)

Analysis of the time-lapse images showed that coordination of BC contractions and dilations appeared to be present. BC movements were classified according to the speed of movement: BC movements within 10 min (fast) and those that continued for more than 30 min (slow). BC movements were also classified according to whether the movements were coordinated or not. Visual analysis of the movie showed that all colonies had BC movements, and 94% of those were coordinated (Table 4-1).

By further observation of time-lapse images, it was found that BC movements could be classified into 3 types. Therefore, 3 typical types of BC movement were shown in Fig. 4-5 although 17 colonies were analyzed. Fig. 4-5 shows BC movements in 3 colonies in which different types of movement occurred. BC dramatically contracted and dilated as shown in Figs. 4-5C, F and I, and coordination of movements was observed. The coordination was observed in the contractions of both fast and slow types and the observation periods are indicated by the closed box (p1–9, Figs. 4-5C, F, I). For quantitative analysis of the coordination, correlation coefficients during periods p1–9 were calculated, and the values are shown in Table 4-2. Thus, Fig. 4-5 shows the BC movements and the values in Table 4-2 show the degree of the coordination corresponding to Fig. 4-5. In this study, BC movements with an absolute correlation coefficient value of more than 0.66, the average value, were presumed to be coordinated. At least one correlation coefficient between the ROIs was more than 0.66 in all periods (asterisks, Table 4-2), which indicates that BC movements occurring in neighboring areas were coordinated. 1) Figs. 4-5A–C show the BC movements which occurred throughout the colony. There were three contractions in the experimental period (arrowheads, Fig. 4-5C). Fig. 4-5C and Table 4-2 show that in the contraction in period p1 (p1, Fig. 4-5C), the values of the correlation coefficients between #1–#4, #2–#3, #2–#4 and #3–#4 were 0.67, 0.93, 0.96 and 0.97, respectively (p1, Table 4-2). Similarly, in the contractions at periods p2 and p4 the correlation coefficients between each ROI were more than 0.86 (p2, p4, Table 4-2). Thus, although the BC in region #1 was about 10 cells distant from that in region #4, BC around the areas including #1, #2, #3 and #4 were synchronously moving. 2) Figs. 4-5D–F show the BC movements, speed of which was relatively fast, and cellular contraction can be observed. The correlation coefficients at periods p5 and p6 showed negative values, proving the BC dilations (#4) were followed by a BC contraction (#1) in the neighboring area (p5–6, Table 4-2). 3) Figs. 4-5G–I show the BC movements, the speed of which was relatively slow.

The correlation coefficient between #1–#3 at the period p8 was positive, while that at the period p9 was negative (p8–9, Table 4-2). These results indicated that BC both in #1 and #3 dilated at period p8, although the BC in #1 contracted at period p9 while BC in #3 dilated.

Table 4-1 Motilities of the BC networks in SH colonies. Each value indicates the number of colonies in which BC movements (upper) or coordinated movements (lower) occurred in the experimental period. Percentages are in brackets. BC movements of 17 colonies were classified into two types depending on the rate of movement, BC movements within 10 min (fast) and those of more than 30 min (slow).

| | Fast | | Slow | | Either |
|---|---|---|---|---|---|
| | Contraction | Dilatation | Contraction | Dilatation | Either |
| Movement | 10 (59%) | 3 (18%) | 11 (65%) | 16 (94%) | 17 (100%) |
| Coordination | 9 (53%) | 3 (18%) | 8 (47%) | 9 (53%) | 16 (94%) |

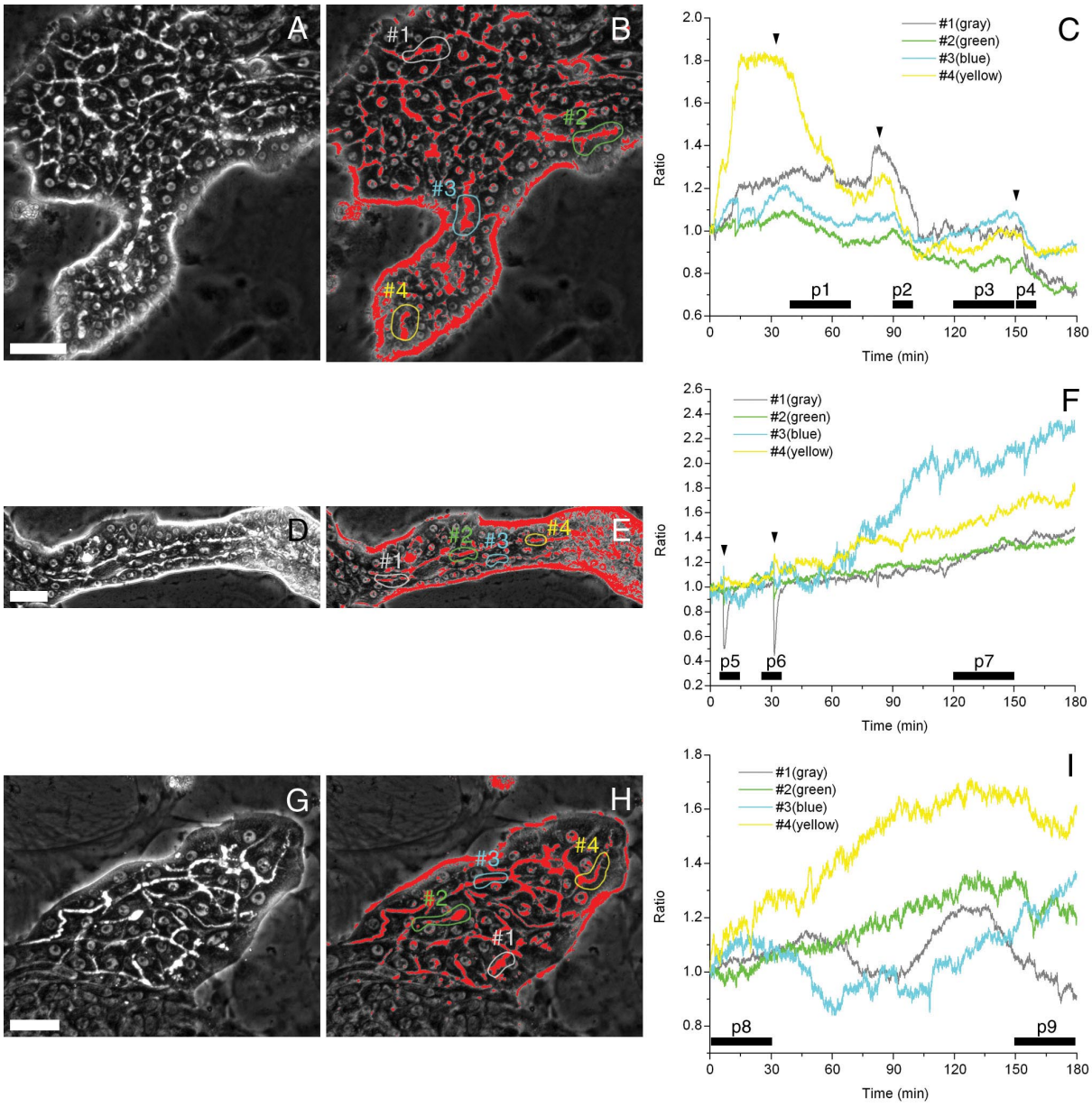


Fig. 4-5 Corresponding phase-contrast (A, D, G), thresholding images (B, E, H), and graphs (C, F, I). Thresholding was applied to phase-contrast images of the piled-up cells at A: day 23, D: day 27 and G: day 23, and B, E, H: the merged images of each phase-contrast and thresholding image are shown. C, F, I: The graphs indicate the variations of the thresholding area in each ROI set on the thresholding image (#1–4, B, E, H), normalized by division by the value at the initial time in the experimental period. Closed boxes (p1–9, C, F, I) indicate observation periods in which correlation coefficients were calculated. Arrowheads indicate contractions. Scale bars, 50 μm (A, D, G).

Table 4-2 Correlation coefficients between BC movements in different ROIs. Correlation coefficients between pairs of thresholding areas in each ROI (#1–4, Figs. 4-5B, E, H) during periods indicated by a closed box (p1–9, Figs. 4-5C, F, I) were calculated. Coefficients whose absolute values were more than 0.66 are presumed to be coordinated (asterisks).

| | | #1 | #2 | #3 | #4 |
|---|---|---|---|---|---|
| p1 | #1 | 1.00 | | | |
| | #2 | 0.65 | 1.00 | | |
| | #3 | 0.61 | 0.93* | 1.00 | |
| | #4 | 0.67* | 0.96* | 0.97* | 1.00 |
| p2 | #1 | 1.00 | | | |
| | #2 | 0.93* | 1.00 | | |
| | #3 | 0.88* | 0.92* | 1.00 | |
| | #4 | 0.96* | 0.95* | 0.94* | 1.00 |
| p3 | #1 | 1.00 | | | |
| | #2 | 0.12 | 1.00 | | |
| | #3 | -0.15 | 0.41 | 1.00 | |
| | #4 | -0.17 | 0.47 | 0.92* | 1.00 |
| p4 | #1 | 1.00 | | | |
| | #2 | 0.90* | 1.00 | | |
| | #3 | 0.95* | 0.88* | 1.00 | |
| | #4 | 0.96* | 0.86* | 0.95* | 1.00 |
| p5 | #1 | 1.00 | | | |
| | #2 | 0.43 | 1.00 | | |
| | #3 | -0.19 | -0.47 | 1.00 | |
| | #4 | -0.67* | -0.16 | -0.24 | 1.00 |
| p6 | #1 | 1.00 | | | |
| | #2 | 0.95* | 1.00 | | |
| | #3 | 0.35 | 0.26 | 1.00 | |
| | #4 | -0.89* | -0.92* | -0.13 | 1.00 |
| p7 | #1 | 1.00 | | | |
| | #2 | 0.83* | 1.00 | | |
| | #3 | 0.02 | 0.04 | 1.00 | |
| | #4 | 0.85* | 0.86* | 0.06 | 1.00 |
| p8 | #1 | 1.00 | | | |
| | #2 | 0.50 | 1.00 | | |
| | #3 | 0.61 | 0.06 | 1.00 | |
| | #4 | 0.74* | 0.70* | 0.40 | 1.00 |
| p9 | #1 | 1.00 | | | |
| | #2 | 0.41 | 1.00 | | |
| | #3 | -0.75* | -0.27 | 1.00 | |
| | #4 | 0.69* | 0.57 | -0.40 | 1.00 |

### 4-2-4 Cytochalasin B treatment (2-3-2, 2-5-5)

CB inhibits polymerization of actin by binding to the barbed ends of actin filaments (Brown *et al.*, 1981; Cooper, 1987; Flanagan *et al.*, 1980). The agent has been widely used to study the role of actin in biological processes (Cooper, 1987). Numerous actin filaments have been observed around the BC in hepatocytes, which suggests that they play an important role in BC contraction (Phillips *et al.*, 1983). Therefore, the role of actin in BC contraction was studied using CB.

As shown in Fig. 4-6, the morphology of BC in piled-up cells treated with CB dramatically changed. The BC started to dilate soon after the addition of CB. When the cells were treated with 1.0 μg/ml CB, BC became progressively dilated for 1 hour, and then maintained that width for more than 2 hours (Figs. 4-6A–C). On the other hand, when the cells were treated with 5.0 μg/ml CB, BC became progressively dilated throughout the experimental period, and cystic structures were observed (arrowheads, Fig. 4-6F inset). Cystic dilation of BC was noticeable near the edges of the colony. Remarkable dilations of the BC network were observed at 60 min after addition of CB (Fig. 4-6E), and canalicular structures changed into cystic ones after 180 min (Fig. 4-6F). The motility of BC was reduced, and no contraction was observed when the cells were treated with CB at concentrations of more than 1.0 μg/ml. In contrast, when the cells were treated with low concentration (0.1 μg/ml) of CB, no remarkable dilatations of BC were observed (data not shown).

As shown in Fig. 4-7, actin filaments were abundant around BC in the cells treated with each concentration of CB. The actin filaments around the BC revealed narrow spaces between them in cells without CB treatment (arrowheads, Fig. 4-7A). On the other hand, when the cells were treated with 1.0 μg/ml CB, the actin filaments around the BC were wider (arrowheads, Fig. 4-7B). In addition, when the cells were treated with a high concentration (5.0 μg/ml) of CB, the actin filaments showed indented distribution around the dilated BC (Fig. 4-7C). Some actin filaments were also distributed in the cytoplasm (asterisks, Fig. 4-7C), and increased intensity of positivity was heterogeneously observed along the BC (arrowheads, Fig. 4-7C).

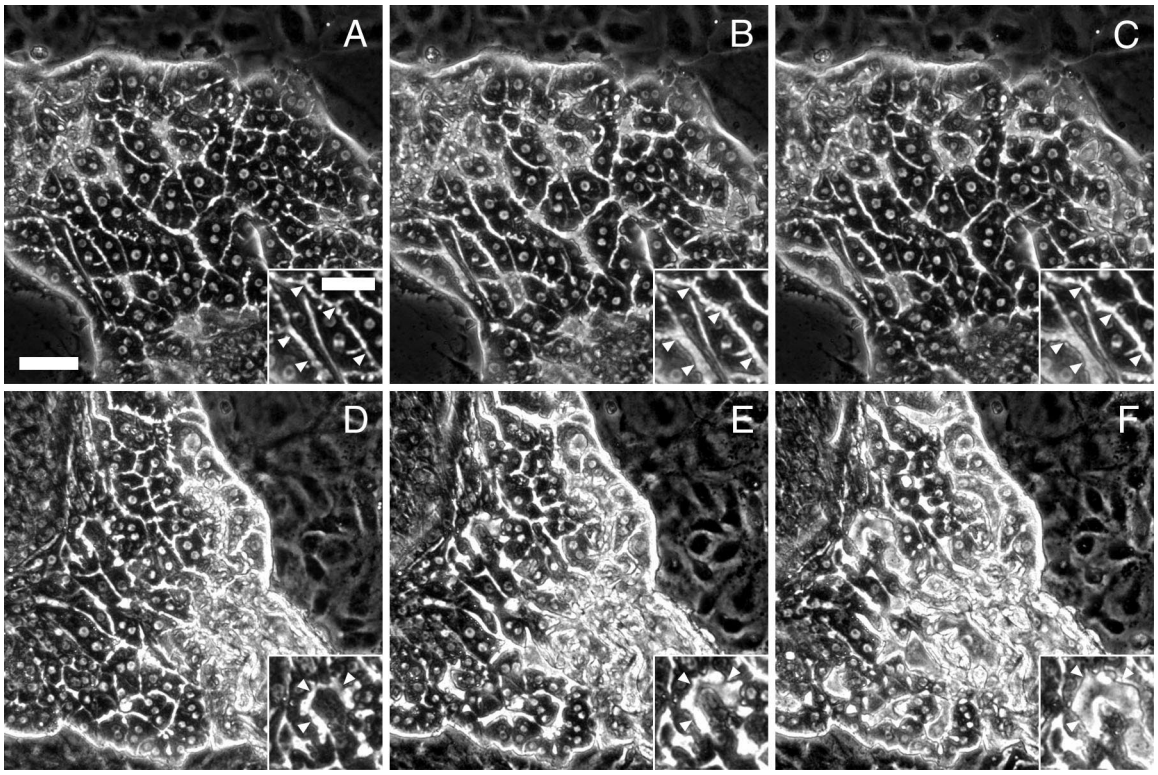


Fig. 4-6 Time series phase-contrast images of the cells reconstructing BC networks at day 43 under administration of CB (1.0 μg/ml: A–C, and 5.0 μg/ml: D–F). Corresponding images of the cells after administration of CB shows dilation of BC networks. A, D: immediately after administration, B, E: after 60 min, C, F: after 180 min. Insets in each figure show magnified images of corresponding BC (arrowheads, A–F insets). Scale bars, 50 μm (A) and 30 μm (A inset).

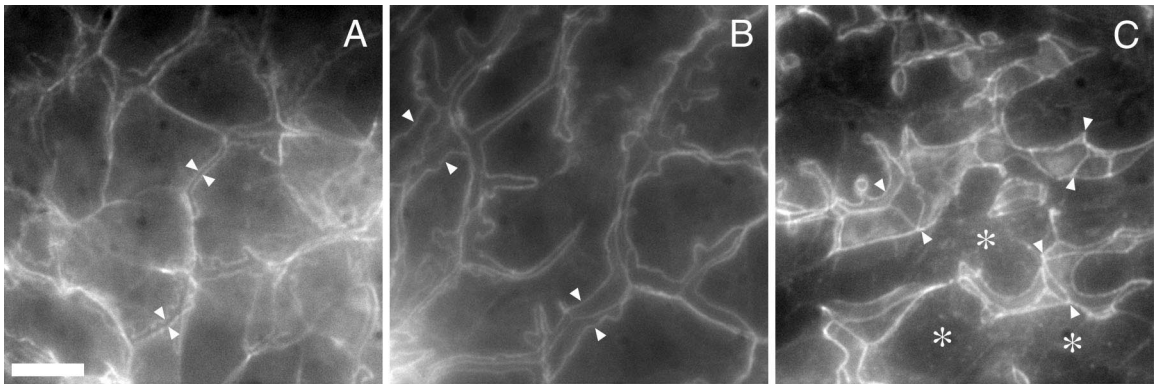


Fig. 4-7 The localization of actin filaments in the piled-up cells reconstructing BC networks at day 43. A: the control cells show intensive expression of actin filaments around BC (arrowheads). B: administration of 1.0 μg/ml CB causes wide spaces between actin filaments coinciding with dilation of BC (arrowheads). C: the actin filaments of the cells treated with 5.0 μg/ml CB show indented distribution around dilated BC (arrowheads). In addition, dotted intensities in the cytoplasm (asterisks) and heterogeneity of the intensity around BC are observed. Scale bar, 20 μm.

## 4-2-5 Immunocytochemistry for connexin 32 (2-5-4)

Immunocytochemistry for Cx 32 was carried out to determine whether the piled-up cells had the ability to communicate via gap junctions. Immunocytochemistry for actin was also carried out to visualize cell–cell borders. Actin in the piled-up cells was intensively stained around the BC (inset, Fig. 4-8C). Cortical actin was observed in those SHs that form no BC between the cells (Fig. 4-8G inset). Dotted expression of Cx 32 was distributed on basolateral membranes that coincided with the translucent belts formed in the piled-up cells, although the expression had heterogeneity (Figs. 4-8A–D). By contrast, no Cx 32 was expressed in the cytoplasm of the flat cells and no localization was observed (Figs. 4-8E–H).

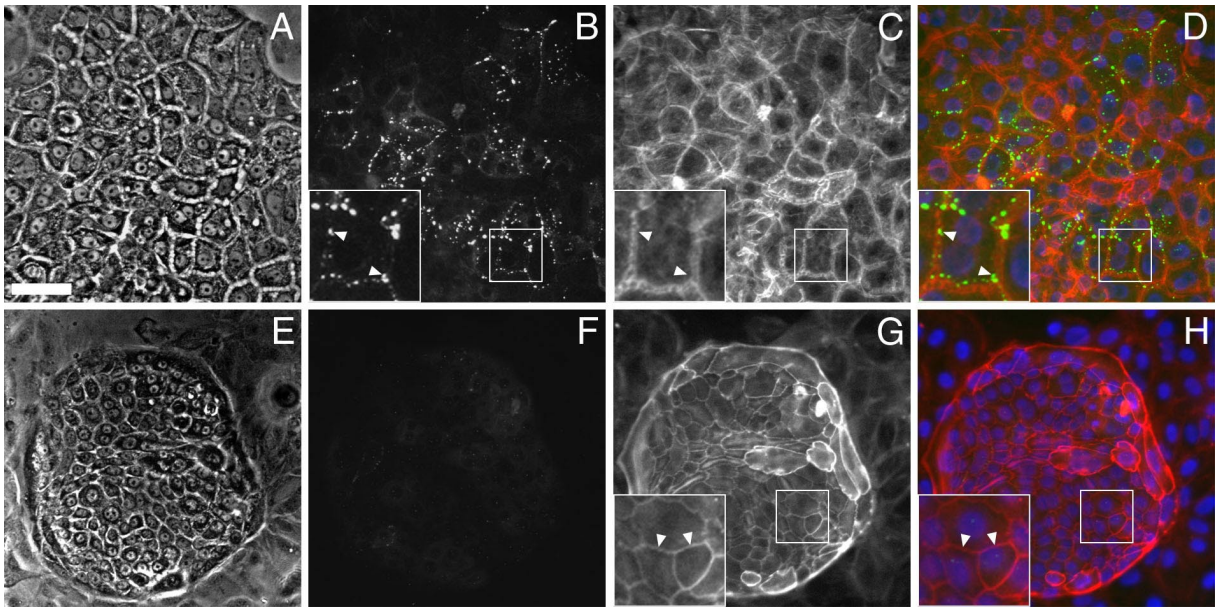


Fig. 4-8 The localization of Cx 32 protein in the flat cells and piled-up cells reconstructing BC. Triple immunostaining for Cx 32 (green), actin (red) and DAPI (blue) was carried out. Phase-contrast micrographs of the cells at day 27 (A) and day 26 (E). Corresponding images of Cx 32 (B, F), actin (C, G), and the merged images of Cx 32, actin, and DAPI (D, H). Dotted expression of Cx 32 was observed along the BC (B–D insets), whereas no expression of Cx 32 was observed in the flat cells (F). Scale bar, 50 μm.

## 4-2-6 Secretion of microinjected dye in piled-up cells [2-7-2]

CMFDA was microinjected into one of the piled-up cells in the colony (asterisk, Fig. 4-9A). It was metabolized within the injected cell and the metabolite was excreted into BC by a transporter such as MRP2. As mentioned in chapter 3, MRP2 is uniformly expressed on BC membranes of the piled-up cells. As shown in Fig. 4-9C, soon after the injection bright fluorescence was observed in the cytoplasm of the cell and a line of fluorescence extended in the direction of the tip of the colony. Two and half minutes later, the dye was clearly detected in 4 cells distant from the injected cell (arrowhead, Fig. 4-9E). The intensity was observed within BC branching toward the tip of the colony. In the piled-up cells, Cx 32 was expressed along the BC. Therefore, the dye might have been transferred through gap junctions although cells adjacent to the injected one were only faintly stained. The fluorescence intensity increased in the route of the transferred dye for several minutes and then gradually decreased.

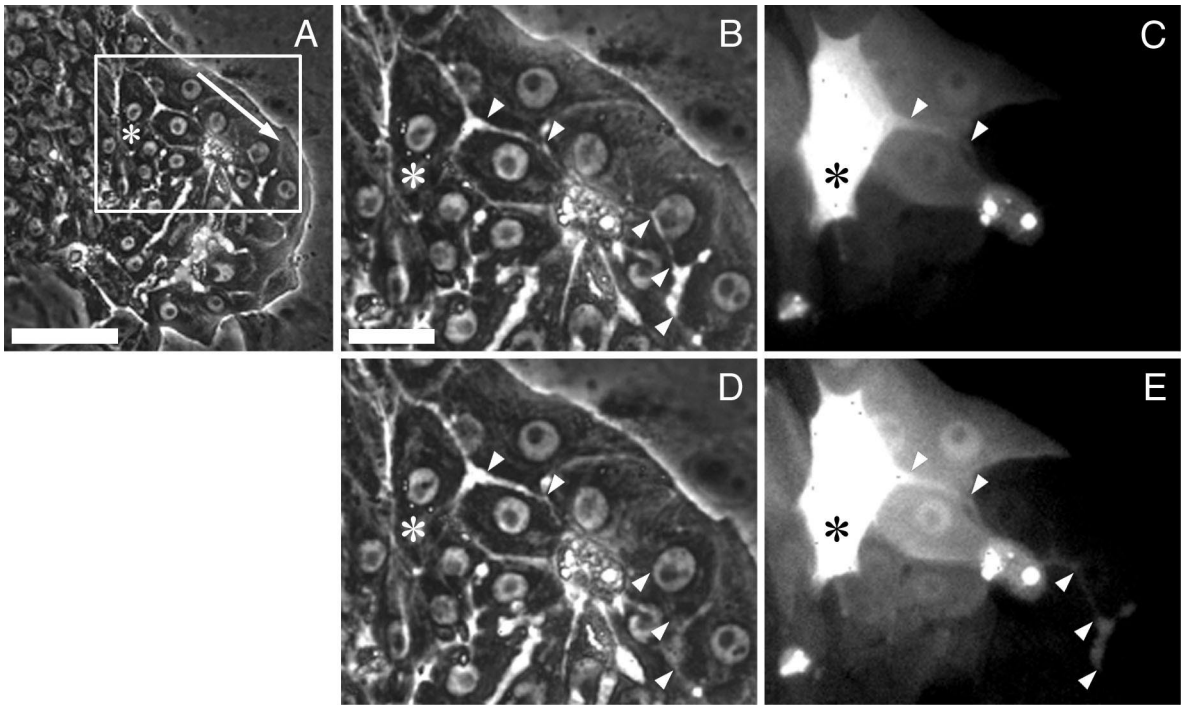


Fig. 4-9 Fluorescent images of microinjected dye in the piled-up cells reconstructing BC. CMFDA was microinjected in a cell (asterisk, A) and the fluorescent image was immediately photographed (C). One time-lapse image (2.5 min after C) is shown in (E). Phase-contrast photographs corresponding to the fluorescent images C and E are shown in B and D, respectively. The arrow shows the observed direction of fluorescein transportation. The arrowheads show the fluorescent line secreted from an injected cell. The transported fluorescein within BC is elongated to the tip of the colony (arrowheads, C, E). Scale bars, 50 μm (A) and 20 μm (B).

## 4-3 Discussion

### 4-3-1 Coordination of bile canalicular contraction

The BC form a pathway to transport bile secreted by hepatocytes. Transportation of bile is very important because disorders of bile transportation are associated with cholestasis. Therefore, motility of BC is necessary for the physiological function. In addition, coordination of BC movements is sequential and synchronous, and therefore essential for transporting bile into bile ducts. BC contractions were first observed in hepatocyte couplets, intact pairs of hepatocytes isolated from rat livers (Oshio *et al.*, 1981). Subsequent studies using couplets demonstrated BC contractions (Phillips *et al.*, 1982; Smith *et al.*, 1985), the $Ca^{2+}$-induced BC contractions (Watanabe *et al.*, 1984) and some agents to increase the BC contractions (Kamimura *et al.*, 1993; Miyairi *et al.*, 1984; Watanabe *et al.*, 1988). Although hepatocyte couplets are useful models for analysis of BC contractions, coordination of adjacent hepatocytes along BC could not be investigated because BC in couplets form a closed sphere, whereas the BC *in vivo* form a tubular structure. BC movements and the coordination of these movements have not been investigated in studies that investigated BC formation using the collagen gel sandwich method (LeCluyse *et al.*, 1994; Talamini *et al.*, 1997) and hepatocyte spheroid culture (Koide *et al.*, 1990; Landry *et al.*, 1985). Therfore, this BC network made it possible to analyze the coordination of the SHs required for tissue-level function.

In the present experiment BC movements were analyzed to determine whether they were coordinated. Time-lapse microscopy revealed sequential contraction along the BC (Fig. 4-2) and coordination of BC contraction (Fig. 4-5). The degree of the coordination was quantified to calculate the correlation coefficient. Although each BC had its own motility (Fig. 4-4), the values of the correlation coefficients during the observed periods (p1–9, Fig. 4-5) were more than 0.66, which suggests coordination of the BC contraction (Fig. 4-5, Table 2). These results suggest that individual cells forming BC act in a coordinated manner to achieve an integrated function for the transportation of bile.

### 4-3-2 Intercellular communication for the coordination

Various intracellular processes in the liver are known to be coordinated by second messengers such as cAMP, cytosolic $Ca^{2+}$ and inositol trisphosphate (Clair *et al.*, 2001; Hayakawa *et al.*, 1990; Saez *et al.*,

1989; Tordjmann *et al.*, 1997; Watanabe *et al.*, 1985). An organ-level response to hormonal stimuli may be produced by integration of signals among hepatocytes within the liver plate (Nathanson *et al.*, 1994, 1995; Tordjmann *et al.*, 1998). Nathanson *et al.* (1999) reported that the organization of second messenger signals across the hepatic lobule played an important role in hormonal regulation of bile secretion in the perfused liver. Serriere *et al.* (2001) reported that unidirectional agonist-induced intercellular $Ca^{2+}$ waves via gap junctions might drive canalicular peristalsis and increase bile flow.

To reconstruct hepatic tissues, proliferation and interaction of SHs and NPCs are essential. It has been reported that hepatocytes can maintain viability for extended periods when the cells form 3D aggregates like spheroids (Koide *et al.*, 1990; Landry *et al.*, 1985). Although the hepatocytes in spheroids could express differentiated functions and form BC-like structures, apical domains of these cells were gradually lost with time in culture (Abu-Absi *et al.*, 2002). On the other hand, after SHs proliferate and form colonies within a couple of weeks, matured SHs appear on the colonies, in which BC networks are well developed.

In the present experiment the cellular ability for the intercellular communication was investigated by immunostaining gap junctional protein Cx 32. The piled-up cells expressed Cx 32 in the basolateral membranes along BC networks although no expression of Cx 32 in the basolateral membranes was observed in the proliferating SHs that were not mature and formed no BC (Fig. 4-8). Cx 32 was expressed heterogeneously along BC networks (Fig. 4-8), which suggested the heterogeneity of BC movements. BC networks started to form in piled-up colonies. As these piled-up areas developed in the colony, the networks gradually expanded. Thus, considering the temporal formation of the BC, BC networks in piled-up colonies might be heterogenous. In addition, analysis of the BC movements revealed that even within a colony there were regions where the BC could act in a coordinated fashion, which was also consistent with the heterogenous expression of Cx 32. Furthermore, treatment with A23187, a $Ca^{2+}$ ionophore, transiently induced coordinated BC contraction (data not shown). Thus, coordination of neighboring and apposing SHs may integrate the action of the whole BC network by second messengers such as $Ca^{2+}$ and inositol trisphosphate via gap junctions.

## 4-3-3 The role of actin in bile canalicular contraction

The role of actin in BC contraction has been investigated using CB. When CB is administered to rats,

dilated BC are visualized in the liver (Watanabe *et al.*, 1991). The dilation is also observed in hepatocyte couplets (Phillips *et al.*, 1983) and hepatocyte spheroids (Abu-Asbi *et al.*, 2002; Yumoto *et al.*, 1996). In the present experiment the morphology of BC networks treated with CB dramatically changed to induce marked dilations of BC. This result showed morphological phenomena similar to those observed when 5.0 μg/ml CB was infused through portal vein and saccular dilatations of BC were induced in the liver (Watanabe *et al.*, 1991). Immunocytochemical staining also revealed that CB treatment caused wide spaces between actin filaments around BC. The pericanalicular actin filaments were present around dilated BC. These results are consistent with the dilations of BC observed under phase-contrast microscopy.

These results may indicate the involvement of actin filaments in the mechanism of BC contraction. Actin filaments can interact with myosin, which is regulated by $Ca^{2+}$-calmodulin-dependent phosphorylation. In hepatocytes, myosin is abundant around BC, and the co-localization of actin and myosin was reported in a model of an isolated BC compartment (Tsukada *et al.*, 1993). In addition, ML-9, a myosin light-chain inhibitor, inhibited BC contraction in hepatocyte couplets. Thus, BC contraction may be achieved by coordination of the actin-myosin system, which is regulated by second messengers via gap junctions.

### 4-3-4 Bile canalicular movements and the flow within bile canaliculi

Although the triggers of the BC contractions are still unclear, some possibilities surfaced in the present experiment. 1) The BC contractions could have occurred when the contents of BC were regurgitated into cytoplasm, observed as diacytotic vacuoles. Kawahara *et al.* (1990) reported that such regurgitation, called diacytosis (Matter *et al.*, 1969), was observed during BC contractions. In this study, similar diacytotic vacuoles were often observed when BC formed in SH colonies contracted. Some small vacuoles were budding off from the BC and this process was simultaneously seen in several parts of BC networks. As described in chapter 3, the tight junctional protein ZO-1 was well expressed along the BC and that accumulated bilirubin did not leak from BC even a few days after the treatment. The results suggested that the reconstructed BC was tightly sealed by the junctions. Therefore, when the pressure in the canalicular lumen was rapidly increased by contractions, biliary content was directed into hepatic cytoplasm and showed diacytosis. 2) The cytokinesis of the cells consisting of BC networks seems to be a trigger for BC

contraction. Analysis of the time-lapse movie revealed that BC contractions were sometimes synchronized with the timing of cytokinesis. When the cells that form BC are dividing, the BC may be transiently deformed and the luminal pressure near the region may increase. The increase of the pressure may induce the contraction.

Luminal contents of the BC network need to move because hepatocytes may secrete bile-like substances into motile BC. In this culture the BC networks were closed. Therefore, luminal contents gathered at certain regions and formed cyst-like structures. These often formed at the peripheral regions of the piled-up colonies because BC networks were gradually developed coinciding with the development of the piled-up colonies. The formation of cystic structures may facilitate BC contractions and the canalicular flow. In fact visual analysis of the time-lapse movie showed the flow of luminal contents directed to the cystic structure. Quantified measurement of BC contractions also confirmed this phenomenon (Figs. 4-5D–F). BC contractions in the root parts of the piled-up colonies caused dilation of BC in the peripheral regions of the colony (Fig. 4-5E), which indicates negative correlation, confirmed by the values of correlation coefficients (p5, Table 4-2).

BC movements revealed various characteristics. All BC moved, although various speeds of contraction and dilation were observed (Table 4-1). Analysis of correlation coefficients revealed that BC had both positive and negative correlations. These results indicate that some BC synchronously contract or dilate, and some BC dilate as a result of the contraction of neighboring BC. Although BC is thought to act as a peristaltic pump, both types of movement can transfer their contents. When the cells were treated with CB, dilations of BC were observed particularly in the peripheral regions of the piled-up colonies (Fig. 4-6). In addition, microinjection studies revealed that the dye secreted from injected cells had a tendency to flow toward the peripheral regions of the piled-up colonies (Fig. 4-9). These results suggest that secreted bile may be transferred to the peripheral regions by the two types of contractions.

Reconstructing well-assembled hepatic tissues is valuable for tissue engineering of the liver because these tissues can maintain hepatic functions during long-term culture and can be useful for bioartificial livers or tissue-engineered organ transplantation. Although the functions of individual cells have been well analyzed, multicellular functions such as coordination of BC movements have not been investigated. In the present experiment BC movements in the organoids were analyzed and coordination of the movements was

verified. Therefore, hepatic organoids reconstructed by SHs have potential for the tissue engineering of the liver, and this culture system is a useful model to investigate how the cells are integrated into the tissue.

## 4-4 Summary

Hepatocytes *in vivo* have the potential for liver regeneration, but it has been very difficult to reconstruct hepatic organoids *in vitro*. Recent studies have shown that small hepatocytes (SHs) can reconstruct hepatic organoids including functional bile canaliculi (BC). In the present study the movement of BC formed in the hepatic organoids was analyzed, focusing on the coordination of contraction and dilation among cells and the mechanism producing the coordination. Hepatic cells, including SHs, were isolated from an adult rat liver and cultured. Time-lapse images of BC movements were taken and analyzed in cells treated with or without cytochalasin B (CB). Time-lapse images revealed that all BC, regardless of region contracted in a coordinated manner. Actin filaments were observed along the BC even after the BC networks treated with CB dilated markedly. Microinjection of dye was also carried out to investigate the flow thorough BC. Secreted fluorescein from the injected cell flowed along BC, and gap junctional protein connexin 32 was expressed along BC networks, suggesting cell-to-cell communication. Thus, groups of hepatocytes in the hepatic organoids act in a coordinated manner through intercellular communication.

## References

Abu-Absi SF, Friend JR, Hansen LK, Hu WS. Structural polarity and functional bile canaliculi in rat hepatocyte spheroids. Exp Cell Res. 2002;274:56–67.

Brown SS, Spudich JA. Mechanism of action of cytochalasin: evidence that it binds to actin filament ends. J Cell Biol. 1981;88:487–491.

Clair C, Chalumeau C, Tordjmann T, Poggioli J, Erneux C, Dupont G, Combettes L. Investigation of the roles of $Ca^{2+}$ and $InsP_3$ diffusion in the coordination of $Ca^{2+}$ signals between connected hepatocytes. J Cell Sci. 2001;114:1999–2007.

Cooper JA. Effects of cytochalasin and phalloidin on actin. J Cell Biol. 1987;105:1473–1478.

Fausto N. Liver regeneration. J Hepatol. 2000;32:19–31.

Flanagan MD, Lin S. Cytochalasins block actin filament elongation by binding to high affinity sites associated with F-actin. J Biol Chem. 1980;255: 835–838.

Hayakawa T, Bruck R, Ng OC, Boyer JL. DBcAMP stimulates vesicle transport and HRP excretion in isolated perfused rat liver. Am J Physiol. 1990;259:G727–735.

Kamimura Y, Sawada N, Aoki M, Mori M. Endothelin-1 induces contraction of bile canaliculi in isolated rat hepatocytes. Biochem Biophys Res Commun. 1993;191:817–822.

Kawahara H, French SW. Role of cytoskeleton in canalicular contraction in cultured differentiated hepatocytes. Am J Pathol. 1990;136:521–532.

Koide N, Sakaguchi K, Koide Y, Asano K, Kawaguchi M, Matsushima H, Takenami T, Shinji T, Mori M, Tsuji T. Formation of multicellular spheroids composed of adult rat hepatocytes in dishes with positively charged surfaces and under other nonadherent environments. Exp Cell Res. 1990;186:227–235.

Landry J, Bernier D, Ouellet C, Goyette R, Marceau N. Spheroidal aggregate culture of rat liver cells: histotypic reorganization, biomatrix deposition, and maintenance of functional activities. J Cell Biol. 1985;101: 914–923.

LeCluyse EL, Audus KL, Hochman JH. Formation of extensive canalicular networks by rat hepatocytes cultured in collagen-sandwich configuration. Am J Physiol. 1994;266:C1764–1774.

Matter A, Orci L, Rouiller C. A study on the permeability barriers between Disse's space and the bile canaliculus. J Ultrastruct Res. 1969;11:1–71.

Michalopoulos GK, Bowen WC, Mule K, Stolz DB. Histological organization in hepatocyte organoid cultures. Am J Pathol. 2001;159:1877–1887.

Michalopoulos GK, Bowen WC, Zajac VF, Beer-Stolz D, Watkins S, Kostrubsky V, Strom SC. Morphogenetic events in mixed cultures of rat hepatocytes and nonparenchymal cells maintained in biological matrices in the presence of hepatocyte growth factor and epidermal growth factor. Hepatology. 1999;29:90–100.

Michalopoulos GK, DeFrances MC. Liver regeneration. Science. 1997;276: 60–66.

Mitaka T, Kojima T, Mizuguchi T, Mochizuki Y. Growth and maturation of small hepatocytes isolated from adult rat liver. Biochem Biophys Res Commun. 1995;214:310–317.

Mitaka T, Mikami M, Sattler GL, Pitot HC, Mochizuki Y. Small cell colonies appear in the primary culture of adult rat hepatocytes in the presence of nicotinamide and epidermal growth factor. Hepatology. 1992a;16:440–447.

Mitaka T, Sato F, Ikeda S, Sugimoto S, Higaki N, Hirata K, Lamers WH, Mochizuki Y. Expression of carbamoylphosphate synthetase I and glutamine synthetase in hepatic organoids reconstructed by rat small hepatocytes and hepatic nonparenchymal cells. Cell Tissue Res. 2001;306:467–471.

Mitaka T, Sato F, Mizuguchi T, Yokono T, Mochizuki Y. Reconstruction of hepatic organoid by rat small hepatocytes and hepatic nonparenchymal cells. Hepatology. 1999;29:111–125.

Mitaka T, Sattler GL, Pitot HC, Mochizuki Y. Characteristics of small cell colonies developing in primary cultures of adult rat hepatocytes. Virchows Arch B Cell Pathol Incl Mol Pathol. 1992b;62:329–335.

Miyairi M, Oshio C, Watanabe S, Smith CR, Yousef IM, Phillips MJ. Taurocholate accelerates bile canalicular contractions in isolated rat hepatocytes. Gastroenterology. 1984;87:788–792.

Nathanson MH, Burgstahler AD, Fallon MB. Multistep mechanism of polarized $Ca^{2+}$ wave patterns in hepatocytes. Am J Physiol. 1994;267:G338–349.

Nathanson MH, Burgstahler AD, Mennone A, Fallon MB, Gonzalez CB, Saez JC. $Ca^{2+}$ waves are organized among hepatocytes in the intact organ. Am J Physiol. 1995;269:G167–171.

Nathanson MH, Rios-Velez L, Burgstahler AD, Mennone A. Communication via gap junctions modulates

bile secretion in the isolated perfused rat liver. Gastroenterology. 1999;116:1176–1183.

Oshio C, Phillips MJ. Contractility of bile canaliculi: implications for liver function. Science. 1981;212:1041–1042.

Phillips MJ, Oshio C, Miyairi M, Katz H, Smith CR. A study of bile canalicular contractions in isolated hepatocytes. Hepatology. 1982;2:763–768.

Phillips MJ, Oshio C, Miyairi M, Smith CR. Intrahepatic cholestasis as a canalicular motility disorder. Evidence using cytochalasin. Lab Invest. 1983;48:205–211.

Phillips MJ, Oshio C, Miyairi M, Watanabe S, Smith CR. What is actin doing in the liver cell? Hepatology. 1983;3:433–436.

Roelofsen H, Soroka CJ, Keppler D, Boyer JL. Cyclic AMP stimulates sorting of the canlicular organic anion transporter (Mrp2/cMoat) to the apical domain in hepatocyte couplets. J Cell Sci. 1998;111:1137–1145.

Saez JC, Connor JA, Spray DC, Bennett MV. Hepatocyte gap junctions are permeable to the second messenger, inositol 1,4,5-trisphosphate, and to calcium ions. Proc Natl Acad Sci U S A. 1989;86:2708–2712.

Seglen PO. Preparation of isolated rat liver cells. Methods Cell Biol. 1976;13:29–83.

Serriere V, Berthon B, Boucherie S, Jacquemin E, Guillon G, Claret M, Tordjmann T. Vasopressin receptor distribution in the liver controls calcium wave propagation and bile flow. FASEB J. 2001;15:1484–1486.

Smith CR, Oshio C, Miyairi M, Katz H, Phillips MJ. Coordination of the contractile activity of bile canaliculi. Evidence from spontaneous contractions in vitro. Lab Invest. 1985;53:270–274.

Sugimoto S, Mitaka T, Ikeda S, Harada K, Ikai I, Yamaoka Y, Mochizuki Y. Morphological changes induced by extracellular matrix are correlated with maturation of rat small hepatocytes. J Cell Biochem. 2002;87:16–28.

Sundback CA, Vacanti JP. Alternatives to liver transplantation: from hepatocyte transplantation to tissue-engineered organs. Gastroenterology. 2000;118:438–442.

Talamini MA, Kappus B, Hubbard A. Repolarization of hepatocytes in culture. Hepatology. 1997;25:167–172.

Tordjmann T, Berthon B, Claret M, Combettes L. Coordinated intercellular calcium waves induced by noradrenaline in rat hepatocytes: dual control by gap junction permeability and agonist. EMBO J. 1997;16:5398–5407.

Tordjmann T, Berthon B, Jacquemin E, Clair C, Stelly N, Guillon G, Claret M, Combettes L. Receptor-oriented intercellular calcium waves evoked by vasopressin in rat hepatocytes. EMBO J. 1998;17:4695–4703.

Tsukada N, Phillips MJ. Bile canalicular contraction is coincident with reorganization of pericanalicular filaments and co-localization of actin and myosin-II. J Histochem Cytochem. 1993;41:353–363.

Watanabe S, Miyazaki A, Hirose M, Takeuchi M, Ohide H, Kitamura T, Ueno T, Kominami E, Sato N. Myosin in hepatocytes is essential for bile canalicular contraction. Liver. 1991;11:185–189.

Watanabe S, Phillips MJ. $Ca^{2+}$ causes active contraction of bile canaliculi: direct evidence from microinjection studies. Proc Natl Acad Sci U S A. 1984;81:6164–6168.

Watanabe S, Smith CR, Phillips MJ. Coordination of the contractile activity of bile canaliculi. Evidence from calcium microinjection of triplet hepatocytes. Lab Invest. 1985;53:275–279.

Watanabe S, Tomono M, Takeuchi M, Kitamura T, Hirose M, Miyazaki A, Namihisa T. Bile canalicular contraction in the isolated hepatocyte doublet is related to an increase in cytosolic free calcium ion concentration. Liver. 1988;8:178–183.

Watanabe N, Tsukada N, Smith CR, Phillips MJ. Motility of bile canaliculi in the living animal: implications for bile flow. J Cell Biol. 1991;113:1069–1080.

Yumoto AU, Watanabe S, Hirose M, Kitamura T, Yamaguchi Y, Sato N. Structural and functional features of bile canaliculi in adult rat hepatocyte spheroids. Liver. 1996;16:61–66.

# Chapter 5

# Reconstruction of 3D stacked-up structures by rat small hepatocytes cultured on microporous membranes

## 5-1 Introduction

The liver has a complex organized architecture in which epithelial cells, such as hepatocytes and BECs, and hepatic NPCs, such as stellate cells, kupffer cells and sinusoidal endothelial cells, form functional units (Desmet *et al.*, 2001). Hepatocytes form liver-cell plates that assemble into cords of adjacent hepatocytes connected by lateral membranes. BC are formed by the apical membranes of adjacent hepatocytes and function as pathways for metabolites. The sinusoidal domains of hepatocytes face the space of Disse, in which a variety of matrix components are sparsely distributed. Thus, hepatocytes *in vivo* extend three-dimensionally, and maintain the specific phenotypes and functions that are caused by cell–cell and cell–ECM interactions.

It has been attempted to reconstruct hepatic organoids using SHs, which are hepatic progenitor cells, in the adult liver (Mitaka *et al.*, 1992, 1995). Although primary hepatocytes lose their specific functions over time in culture, SHs can proliferate and reconstruct hepatic organoids, including NPCs (Mitaka *et al.*, 1999). As described in chapters 3 and 4, functional BC could be reconstructed using SHs. Although SH colonies become flat clusters during the early stage of the culture, they later expand to form large colonies, some of which are composed of piled-up cells that have the appearance of MHs. BC form between the differentiated hepatocytes and bile canalicular proteins, such as ectoATPase, 5′NT, DPPIV and MRP2, localize in the lumina of the BC. Bilirubin added to the medium is secreted into the BC and accumulates without leakage. Furthermore, the BC can continuously contract and dilate in a coordinated manner. Thus, SHs can differentiate into MHs with membrane polarity, secretory ability and motility. SHs are therefore

considered to be suitable cells for the reconstruction of functional tissues.

The 3D culture of hepatocytes is essential in order to reconstruct functional hepatic tissues *in vitro*. Several approaches for producing 3D cultures have been suggested to maintain the function of primary hepatocytes. When hepatocytes were cultured in 3D aggregates, known as hepatocyte spheroids, liver-specific functions were maintained for extended culture periods (Landry *et al.*, 1985; Koide *et al.*, 1990; Abu-Absi *et al.*, 2002). However, although spheroids are useful as a cell source for BAL reactors (Matsushita *et al.*, 1991; Yamashita *et al.*, 2003; Gerlach *et al.*, 1995; Sakai *et al.*, 1996), their structures differ from those of the liver *in vivo*. Hepatocytes *in vivo* construct hepatic cords, and organization of the cells is achieved by the interaction of MHs, NPCs and the ECM, whereas spheroids are simple aggregates composed of MHs alone. Another method for 3D culture uses scaffolds, such as paper (Mizuguchi *et al.*, 2000), poly-L-lactic-acid scaffolds (Mooney *et al.*, 1995; Jiang *et al.*, 2002) or 3D-perfused microarray bioreactors (Powers *et al.*, 2002). The hepatocytes in the scaffold tend to form spheroids. SHs have also been cultured in 3D scaffolds. However, although culturing SHs in 3D collagen sponges enhanced the formation of hepatic organoids, the size of the cell aggregates was limited by the topology of the surface pits (Harada *et al.*, 2003). Considering the structure of the liver, it might be difficult to reconstruct well-assembled tissue in the scaffold spontaneously, because the assembly of cells into tissues is a highly organized process that is achieved by several kinds of cell. Precise manipulation of the cells is necessary to facilitate their organization. Therefore, it was hypothesized that a stepwise method is necessary to reconstruct well-assembled 3D hepatic tissues from 2D tissues.

Combining SHs and the stepwise-culture method, a simple 3D-culture technique that mimics the structure of the hepatocytes *in vivo* was developed. In the present experiments, 2D tissues composed of SHs and NPCs were stacked up in order to reconstruct 3D tissues. Pairs of membranes were prepared and the cells were separately cultured on each membrane. After SH colonies developed, one membrane was inverted on top of the other, which resulted in the SHs becoming attached to one another. To organize the SHs into the tissue, the cells must mimic the structure of the hepatic cords in the 3D stacked-up structures. In order to evaluate their organization, it was ascertained whether the cells adhered to each other and formed BC in the attached portions.

## 5-2 Results

### 5-2-1 Small hepatocyte colonies developed on the microporous membranes [2-1]

The GFP-labeled SHs could proliferate and formed colonies on the microporous membranes (Figs. 5-1A, B). Although individual cells could not be clearly observed under phase-contrast microscopy, an outline of the SH colony could be seen (Fig. 5-1B). However, fluorescent microscopy revealed that the GFP-labeled NPCs were also present in the culture and surrounded the colonies (Fig. 5-1A). The cells in the colonies were immunocytochemically positive for albumin, and some that were positive for desmin were located under and adjacent to the colonies (Fig. 5-1C). Although most of the surrounding cells seemed to be stellate cells, ED-1, SE-1 and vimentin-positive cells were also present (data not shown). 3D deconvolution microscopy revealed that the stellate cells were present under the SH colonies and the membranes (Figs. 5-1D–G). The tight-junction-associated protein ZO-1 was strongly expressed at the cell–cell borders of the SH colony (Fig. 5-1D). Some stellate cells were observed under the colonies or membranes (Figs. 5-1E, F). The vertical section in Fig. 5-1G shows the top layer of SHs, and the middle and bottom layers of stellate cells.

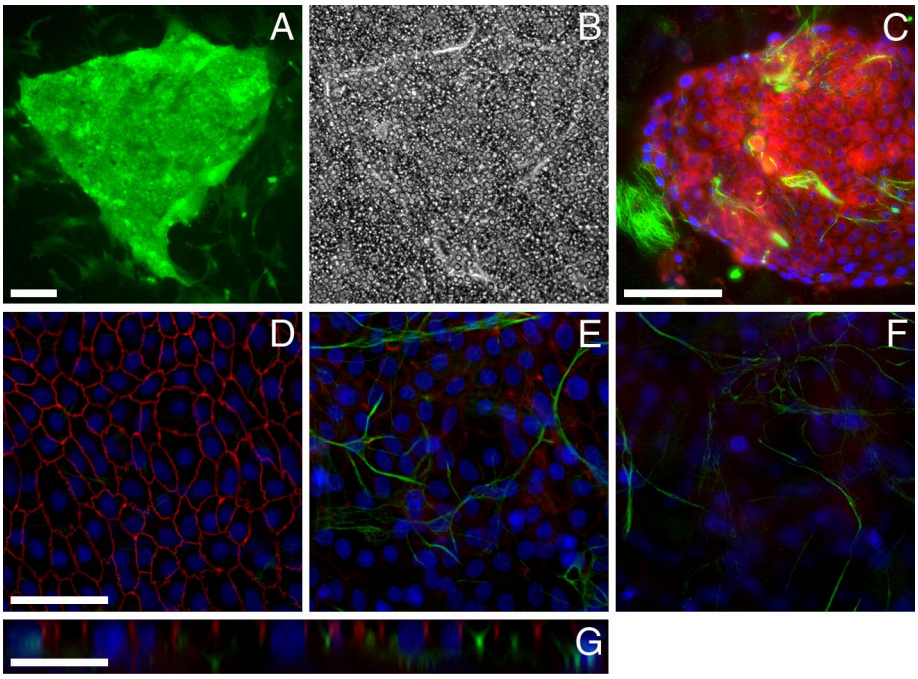


Fig. 5-1 Fluorescent and phase-contrast micrographs of cells cultured on microporous membranes. A, B: A fluorescent micrograph of the cells isolated from EGFP rats (A) and the corresponding phase-contrast micrograph at day 14 (B). An outline of the colony and the randomly distributed micropores can be distinguished under phase-contrast microscopy. C: The distribution of the SHs and stellate cells. Triple immunostaining for desmin (green), albumin (red) and DAPI (blue) was carried out on day 16. D–G: The 3D distribution of SHs and stellate cells at day 21. Triple immunostaining was carried out for desmin (green), ZO-1 (red) and DAPI (blue), and the cells were photographed using 3D deconvolution microscopy. The images were three-dimensionally reconstructed by calculating 29 planes at 0.675-μm intervals: the 10th (F), 18th (E) and 24th (D) planes are shown. The x-z axes in the center of the 3D image are shown in (G). Scale bars: 100 μm (A, C, G) and 50 μm (D).

## 5-2-2 The 3D stacked-up culture [2-2]

As illustrated in Fig. 2-2, four different methods of stacking the membranes were investigated in order to reconstruct the 3D structures: in the case of Figs. 2-2A and C, the upper cells were inverted and faced the lower cells; by contrast, in the cases shown in Figs. 2-2B and D, the lower cells faced the membranes. The cells could directly adhere to each other, so the cells in Figs. 2-2A and C were more strongly attached than those in Figs. 2-2B and D. In terms of re-stacking the membrane, the method shown in Fig. 2-2A was the easiest to manipulate and was therefore chosen for the subsequent experiments.

## 5-2-3 Cell adhesion and bile canalicular formation in the 3D stacked-up structures [2-6-2, 2-7-3, 2-8]

After the cells were cultured on the membranes and allowed to develop, they were stacked as shown in Fig. 2-2A. FD treatment revealed that although fluorescein was observed in the cytoplasm 1–3 days after stacking, the secretion of fluorescein into the BC was first detectable 3 days after stacking. The lined BC then formed between the cells in the 3D stacked-up structure (Fig. 5-2A). The length of the fluorescent lines gradually increased with the culture time (Fig. 5-2B), and the BC rapidly developed and constructed anastomosing networks (Figs. 5-2B–D). Some parts of the BC dilated and formed cyst-like structures (asterisks, Fig. 5-2D). BC formation was only observed in the region where the membranes were stacked up, and the fluorescein stopped at the edge of the upper membrane (Fig. 5-2E). Although the membranes were stacked up, it could not be verified whether the cells were directly attached to each other. Therefore, the cells on each membrane were labeled with DiI and GFP in order to distinguish the upper and lower cells, respectively.

Fig. 5-3 shows BC formation in 3D stacked-up structures in which GFP-labeled cells were stacked onto the DiI-labeled cells. Black branching lines were observed between the GFP-labeled cells (arrowheads, Figs. 5-3B, C, E, F) although no lines were identified in regions where both sides of the cells remained unattached (asterisks, Figs. 5-3B, C, E, F). CMTPX treatment revealed red fluorescent secretions in the spaces corresponding to the black branching lines between the GFP-labeled cells (arrows, Figs. 5-3G–I). These results suggest that the black branching lines represent the BC. Although it is possible that the BC formation occurred in the region between the neighboring cells on each side, this was difficult to confirm

using the labeling method described. Therefore, vertical sections of the 3D stacked-up structures were analyzed using TEM.

Perpendicular sections of the stacked cells showed that the hepatocytes of the upper and lower layers adhered to each other and formed a bilayer that was sandwiched between the membranes (Figs. 5-4A, C). Between the cells of the upper and lower layers, a well-developed BC was observed that formed a tubular structure (arrows, Fig. 5-4A). As shown in the enlarged image in Fig. 5-4B, the BC was about 1 μm in diameter and possessed many microvilli. The structure was bounded by cell–cell junctions, such as tight junctions and desmosomes (Figs. 5-4B, D). In addition, NPCs with flat shapes were observed between the hepatocytes and the membranes. By contrast, dilated BC were observed when cells were cultured for 48 days after being stacked (arrows, Fig. 5-4C).

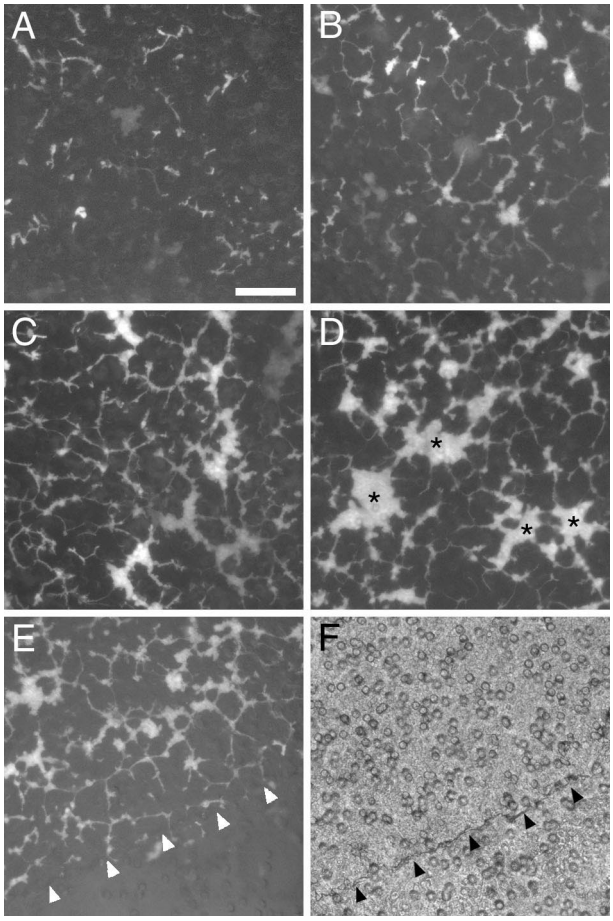


Fig. 5-2 Fluorescent images of the cells in 3D stacked-up structures treated with FD. A–D: Uptake and metabolization of FD by the cells 5 (A), 7 (B), 14 (C) and 20 (D) days after stacking. The cells were stacked at day 19. Pools of fluorescein are observed 20 days after stacking (asterisks, D). E, F: Corresponding fluorescent (E) and phase-contrast (F) images of the cells 20 days after stacking at the edge of one membrane (arrowheads). BC are formed in the region where the membranes are stacked. Scale bar: 100 μm.

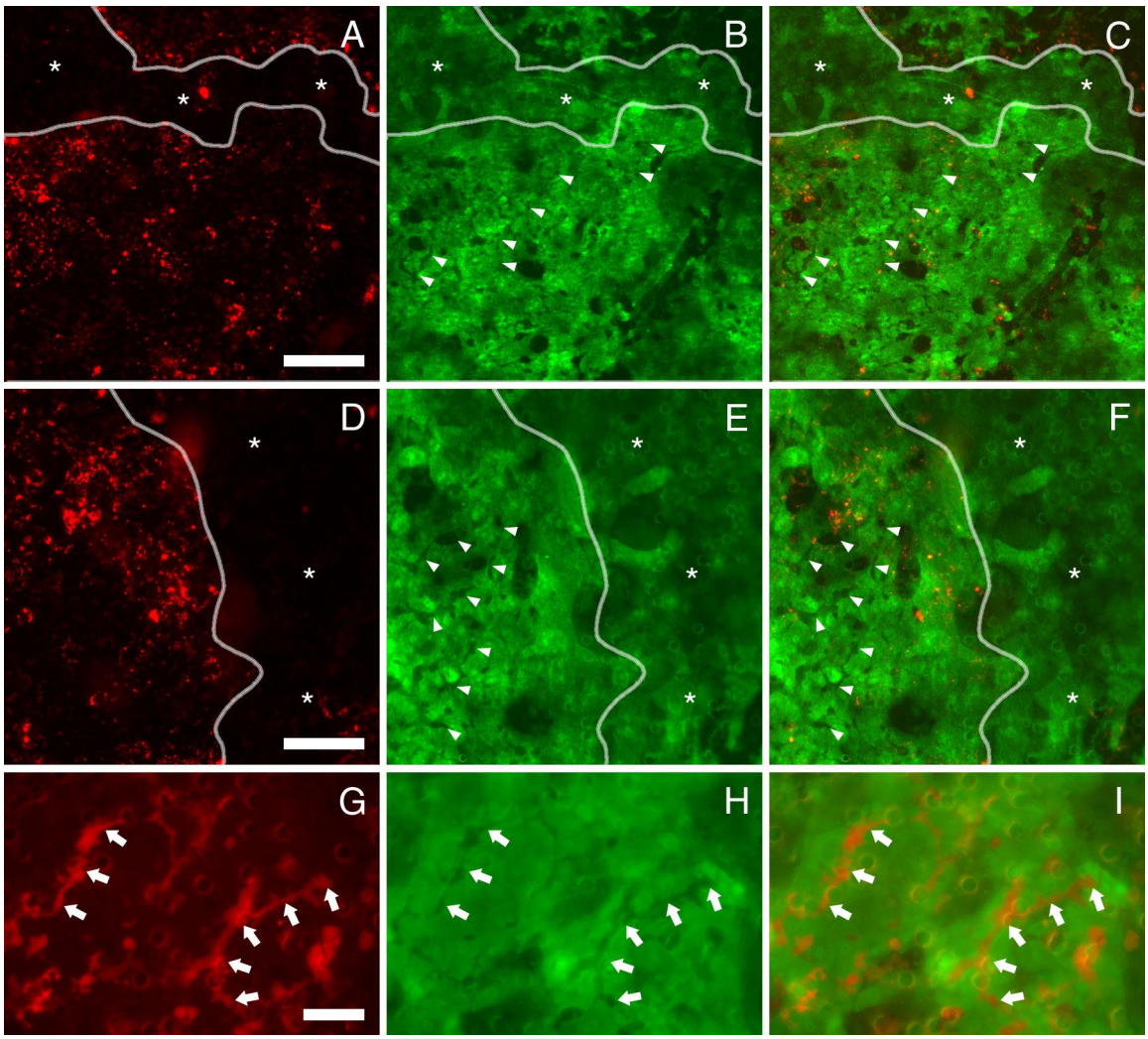


Fig. 5-3 BC formation in the GFP- and DiI-labeled cells. A–F: Corresponding images of the lower layer of the DiI-labeled cells (A, D), the upper layer of the GFP-labeled cells (B, E) and the merged layers (C, F) in the 3D stacked-up structures. The cells were stacked at day 31 and photographed 15 days after stacking. Outlines of DiI-labeled cell colonies are traced with white lines. Regions where the cells are not directly attached are marked with asterisks. BC are observed as black branching lines, which are only seen in the region where the cells of the upper and lower layers coexist (arrowheads, B, C, E, F). G–I: Corresponding images of the CMTPX (G), GFP (H) and merged (I) cells in the structure. Cells were isolated from SD and EGFP rats on each day, and the normal cells at day 25 were stacked onto the GFP-labeled cells at day 24. The cells were then photographed 10 days after stacking. Arrows show the CMTPX secreted into the branching BC. Scale bars: 200 μm (A), 100 μm (D) and 50 μm (G).

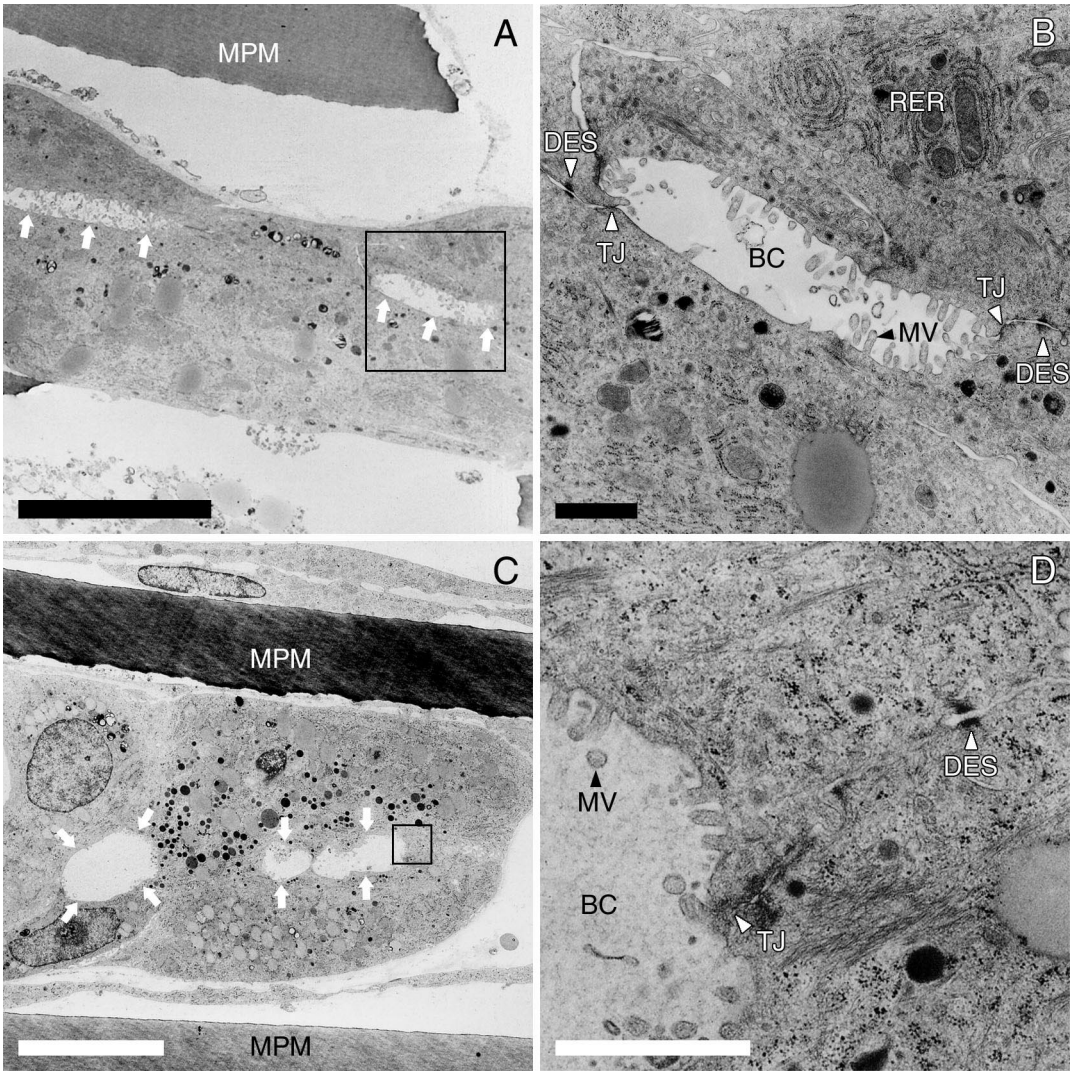


Fig. 5-4 Electron micrographs of vertical sections of the 3D stacked-up structures. A: The cells were stacked at day 19 and fixed 24 days after stacking. The upper and lower layers adhere to each other to form a bilayer sandwiched by the microporous membranes (MPMs). Tubular BC are observed between the cells of the upper and lower layers (arrows). B: An enlarged image of the region indicated by the box in A. BC with luminal microvilli (MV) are formed between the cells, and are bounded both by tight junctions (TJ) and desmosomes (DES). Rough endoplasmic reticulum (RER) is visible within the cells. C: The cells were stacked at day 31 and fixed 48 days after stacking. Dilated BC were observed (arrows). NPCs with flat shapes were observed between the hepatocytes and the membranes, as well as on the membranes. D: An enlarged image of the region indicated by the box in C. The dilated BC possess MV and maintain the cell–cell junctions, such as TJ and DES. Scale bars: 10 μm (A, C) and 1 μm (B, D).

## 5-2-4 Localization of ectoATPase in the 3D stacked-up structures [2-5-6]

3D deconvolution microscopy revealed that ectoATPase, which is known to be expressed in BC, was present along the tubular structures (arrowheads, Figs. 5-5A–C). Actin filaments were abundant on the outer surface of the ectoATPase-positive structure. These results indicate that ectoATPase was localized on the extracellular side of the apical membrane and that actin filaments accumulated beneath the apical membrane. Therefore, hepatocytes in the 3D stacked-up structures might acquire membrane polarity.

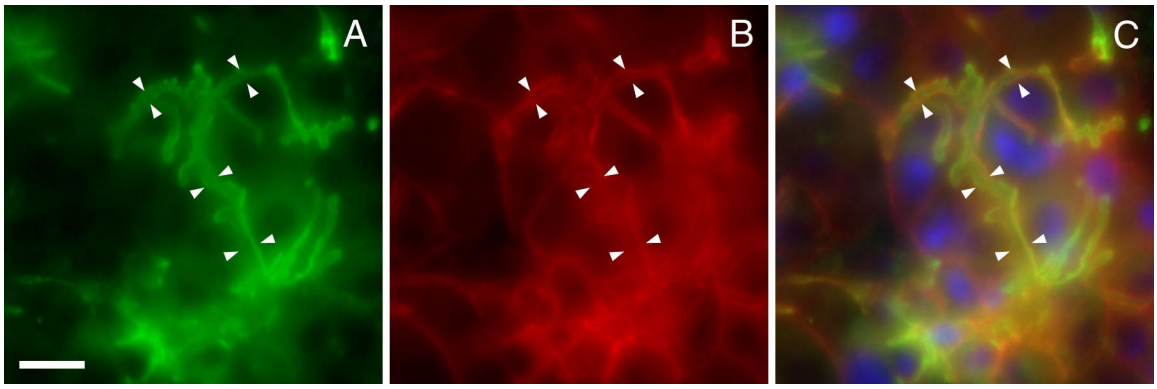


Fig. 5-5 Localization of ectoATPase and actin in the cells within the 3D stacked-up structure. The membrane was stacked at day 25 and fixed 15 days after stacking. Triple immunostaining was carried out for ectoATPase (green), actin (red) and DAPI (blue). The corresponding ectoATPase (A), actin (B) and merged (C) images are shown in produced using the 3D deconvolution microscopy. The branching tubular structures consist of an inner layer of ectoATPase and an outer layer of actin (arrowheads). The images were three-dimensionally reconstructed by calculating 26 planes at 0.65-μm intervals. Scale bar: 20 μm.

## 5-2-5 Albumin secretions and gene expression of the hepatic differentiation markers

(2-9, 2-11)

When the cells were stacked up, the amount of albumin secreted into the medium rapidly increased within 2 days, and remained high for more than 2 weeks (S1, S2, Fig. 5-6). By contrast, the level of albumin secretion gradually diminished in the cells that were cultured on a membrane (NS, Fig. 5-6).

It was next examined whether the cells within the 3D stacked-up structures could express hepatic-differentiation markers. RT-PCR analysis revealed that the mRNA expression of albumin, MRP2, HNF-4 and TAT persisted at 10 days after stacking (Fig. 5-7). In addition, although the expression level of TO mRNA was low compared to that of the primary hepatocytes, the gene was detected 10 days after the stacking. By contrast, the TO expression was diminished when the cells were not stacked.

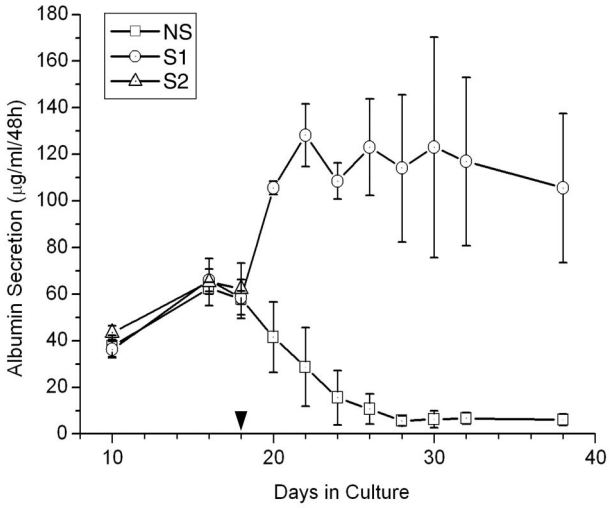


Fig. 5-6 Albumin secretion into the medium during 48-hour periods. The samples were collected from the dishes 48 hours after the change of the medium. One membrane (S2) was stacked on top of the other (S1) at day 18 (arrowhead). The media were also collected from the dishes, in which the cells were not stacked (NS).

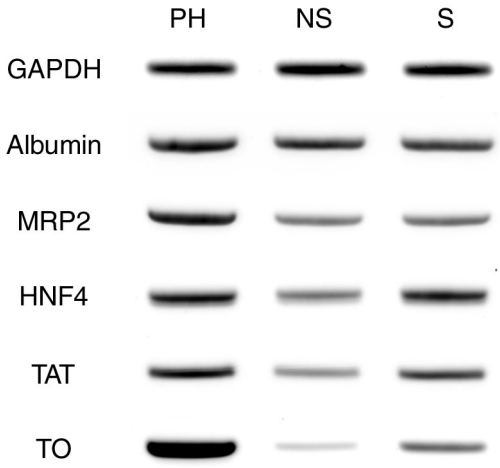


Fig. 5-7 Gene expression of the hepatic-differentiation markers in cells within the 3D stacked-up structures. The cells were stacked at day 20. Total RNA samples were prepared from the cells 10 days after stacking (S). The samples were also prepared from the cells cultured on membranes that were not stacked (NS). As a positive control, those of freshly isolated primary hepatocytes (PH) were prepared. The samples were analyzed using RT-PCR to detect albumin, MRP2, HNF4, TAT, TO and GAPDH mRNAs.

## 5-3 Discussion

### 5-3-1 Reorganization of small hepatocytes in the 3D stacked-up structures

A tissue is an organized structure, in which cells assemble into an appropriate configuration in order to achieve a specific function. In the liver, the hepatocytes assemble into interconnected lines of cells, which are separated by BC. The hepatic cords achieve the functional structure, which has interfaces with both blood and bile. These structures seem to be important for the reconstruction of functional hepatic organoids.

In the present experiment, 3D stacked-up structures that mimic the structures of the hepatic cords were reconstructed. In order to organize the cells within these structures, the SHs of the upper and lower layers must first adhere to one another. When the cells have only physical contact between the upper and lower layers, they are unable to organize into tissues. Therefore, vertical sections of the structures were investigated to determine whether the cells of the upper and lower layers reconstructed cell−cell junctions. The TEM results revealed that both tight junctions and desmosomes were constructed between the cells, as well as BC with many microvilli (Fig. 5-4). These findings indicate that the cells of the upper and lower layers physiologically adhere to each other within the structures, which are not merely stacked-up layers of cells.

BC are highly differentiated structures that cannot be produced by individual cells. The membrane polarity of the hepatocyte needs to be maintained for BC formation, because the apical domains of adjacent hepatocytes form the BC. Although freshly isolated hepatocytes retain partial BC in paired cells, they are rapidly lost over time in culture (Oshio *et al.*, 1981). SHs can reconstruct functional BC that interact with NPCs when they are cultured on collagen-coated dishes (chapter 3). However, SHs cultured on collagen gels continue to proliferate without BC formation (Mitaka *et al.*, 2002). Thus, the growth and maturation of SHs depend on surface conditions, such as the ECM concentration, and on the surface topology. In the present experiment, SHs were cultured on microporous membranes coated with rat-tail collagen. Although these SHs formed some BC, they were less frequent compared to those produced in cells cultured on collagen-coated dishes. However, most of the cells in the 3D stacked-up structures formed BC between vertically neighboring cells as well as between horizontal neighbors. These cells maintained their

membrane polarity, as illustrated by the fact that ectoATPase was expressed in intercellular spaces (Fig. 5-5). Our findings indicate that these cells can be organized into orchestrated tissues in which they form interconnected lines that include functional BC.

## 5-3-2 Schematic diagram of the 3D stacked-up culture

The schematic diagram shown in Fig. 5-8 summarizes the 3D stacked-up structures produced by SHs and NPCs. Initially, a single SH proliferates and forms a colony on each membrane, which is then separately cultured in order to produce the structures (Fig. 5-8A). Next, NPCs, such as stellate cells, proliferate and surround the colony. Then, the surrounding cells translocate beneath the colony and some NPCs infiltrate under the membranes through the micropores. SH colonies gradually develop over time in culture (Fig. 5-8B). About 20 days after inoculation, one membrane is inverted on top of the other, which results in the SHs becoming attached to one another. The cells can then extend three-dimensionally into the 3D stacked-up structures (Fig. 5-8C). Subsequently, the SHs of the upper and lower layers adhere to each other, and cell–cell junctions, such as desmosomes and tight junctions, develop between the cells. After the cells are stacked, BC start to form between the hepatocytes of the upper and lower layers, as well as between horizontally neighboring cells. Thereafter, the short BC gradually elongate and develop into anastomosing networks (Fig. 5-8D). Thus, 3D structures in which SHs differentiate into MHs can be reconstructed by stacking up the membranes.

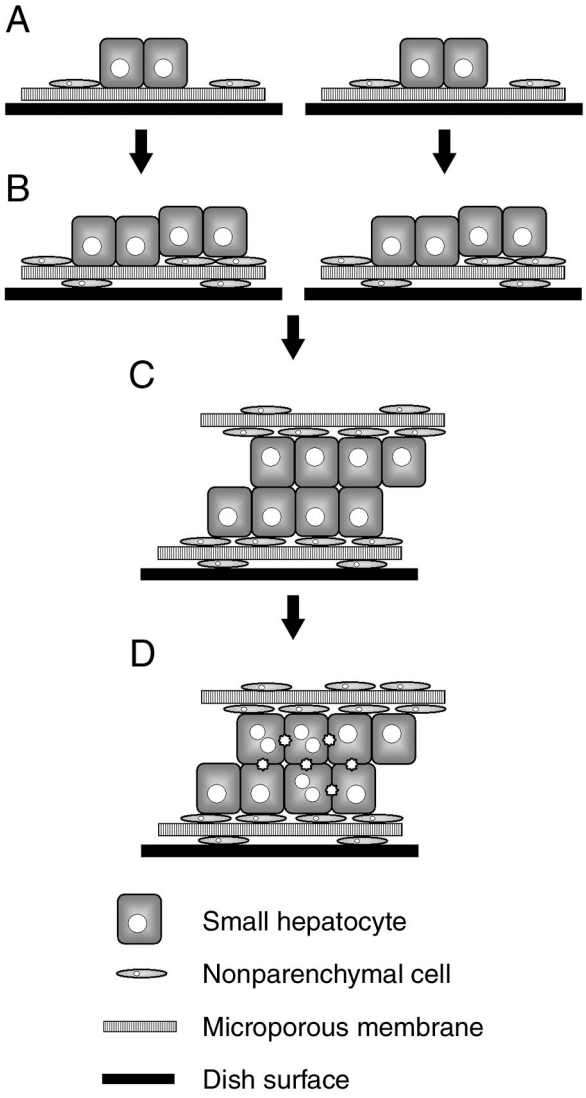


Fig. 5-8 Schematic representation of the formation of 3D stacked-up structures by SHs and NPCs. For details of stages A–D see the Discussion section.

## 5-3-3 Maintenance of liver-specific function of the cells in the 3D stacked-up structures

Cell shape is reported to be closely associated with function (Folkman *et al.*, 1978; Ben-Ze'ev *et al.*, 1988; Mooney *et al.*, 1992; Watt *et al.*, 1988). When hepatocytes were cultured in rectangular cell-adhesive islands, which were designed to prevent individual cells from spreading, the resulting cells exhibited low levels of DNA synthesis and high levels of albumin secretion compared to cells cultured on unpatterned surfaces (Singhvi *et al.*, 1994). These results suggest that the differentiation of hepatocytes is strongly affected by the shape of the individual cells. By contrast, when hepatocytes were cultured as slices of tissues in which the *in vivo* architecture was retained, liver-specific mRNA synthesis was maintained in a culture, whereas hepatocytes that were cultured in monolayers rapidly lost their functions (Clayton *et al.*, 1985). *In vivo*, hepatocytes seem to maintain their liver-specific function by forming 3D complex architectures interacting with NPCs and the ECM. Therefore, the maintenance of the 3D microarchitecture for the cuboidal cell shape is important for reconstructing functional liver tissues *in vitro*.

In the present experiment, the SHs in 3D stacked-up structures assembled into cords in which BC were produced. These structures mimicked those of the hepatic cords. In these structures, the cells could extend three-dimensionally while maintaining both cell–cell and cell–ECM contacts. By contrast, when SHs were sparsely inoculated onto collagen-coated dishes, they only attached onto the surface of the dish and did not maintain their cell–cell interactions. As a result, the cells extended two-dimensionally and the cells became flat. By contrast, SHs in the 3D stacked-up structures could maintain both vertical and horizontal cell–cell interactions, as well as cell–ECM interactions. These microarchitectures might enhance the differentiation of SHs through maintenance of the cuboidal cell shape. Thus, albumin secretion by the cells in the 3D stacked-up structures was enhanced compared to that in the cells on the membranes (Fig. 5-6).

The microarchitecture in the 3D stacked-up structures might also enhance the synthesis of liver-specific mRNAs (Fig. 5-7). Cells in these structures transcribed the mRNA of MRP2, which is a bile canalicular protein. Although the localization of ectoATPase was shown in the present experiment, MRP2 was also localized on the lumina of BC that were reconstructed in SHs cultured on a collagen-coated dish (Fig. 3-2F, chapter 3). The characteristics of the BC in the present experiment might be similar to those described in chapter 3. HNF-4 is a liver-enriched transcription factor that regulates liver-specific gene

expression (Cereghini *et al.*, 1996). The morphological changes in the SHs induced by Matrigel overlay correlated with the maturation of the cells, including the expression of HNF-4 (Sugimoto *et al.*, 2002). TAT and TO, which are markers of hepatocytes at a terminal differentiation stage, were also detected.

### 5-3-4 Stepwise reconstruction of 3D stacked-up tissues from 2D structures

Tissue engineering is necessary to reconstruct well-organized 3D tissues. Although 3D-culture methods, such as hepatocyte spheroids and cultures in 3D scaffolds, have been reported, the formation of the tissues depends on the spontaneous behavior of the cells. The cells in the spheroids tend to form compact aggregates; therefore, manipulation of the cells is necessary to facilitate their organization. In the present experiment, it was demonstrated that a simple 3D-culture method could successfully reconstruct 3D stacked-up tissues from 2D structures. Moreover, within these structures, the SHs could organize themselves into orchestrated tissues with liver-specific functions. In a recent study, Ogawa *et al.* (2004) reported that rolled layers of SHs could be rearranged into functionally differentiated 3D hepatic tissues when they were implanted into the rat omentum. These results suggest that a stepwise progression from 2D to 3D is an essential step in the reconstruction of well-organized hepatic organoids.

Liver transplantation is the only treatment for end-stage liver disease, but donor organ shortages are a serious issue. Therefore, many researchers have attempted to restore liver function using the BAL. Although many cell types have been examined for use in the BAL reactor, it is extremely difficult to maintain hepatocyte function *in vitro* (Strain *et al.*, 2002). Therefore, tissue-engineered livers are thought to be an alternative source for the BAL (Sundback *et al.*, 2000; Griffith *et al.*, 2002). In the present experiment, the cells were stacked onto those cultured on the membrane, which suggests the potential for multiple stacking; although only two membranes were stacked in the present experiment, three were successfully stacked in the preliminary study (data not shown). Although further improvements will be necessary to achieve thicker complex tissues, the 3D stacked-up culture described here will be useful in the construction of tissue-engineered livers.

## 5-4 Summary

The three-dimensional (3D) culture of hepatocytes is essential for the reconstruction of functional hepatic tissues *in vitro*. In the present experiment a 3D-culture method was developed in order to reconstruct hepatic cord-like structures by stacking up two-dimensional tissues composed of rat small hepatocytes (SHs), which are hepatic progenitor cells. Pairs of membranes were prepared and the cells were separately cultured on each membrane. After the SH colonies had developed, one membrane was inverted on top of the other to form an SH bilayer. Thereafter, it was investigated whether the stacked cells were organized into differentiated tissues. In the 3D stacked-up structures, bile canaliculi (BC) started to form and gradually developed into anastomosing networks. Transmission electron microscopy revealed that the SHs of the upper and lower layers adhered to one another, and that BC formed between them. EctoATPase, a bile canalicular protein, was localized along the tubular structures. Furthermore, the cells within the structures exhibited mRNA transcription of the hepatic-differentiation markers and maintained a relatively high level of albumin secretion. It was concluded that highly differentiated 3D tissues, including functional BC, could be reconstructed by stacking up layers of SHs. This 3D stacked-up culture is useful for the reconstruction of tissue-engineered livers.

## References

Abu-Absi SF, Friend JR, Hansen LK, Hu WS. Structural polarity and functional bile canaliculi in rat hepatocyte spheroids. Exp Cell Res. 2002;274:56–67.

Ben-Ze'ev A, Robinson GS, Bucher NL, Farmer SR. Cell–cell and cell–matrix interactions differentially regulate the expression of hepatic and cytoskeletal genes in primary cultures of rat hepatocytes. Proc Natl Acad Sci U S A. 1988;85:2161–2165.

Cereghini S. Liver-enriched transcription factors and hepatocyte differentiation. FASEB J. 1996;10:267–282

Clayton DF, Harrelson AL, Darnell JE Jr. Dependence of liver-specific transcription on tissue organization. Mol Cell Biol. 1985;5:2623–2632.

Desmet VJ. Organizational principles. In: Arias JM, Boyer JL, Chisari F, Fausto N, Schachter D, Shafritz, DA. eds. The liver biology and pathobiology fourth edition Philadelphia: Lippincott Williams & Wilkins, 2001:3–15.

Folkman J, Moscona A. Role of cell shape in growth control. Nature. 1978;273:345–349.

Gerlach JC, Schnoy N, Encke J, Smith MD, Muller C, Neuhaus P. Improved hepatocyte in vitro maintenance in a culture model with woven multicompartment capillary systems: electron microscopy studies. Hepatology. 1995;22:546–552.

Griffith LG, Naughton G. Tissue engineering--current challenges and expanding opportunities. Science. 2002;295:1009–1014.

Mitaka T, Mikami M, Sattler GL, Pitot HC, Mochizuki Y. Small cell colonies appear in the primary culture of adult rat hepatocytes in the presence of nicotinamide and epidermal growth factor. Hepatology. 1992;2:440–447.

Harada K, Mitaka T, Miyamoto S, Sugimoto S, Ikeda S, Takeda H, Mochizuki Y, Hirata K. Rapid formation of hepatic organoid in collagen sponge by rat small hepatocytes and hepatic nonparenchymal cells. J Hepatol. 2003;39:716–723.

Jiang J, Kojima N, Kinoshita T, Miyajima A, Yan W, Sakai Y. Cultivation of fetal liver cells in a three-dimensional poly-L-lactic acid scaffold in the presence of oncostatin M. Cell Transplant.

2002;11:403–406.

Koide N, Sakaguchi K, Koide Y, Asano K, Kawaguchi M, Matsushima H, Takenami T, Shinji T, Mori M, Tsuji T. Formation of multicellular spheroids composed of adult rat hepatocytes in dishes with positively charged surfaces and under other nonadherent environments. Exp Cell Res. 1990;186:227–235.

Landry J, Bernier D, Ouellet C, Goyette R, Marceau N. Spheroidal aggregate culture of rat liver cells: histotypic reorganization, biomatrix deposition, and maintenance of functional activities. J Cell Biol. 1985;101:914–923.

Matsushita T, Ijima H, Koide N, Funatsu K. High albumin production by multicellular spheroids of adult rat hepatocytes formed in the pores of polyurethane foam. Appl Microbiol Biotechnol. 1991;36:324–326.

Mitaka T. Reconstruction of hepatic organoid by hepatic stem cells. J Hepatobiliary Pancreat Surg. 2002;9:697–703.

Mitaka T, Kojima T, Mizuguchi T, Mochizuki Y. Growth and maturation of small hepatocytes isolated from adult rat liver. Biochem Biophys Res Commun. 1995;214:310–317.

Mitaka T, Sato F, Mizuguchi T, Yokono T, Mochizuki Y. Reconstruction of hepatic organoid by rat small hepatocytes and hepatic nonparenchymal cells. Hepatology. 1999;29:111–125.

Mizuguchi T, Mitaka T, Sato F, Mochizuki Y, Hirata K. Paper is a compatible bed for rat hepatocytes. Artif Organs 2000;24:271–277.

Mooney D, Hansen L, Vacanti J, Langer R, Farmer S, Ingber D. Switching from differentiation to growth in hepatocytes: control by extracellular matrix. J Cell Physiol. 1992;151:497–505.

Mooney DJ, Park S, Kaufmann PM, Sano K, McNamara K, Vacanti JP, Langer R. Biodegradable sponges for hepatocyte transplantation. J Biomed Mater Res. 1995;29:959–965.

Ogawa K, Ochoa ER, Borenstein J, Tanaka K, Vacanti JP. The generation of functionally differentiated, three-dimensional hepatic tissue from two-dimensional sheets of progenitor small hepatocytes and nonparenchymal cells. Transplantation. 2004;77:1783–1789.

Oshio C, Phillips MJ. Contractility of bile canaliculi: implications for liver function. Science. 1981;212:1041–1042.

Powers MJ, Janigian DM, Wack KE, Baker CS, Beer Stolz D, Griffith LG. Functional behavior of primary rat liver cells in a three-dimensional perfused microarray bioreactor. Tissue Eng. 2002;8:499–513.

Sakai Y, Naruse K, Nagashima I, Muto T, Suzuki M. Large-scale preparation and function of porcine hepatocyte spheroids. Int J Artif Organs. 1996;19:294–301.

Singhvi R, Kumar A, Lopez GP, Stephanopoulos GN, Wang DI, Whitesides GM, Ingber DE. Engineering cell shape and function. Science. 1994;264:696–698.

Sugimoto S, Mitaka T, Ikeda S, Harada K, Ikai I, Yamaoka Y, Mochizuki Y. Morphological changes induced by extracellular matrix are correlated with maturation of rat small hepatocytes. J Cell Biochem. 2002;87:16–28.

Sundback CA, Vacanti JP. Alternatives to liver transplantation: from hepatocyte transplantation to tissue-engineered organs. Gastroenterology. 2000;118:438–442.

Strain AJ, Neuberger JM. A bioartificial liver-state of the art. Science. 2002;295:1005–1009.

Yamashita Y, Shimada M, Tsujita E, Shirabe K, Ijima H, Nakazawa K, Sakiyama R, Fukuda J, Funatsu K, Sugimachi K. Efficacy of a larger version of the hybrid artificial liver support system using a polyurethane foam/spheroid packed-bed module in a warm ischemic liver failure pig model for preclinical experiments. Cell Transplant. 2003;12:101–107.

Watt FM, Jordan PW, O'Neill CH. Cell shape controls terminal differentiation of human epidermal keratinocytes. Proc Natl Acad Sci U S A 1988;85:5576–5580.

# Chapter 6

# Concluding remarks

## 6-1 Summary

This thesis deals with hepatic organoid formation using a primary culture of SHs. SHs are hepatic progenitor cells that are present in the adult liver. Although primary hepatocytes rapidly loose their liver-specific functions in culture, SHs can proliferate and retain their functions. In addition, they have a capability to reconstruct the hepatic organoid. Therefore, the cells are considered suitable for the reconstruction of functional hepatic tissues.

Chapter 3 shows that SHs can reconstruct functional BC with their maturation. SHs form colonies within 10 days and the colonies are surrounded by NPCs, such as LECs and stellate cells. The NPCs invade under the SH colonies and accumulate ECM. After that, the morphology of the SHs changes from flat to plied-up and the cells differentiate into MHs. The differentiated cells form BC with luminal microvilli that are similar to hepatocytes *in vivo*. In addition to the morphological characteristics of the BC, their physiological functions are also investigated. The differentiated cells recover membrane polarity. The cells also receive bilirubin in the medium and excrete metabolites into the BC, which suggests bilirubin-metabolic function of the hepatocytes. Thus, SHs were shown to have the capability to proliferate and differentiate into MHs with functional BC. Pairs of SHs were integrated through the formation of BC.

In addition to the structure of the reconstructed BC, their function was also analyzed. In chapter 4, the BC movements are analyzed using time-lapse microscopy and their coordinated behavior is investigated. The results indicate that the BC contract and dilate spontaneously and the movements occur in a coordinated manner. BC in different regions contract and dilate synchronously. Although each SH proliferates individually in the early stage of the culture, the cells seem to develop intercellular communication with their maturation and behave themselves like an integrated multi-cellular system. Thus,

the hepatic organoids formed by SHs are functional tissues and not merely aggregated cells.

Although the functional tissues are successfully reconstructed in a 2D culture, the liver has a 3D configuration. A precise manipulation of SHs was performed to expand the hepatic organoids into a 3D configuration. In the field of liver tissue engineering, it is still unclear how we can reconstruct a complicated tissue maintaining various functions *in vitro*. The liver structure is composed of continuous stacked cell-layers (Fig. 6-1). Hepatocytes form the hepatic cords, which are interconnected lines of cells. The 3D stacked-up culture tried to mimic these structures. In the reconstructed 3D stacked-up structures, SHs physiologically adhered to each other and formed functional BC, mimicking the hepatic cords. *In vivo*, hepatocytes seem to maintain their liver-specific function by forming 3D complex architectures interacting with NPCs and the ECM. It is possible that these microarchitectures might enhance the differentiation of SHs through maintenance of the cuboidal cell shape. The 3D stacked-up culture enhanced albumin secretion and transcriptions of liver-specific mRNAs. Thus, the SHs achieved liver-specific functions by assembling into an appropriate configuration. These results can be considered as a first step in the reconstruction of complicated liver tissues so that 3D stacked-up culture can play a useful part in the construction of tissue-engineered livers.

The self-organization of SHs was observed in the reconstruction of hepatic organoids (Fig. 6-2). Although SHs are randomly distributed in the early stages of the culture, the cells proliferate and migrate to form colonies. Some SHs differentiate into MHs and the differentiated cells form BC between them. Pairs of the cells are integrated through the BC formation. The BC gradually elongate and develop into anastomosing networks. Groups of the cells behave in a coordinated manner, which suggests integration of the cells in the 2D tissue of SHs. Although the cells cannot develop into 3D tissues spontaneously, certain manipulation enhances the next step of self-organization. The stacked layers of SHs are rearranged into 3D tissues. Thus, the process of self-organization progresses in a phased manner, which suggests certain switches for self-organization.

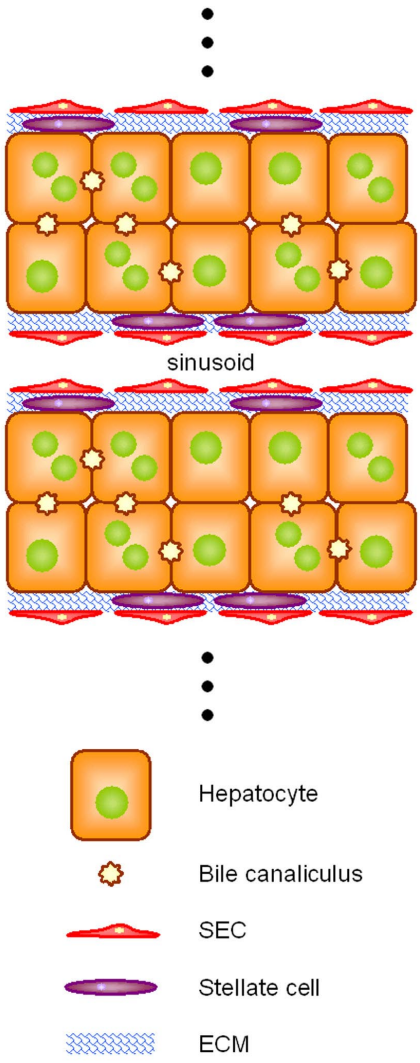


Fig. 6-1 Schematic diagram of a normal liver tissue. The liver structure is composed of continuously stacked cell-layers.

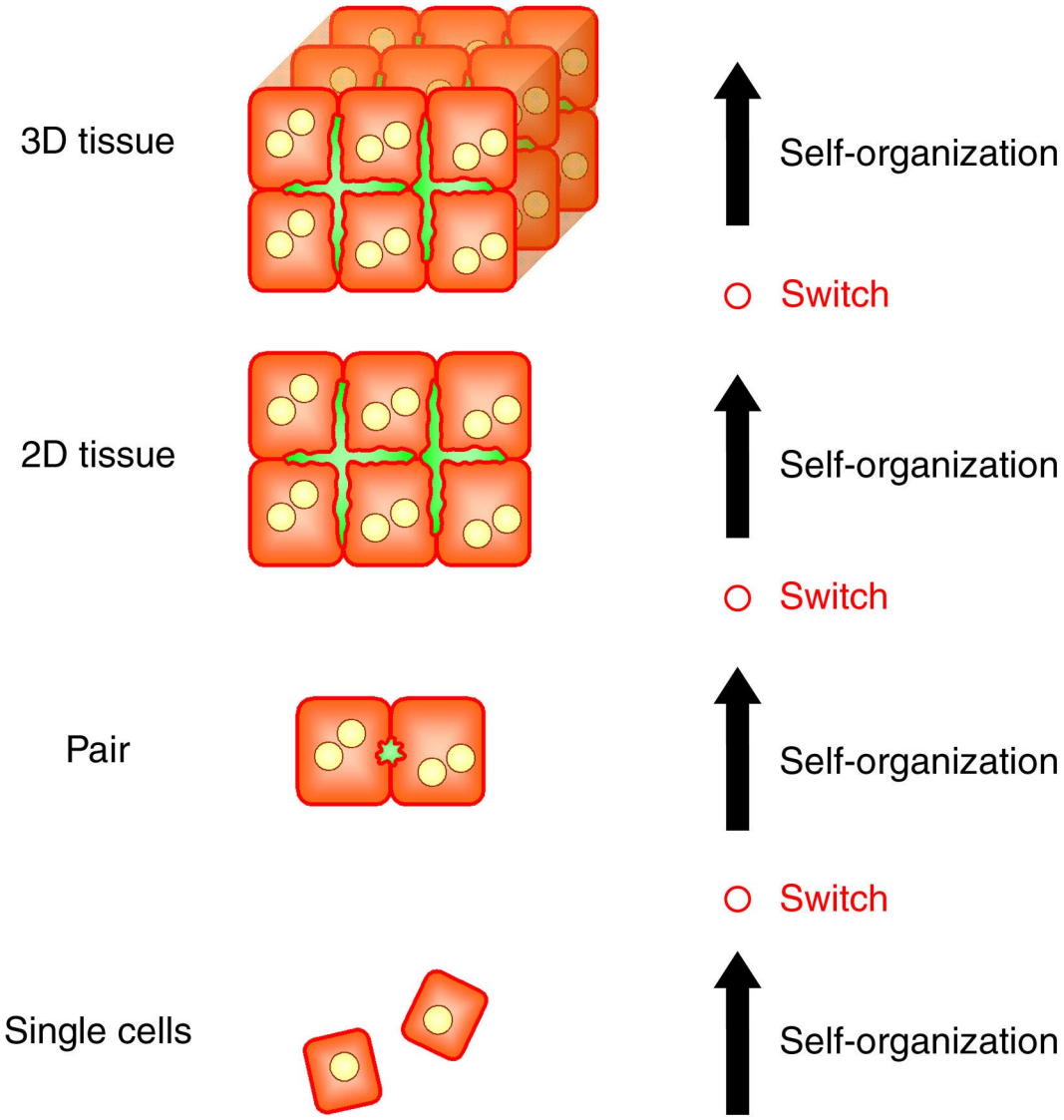


Fig. 6-2 The self-organization of SHs in the reconstruction of hepatic organoids. The cells are integrated in the self-organization process. The process progresses in a phased manner, which suggests possible switches for the next step of self-organization.

## 6-2 Perspectives

Liver transplantation is the only treatment for end-stage liver diseases, but donor organ shortages are a serious issue. Therefore, research concentrates on restoring liver functions using BAL. Various cell types have been examined for use as BAL reactor, however it is extremely difficult to maintain hepatocyte functions *in vitro*. Therefore, tissue-engineered livers are needed as an alternative to BAL bioreactor. Although the reconstruction of functional tissues was demonstrated in this thesis, larger tissues will be needed for transplantation.

Chapter 5 explains how cells are stacked onto ones cultured on membranes, which allows for multiple stacking. Although only two membranes were stacked in the experiment, more can be stacked in future work (Fig. 6-3A). Further improvements will be needed to achieve thicker complex tissues. For the reconstruction of the hepatic organoid without non-biomaterials, biodegradable polymers, such as poly-lactic-acid and poly-glycolic-acid, can be used as a material for membranes in 3D stacked-up cultures. If the cells are cultured on biodegradable membranes instead of polycarbonate membranes, the membranes will gradually degrade over time in culture (Fig. 6-3B). In addition to the multiple stacking and use of biodegradable membranes, there are still two big challenges facing those who try to reconstruct liver tissues: the reconstruction of sinusoids and bile ducts.

Sinusoids are capillary vessels in the liver. As the reconstructed tissues become thicker, the reconstruction of sinusoids is essential because the supply of oxygen and nutrients is necessary for the maintenance of 3D tissues. Isolation and culture of SECs is an ongoing study. Although further studies are needed to maintain intact SECs *in vitro*, other type of endothelial cells also have the potential to reconstruct 3D capillary vessels in collagen gel (Ueda *et al.*, 2004). Endothelial progenitor cells (EPCs) are also known to enhance the vascularization of tissues (Asahara *et al.*, 1997, 2004; Murayama *et al.*, 2002). EPCs are easy to use as a culture system as described in this thesis because they can be isolated from the bone marrow of rats as well as of humans. 3D configuration of these endothelial cells will be studied in 3D stacked-up culture in future (Fig. 6-3C).

Bile ducts are tubular structures that are formed by BECs. *In vivo*, BC merge into bile ducts via canals of Hering (Fig. 6-4). Hepatocytes produce bile and secrete it into the BC. The secreted bile flows within the

BC and is transported to the bile ducts. The reconstructed BC networks are closed due to the absence of BECs. Therefore, the contents of the BC accumulate and cyst-like structures are formed, which suggests pathological conditions such as cholestasis. The reconstruction of bile ducts is needed to drain the contents within the BC. Ongoing studies using primary culture of rat BECs show some encouraging results, but further studies will be needed before intact bile ducts can be constructed in culture.

To reconstruct complicated biological tissues, integrated studies are esential. New concepts for integrative studies, such as physiome (Bassingthwaighte, 2000; Hunter *et al.*, 2003) and systems biology (Kitano, 2002), have been proposed, including the concept of 'System Design'. These concepts take life as a system, which has a hierarchical structure containing various subsystems (Fig. 6-5). Focusing on each subsystem, it is important to design each one considering the characteristics of its components in the reconstruction of the multicellular systems. In the liver, it is important to consider the interactions between SHs and other components, such as neighboring SHs, NPCs, ECM and growth factors in culture system. The cells are integrated into tissues thorough a self-organization process. They must have a switch allowing the self-organization to reconstruct tissues. Further studies will be needed to elucidate the mechanism that operates these switches.

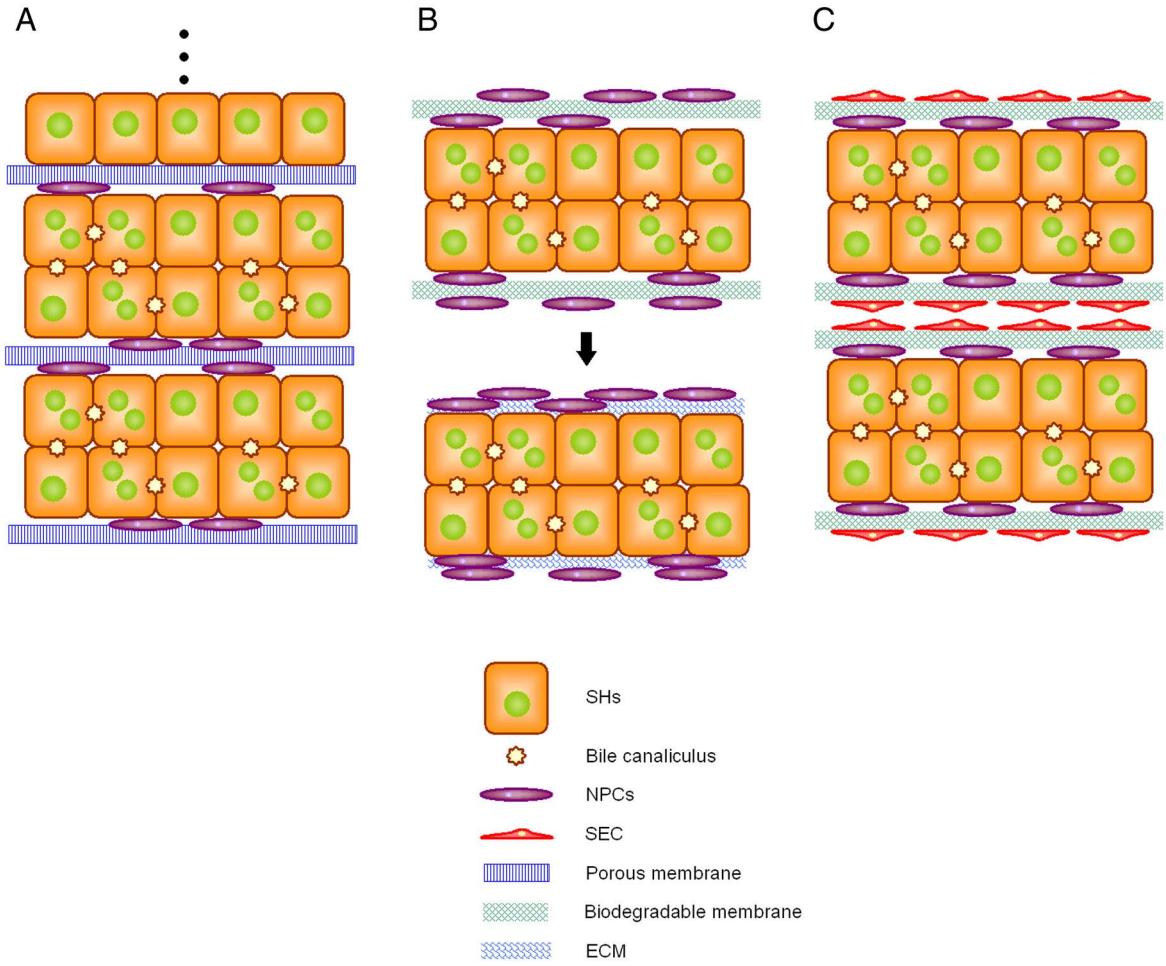


Fig. 6-3 The application of 3D stacked-up culture in future. A: Multiple stacking of the cell-layers cultured on porous membranes. Cells are separately cultured on each membrane and then stacked to reconstruct thick tissues. B: Schematic diagram of 3D stacked-up culture using biodegradable membranes. Biodegradable membranes gradually degrade over time in culture. SHs and NPCs such as stellate cells produce ECM. C: Vascularization of 3D stacked-up structure. SHs and NPCs such as stellate cells and SECs are co-cultured using biodegradable membranes.

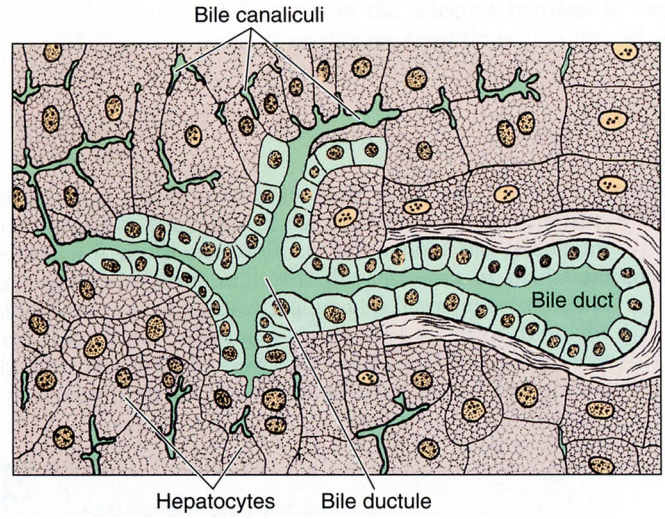


Fig. 6-4 The confluence of BC and bile ducts (Junqueira *et al*., 2003). BC are formed by hepatocytes and bile ducts are formed by BECs. Canals of Hering (also called bile ductules) connect the BC with the bile ducts.

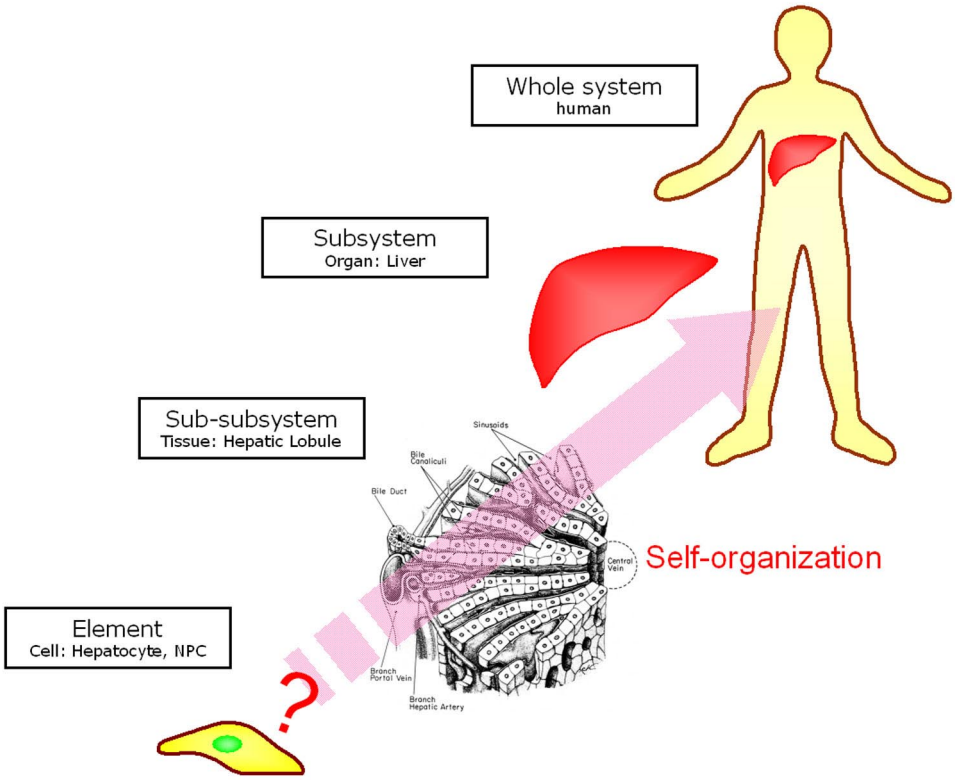


Fig. 6-5 'System Design' of the liver. Life is a system, which has a hierarchical structure of subsystems. The liver is one subsystem. The hepatic lobules are sub-subsystems of the liver composed of individual cells including hepatocytes and NPCs.

## References

Asahara T, Kawamoto A. Endothelial progenitor cells for postnatal vasculogenesis. Am J Physiol Cell Physiol. 2004;287:C572–579.

Asahara T, Murohara T, Sullivan A, Silver M, van der Zee R, Li T, Witzenbichler B, Schatteman G, Isner JM. Isolation of putative progenitor endothelial cells for angiogenesis. Science. 1997;275:964–967.

Bassingthwaighte JB. Strategies for the physiome project. Ann Biomed Eng. 2000;28:1043–1058.

Hunter PJ, Borg TK. Integration from proteins to organs: the Physiome Project. Nat Rev Mol Cell Biol. 2003;4:237–243.

Junqueira LC, Carneiro J. Basic histology: text & atlas, 10th edition. New York, NY: Lange Medical Book McGraw-Hill, 2003: 332–347.

Kitano H. Systems biology: a brief overview. Science. 2002;295:1662–1664.

Murayama T, Asahara T. Bone marrow-derived endothelial progenitor cells for vascular regeneration. Curr Opin Mol Ther. 2002;4:395–402.

Ueda A, Koga M, Ikeda M, Kudo S, Tanishita K. Effect of shear stress on microvessel network formation of endothelial cells with in vitro three-dimensional model. Am J Physiol Heart Circ Physiol. 2004;287:H994–1002.

# Bibliography

## Publications

1. Ryo Sudo, Shinichiro Ikeda, Shinichi Sugimoto, Keisuke Harada, Koichi Hirata, Kazuo Tanishita, Yohichi Mochizuki and Toshihiro Mitaka. Bile canalicular formation in hepatic organoid reconstructed by rat small hepatocytes and nonparenchymal cells. *Journal of Cellular Physiology* 199 (2): 252–261, 2004.

2. Ryo Sudo, Hiroshi Kohara, Toshihiro Mitaka, Mariko Ikeda and Kazuo Tanishita. Coordinated movement of bile canalicular networks reconstructed by rat small hepatocytes. *Annals of Biomedical Engineering* (in press).

3. Ryo Sudo, Toshihiro Mitaka, Mariko Ikeda and Kazuo Tanishita. Reconstruction of 3D stacked-up structures by rat small hepatocytes on microporous membranes. (submitted for publication).

## Proceedings (International)

1. Ryo Sudo, Hiroshi Kohara, Toshihiro Mitaka, Mariko Ikeda and Kazuo Tanishita. Bile canalicular reconstruction by rat small hepatocytes, and its dynamic analysis. *Fourth World Congress of Biomechanics* Calgary, Canada, August 2002.

2. Ryo Sudo, Hiroshi Kohara, Toshihiro Mitaka, Mariko Ikeda and Kazuo Tanishita. Functional repolarization of reconstructed hepatic organoid -- Pumping function of bile canaliculi. *JSME International Symposium on Cell Biomechanics & Tissue Engineering* Tokyo, Japan, September 2002.

3. Ryo Sudo, Toshihiro Mitaka, Mariko Ikeda and Kazuo Tanishita. Coordinated contraction of bile canaliculi reconstructed in rat small hepatocytes. *ASME 2003 Summer Bioengineering Conference* Miami, Florida, USA, July 2003.

4. Ryo Sudo, Toshihiro Mitaka, Mariko Ikeda and Kazuo Tanishita. In vitro multicellular system reconstructed by small hepatocytes and nonparenchymal cells. *International*

*Symposium of 21st Century COE Program, Keio University, Understanding and Control of Life's Function via Systems Biology* Kanagawa, Japan, November 2003.

5. Ryo Sudo, Toshihiro Mitaka, Mariko Ikeda and Kazuo Tanishita. Bile canalicular formation in the reconstructed 3D structure of rat small hepatocytes sandwiched by microporous membranes. *FASEB 2004 Summer Research Conference: Mechanisms of liver growth, development and disease* Snowmass, Colorado, USA, August 2004

## Proceedings (Japanese)

1. 須藤 亮, 池田 満里子, 谷下 一夫. 肝細胞コロニーの形態形成に関する幾何学的評価. 日本機械学会第 11 回バイオエンジニアリング講演会秋季セミナー. 新潟, 2000 年 10 月.

2. 須藤 亮, 三高 俊広, 池田 慎一郎, 杉本 真一, 原田 敬介, 望月 洋一, 池田 満里子, 谷下 一夫. 小型肝細胞によって形成される再構成肝組織における毛細胆管の運動. 第 24 回日本バイオレオロジー学会. 神奈川, 2001 年 6 月.

3. 須藤 亮, 三高 俊広, 池田 慎一郎, 杉本 真一, 原田 敬介, 池田 満里子, 谷下 一夫, 望月 洋一. Small Hepatocytes によって形成される再構成肝組織における毛細胆管の機能. 第 8 回肝細胞研究会. 東京, 2001 年 6 月.

4. 須藤 亮, 小原 洋志, 三高 俊広, 池田 満里子, 谷下 一夫. 再形成毛細胆管の収縮に対する A23187 と Endothelin-1 の影響. 日本機械学会第 14 回バイオエンジニアリング講演会. 東京, 2002 年 3 月.

5. 須藤 亮, 小原 洋志, 三高 俊広, 池田 満里子, 谷下 一夫. ラット小型肝細胞による再生毛細胆管の形成と運動解析. 第 41 回日本エム・イー学会. 京都, 2002 年 5 月.

6. 須藤 亮, 小原 洋志, 三高 俊広, 池田 満里子, 谷下 一夫. 培養肝細胞による生体外での組織形成. 第 35 回日本発生生物学会. 神奈川, 2002 年 5 月.

7. 須藤 亮, 三高 俊広, 池田 満里子, 谷下 一夫. 小型肝細胞による毛細胆管の形成とビリルビン排出機能. 第 2 回日本再生医療学会. 兵庫, 2003 年 3 月.

8. 須藤 亮, 三高 俊広, 池田 満里子, 谷下 一夫. 凍結保存小型肝細胞における毛

細胆管の形成と運動．第 42 回日本エム・イー学会．北海道，2003 年 6 月．

9. 須藤 亮，三高 俊広，池田 満里子，谷下 一夫．毛細胆管の構造と運動に対する Cytochalasin B の影響．第 10 回肝細胞研究会．東京，2003 年 7 月．

10. 須藤 亮，三高 俊広，池田 満里子，谷下 一夫．小型肝細胞が形成する毛細胆管運動とアクチンフィラメントの関係．第 6 回肝臓生物学研究会．北海道，2003 年 7 月．

11. 須藤 亮，高橋 憲生，池田 満里子，三高 俊広，谷下 一夫．多孔性膜を用いた小型肝細胞の積層培養．第 3 回日本再生医療学会．千葉，2004 年 3 月．

12. 須藤 亮，高橋 憲生，三高 俊広，池田 満里子，谷下 一夫．小型肝細胞の積層培養における毛細胆管の形成．第 11 回肝細胞研究会．山口，2004 年 7 月．

13. 須藤 亮，三高 俊広，池田 満里子，谷下 一夫．多孔性膜の積層による小型肝細胞の三次元培養. 日本機械学会第 17 回バイオエンジニアリング講演会. 愛知, 2005 年 1 月．

## Patent (International)

1. PCT835: Methods of cell culture, cell 3D culture, and tissue transplantation, and 3D tissue and artificial organ made thereby, November 2004.

## Patent (Japanese)

1. 特願 2003-385677, 細胞培養法，細胞の三次元培養法，三次元組織，人工臓器，及び組織移植方法，2003 年 11 月．

# Acknowledgments

My research activities for this thesis were carried out at the School of Fundamental Science and Technology, Keio University under the guidance of Prof. Kazuo Tanishita. First of all, I would like to thank him for his encouragement and guidance on my research. He has taught me the fascinating aspect of research from the standpoint of bioengineering. I am also pleased to thank Prof. Mariko Ikeda for her encouragement and valuable scientific suggestions. She has taught me many things from the standpoint of biology.

In my first year of the graduate school, I had been to Sapporo Medical University for 8 months to study under Profs. Toshihiro Mitaka and Yohichi Mochizuki. I would like to thank Prof. Toshihiro Mitaka for teaching me the fundamental idea of a research scientist and for his impressive advice. I am also grateful to the members of his laboratory–Ms. Minako Kuwano, Drs. Shinichi Sugimoto, Shinichiro Ikeda, and Keisuke Harada–for their technical guidance on the isolation of small hepatocytes and some biochemical analyses.

I would like to acknowledge Profs. Motonori Hoshi and Kazuo Umezawa and Associate Prof. Keiji Fujimoto for taking time for careful review of this thesis.

I also thank the members of Tanishita Lab. for their supports. I am grateful to the members of Cell Group in the Lab. for their technical supports. In particular, I am grateful to Mr. Hiroshi Kohara for his help with launching experimental setup at Keio University as well as my experiment of time-lapse microscopy. I am also grateful to Dr. Toshihiro Sera for his support that made my academic life enjoyable. I am also indebted to all of my friends, in particular Ms. Hitomi Ohishi for her moral support.

I am also grateful to Prof. Reuben M. Gerling for his help to improve my English.

Finally, I wish to express my thanks to my family for many years of support, understanding and encouragement.

February 2005

Ryo Sudo